Role of Proteinase 3 in bone marrow hematopoiesis and neutrophil function

Dissertation Advisor: Dr. Hongbo R. Luo Kutay Karatepe

Role of Proteinase 3 in bone marrow hematopoiesis and neutrophil function

Abstract

The hematopoietic system requires finely-tuned regulatory mechanisms to supply the continuous demand of short-lived blood cells while maintaining a healthy hematopoietic stem cell compartment. Proteinase 3 (PR3), a member of neutrophil serine proteases, has a unique role in the regulation of hematopoiesis among its family members. *Pr3*, which has been thought to be expressed exclusively in mature myeloid cells and myeloid progenitors, is expressed in hematopoietic stem cells. *Pr3* deletion expanded the hematopoietic stem and progenitor cell compartments. Absence of PR3 led to increased short-term regeneration potential, accompanied with a defect in production of lymphoid cells, particularly T cells. A more focused analysis led to identification of reduced cell death due to a defect in caspase 3 cleavage, but not proliferation, as the mechanism for elevated hematopoiesis seen in PR3 deficiency. PR3-deficient hematopoietic stem cells displayed exacerbated features associated with ageing. In spite of the previously proposed roles of PR3 in neutrophil function such as microbicidal activity, PR3 deficiency did not reveal a major defect in neutrophil functions except for IL1β secretion. Overall, this study identifies PR3 as a physiological regulator of hematopoietic stem cell compartment and function.

Acknowledgements

Throughout my graduate studies, I was very lucky to have the support of many amazing people. I would like to express my sincerest gratitude to all for their endless ideas, support, patience and love.

I would like to sincerely thank my advisor, Dr. Hongbo R. Luo. I joined his lab in a hard time in my life. I couldn't have asked for a better mentor after deciding to change my lab during my Ph.D. His invaluable guidance, mentorship and the example he set allowed me to grow as a scientist and as a person. Thank you for having confidence in me and teaching me to reach for higher with patience. I learned how to tackle problems, ask important questions, be patient when experiments did not work for long periods of time (after all I can get 500 HSCs from one mouse after sorting) along with so many different techniques.

I would also like to express my gratitude to all of the Luo Lab, past and present. You've provided a very friendly environment for me. I was very happy to share all the excitements of science with all of you.

Subhanjan Mondal, Yonghui Jia and Hyun-Jeong Kwak deserve a special thank you. You have helped me to get settled in the lab while I was unfamiliar with many of the surgeries and techniques. Li Zhao deserves a "very" special thank you. Whenever I was overwhelmed with the number of mice and experiments going on, she kindly offered her help.

I would like to also thank Christie Zhang, Qingming Hou and Hiroto Kambara for their close friendships and suggestions.

Thank you Xiao Luo, who spent a year in our lab as a volunteer, for your

outstanding help.

Thank you to the Joslin Diabetes Research Center Flow Cytometry Core and especially Girijesh Buruzula. I have spent long days in challenging sorts but your expertise and friendship made it all possible.

I would like to thank all of my collaborators, past and present across various labs. It was a pleasure to have worked with such wonderful people. We had a long-standing collaboration with Tao Cheng's Lab and I would like to especially thank Haiyan Zhu.

I would like to acknowledge and thank all the past and present members of my thesis committee, Dr. Joseph Mizgerd, Dr. Wendy Garrett and Dr. Francis W. Luscinskas for all of your helpful guidance with this challenging project.

On a personal note, I would like to especially thank my parents, Aysegul and Kudret Karatepe and my little sister Ayca for being there every step of the way and for making me who I am. Finally, I would like to thank my lovely wife, Esen Sefik. I was so lucky to meet you on the first day of classes at Harvard and I am so happy that we will be spending our lives together. You have provided me with an unbelievable amount of love and support in the tough times and shared my happiness in my successes.

TABLE OF CONTENTS

Chapter 1: Introduction

1.1: The hematopoietic system and hematopoietic stem cells (HSCs)

The hematopoietic system is responsible for replenishing short-lived blood cells while regulating the differentiation, self-renewal and apoptosis of hematopoietic stem cells (HSCs). During development, the earliest site of hematopoiesis in mammals is yolk sac where red blood cells that can transport oxygen to rapidly growing tissues are generated (Orkin and Zon, 2008). The next site of hematopoietic development is the aorta-gonad mesonephros (AGM) region. In mice, HSC activity with engraftment capacity as well as white blood cell differentiation potential can be detected as early as embryonic day 11 (Muller et al., 1994). Subsequent sites that can promote hematopoiesis are fetal liver, thymus, spleen and finally the bone marrow.

HSCs are historically defined by two criteria: (1) the ability to give rise to all mature blood cells, and (2) the ability to self-renew without differentiating into a mature blood cell. The number of HSCs in the adult bone marrow is limited, they have a finite lifespan and most of them reside in a quiescent state (Rossi et al., 2007b). More than one million blood cells are produced in the adult human every second (Ogawa, 1993). While HSCs must self-renew to supply this continuous demand, uncontrolled HSC proliferation can also lead to leukemia. Hence, the processes involving self-renewal, differentiation and lifespan of HSCs are tightly regulated.

1.1.1: History of HSCs and markers used for HSC identification

The first study that showed the proof-of-concept for the existence of stem cells was published in 1961 (Till and Mc, 1961). Authors showed that transplantation of bone marrow cells into recipient mice yielded erythrocytic, granulocytic and megakaryocytic colonies in the spleens of recipient mice.

In 1988, researchers achieved the first prospective isolation of hematopoietic stem cells from mouse bone marrow using fluorescence activated cell sorting and monoclonal antibodies against cell surface molecules. In this study, HSCs were identified as Lineage$^-$ (a combination of markers that distinguish various mature cells) Thy1^{low} Sca-1$^+$ (Spangrude et al., 1988). They showed that 30 Lineage$^-$ Thy1^{low} Sca-1$^+$ cells could rescue half of lethally irradiated mice. In 1991, another group established c-Kit as a vital marker for hematopoietic stem and progenitor cells (Ogawa et al., 1991). They determined Lineage$^-$ Sca-1$^+$ c-Kit$^+$ (LSK) cells as the highly enriched population containing HSCs and Lineage$^-$ Sca-1$^-$ c-Kit$^+$ (LK) cells as hematopoietic progenitor cells. Since then, LSK staining has been routinely used to identify the enriched population for HSCs.

Later, the heterogeneity of LSK cells was gradually understood (Morrison and Weissman, 1994). In 1996, transplantation of a single CD34$^-$ LSK cell has been shown to rescue 21% of lethally irradiated recipients paving the way for the use of CD34 as a marker to identify HSCs with long-term reconstitution potential (Osawa et al., 1996). Using serial dilution assays, 1 out of 5 CD34- LSK cells has been shown to be true HSCs. With the introduction of Flk2 (also known as Flt3 or CD135), LSK cells have

been suggested to contain 3 distinct populations based on their reconstitution and self-renewal capacity in 2001 (Christensen and Weissman, 2001). Results from these studies suggested that $CD34^-$ $Flk2^-$ LSK fraction contained cells with long-term (LT) reconstitution capacity and self-renewal capability. Hence, this population was identified as LT-HSCs. Later, $CD34^+$ $Flk2^-$ LSK cells were shown to exhibit short-term (ST) reconstitution capacity and limited self-renewal (Yang et al., 2005). This population was termed as ST-HSCs. Although $CD34^+$ $Flk2^+$ LSK cells retained the ability to generate cells belonging to multiple lineages, they lost self-renewal capacity (Adolfsson et al., 2001). This latter population was named as multipotent progenitors (MPPs). More recently, an alternative method for purification of HSCs that is based on the expression pattern of CD48 and CD150 that belong to signaling lymphocytic activation molecule (SLAM) family of proteins has been reported (Kiel et al., 2005). In this study, 1 out of 2 $CD48^-$ $CD150^+$ LSK cells has shown HSC activity.

In the traditional hierarchical model for the generation of mature blood cells, the most primitive LT-HSCs give rise to ST-HSCs and MPPs (Figure 1). MPPs generate oligoclonal progenitors that are capable of leading to uniclonal progenitors. In turn, these uniclonal progenitors become mature, differentiated blood cells. Two oligoclonal progenitors downstream of MPPs have been identified: (1) the common lymphoid progenitor (CLP), and (2) the common myeloid progenitor (CMP). CLPs, which can give rise to T and B cells, have a surface marker phenotype of Lin^- $Sca\text{-}1^{low}$ $c\text{-}Kit^{low}$ $IL\text{-}7R^+$ (Kondo et al., 1997). Meanwhile, CMPs have a surface marker phenotype of Lin^- $Sca\text{-}1^-$ $c\text{-}Kit^+$ $CD34^+$ $CD16/32^-$ (Akashi et al., 2000). CMPs can later become

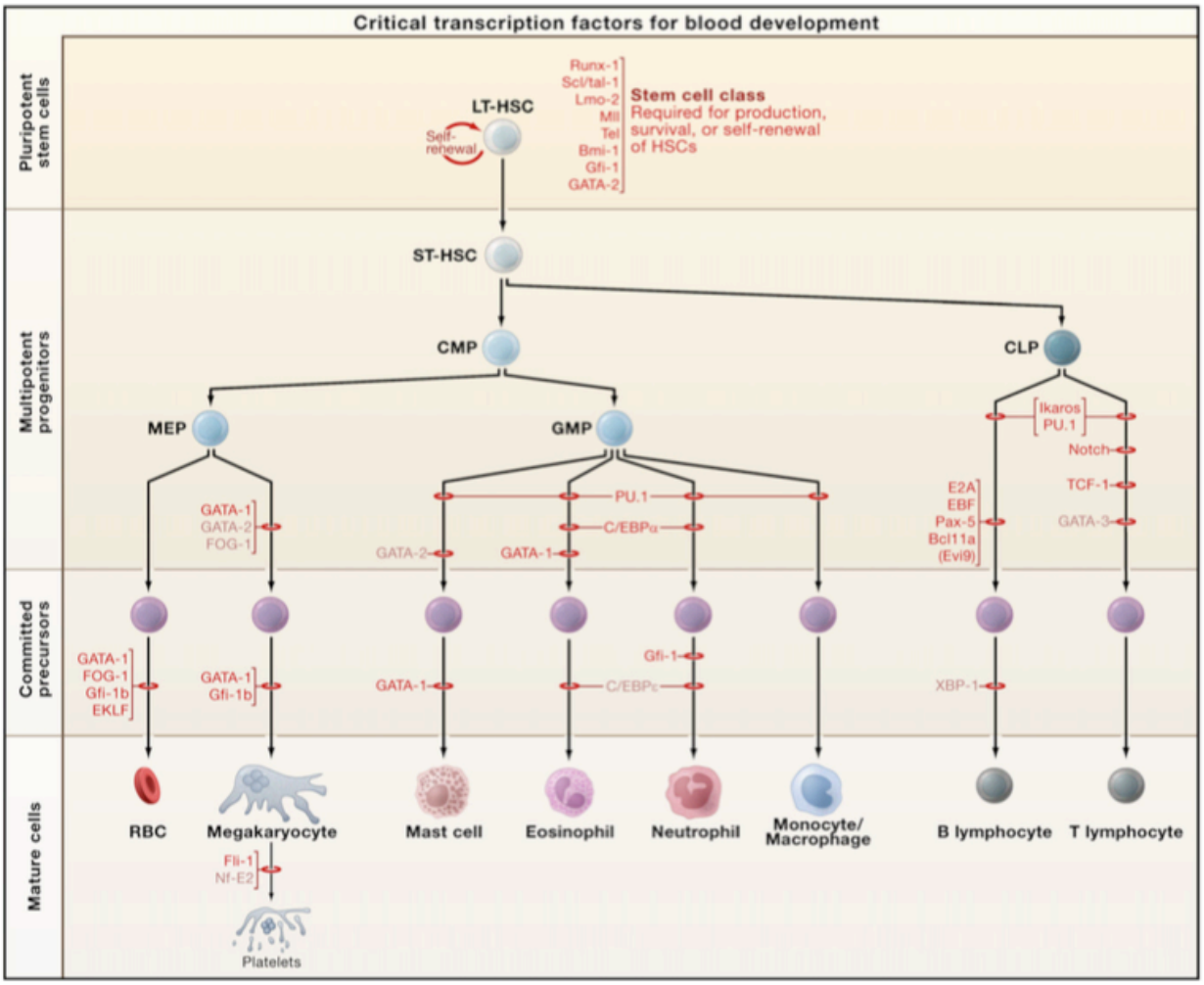

Figure 1. The hematopoietic system
There is a well-established cascade of blood cell development in which hematopoietic stem cells lose their ability to self-renew as they generate fully mature, short-lived blood cells. Critical transcription factors are listed next to the associated step. This illustration is taken from (Orkin and Zon, 2008).

megakaryocyte/erythrocyte progenitors (MEPs) and granulocyte/macrophage progenitors (GMPs). While MEPs are identified as Lin^- $Sca\text{-}1^-$ $c\text{-}Kit^+$ $CD34^-$ $CD16/32^-$ cells, GMPs are identified with the surface marker phenotype of Lin^- $Sca\text{-}1^-$ $c\text{-}Kit^+$ $CD34^+$ $CD16/32^+$ (Akashi et al., 2000).

Various aspects of this well-defined hierarchy such as the relative contribution of HSCs to the peripheral cell pool and the presence of multipotent progenitors in adult

bone marrow have recently been challenged (Notta et al., 2016; Paul et al., 2015; Sun et al., 2014). Our understanding of the hematopoietic system is largely based on transplantation studies. While a few HSC clones have the capability to generate mature blood cells throughout the organism's lifespan in transplantation studies (McKenzie et al., 2006), the contribution of HSCs to the hematopoietic compartment in the naïve state was unknown until recently.

In an elegant study, Sun et al. cloned a transposon system into mice so that the transposon would be randomly inserted into the genomic DNA in each HSC, which would allow for further tracking of its progeny (Sun et al., 2014). The authors observed an unexpectedly large clonal diversity in the mature blood cells. These results suggested that hematopoiesis in the naïve state is sustained by the successive recruitment of many clones, each with a small contribution to the mature blood cell pool. Hence, the authors proposed a model in which a large pool of progenitor cells are the main drivers of hematopoiesis in the steady state rather than a few classically defined HSCs.

Two recently published studies challenge the idea of multipotent progenitor cells in the mouse and human bone marrow. In the first study, Paul et al. performed single-cell transcriptomic analysis of 2,700 myeloid progenitors in the mouse bone marrow (Paul et al., 2015). Cluster analysis of their gene expression revealed distinct subpopulations, which were primed toward a specific myeloid cell fate. In another study, Notta et al. separated human MPPs, CMPs and MEPs into further subsets with the use of additional cell markers (Notta et al., 2016). The authors observed that all of these populations in human adult bone marrow were heterogenous and consisted largely of

unipotent progenitor cells. Hence, they proposed a two-tier model in hematopoietic hierarchy, in which the top tier contains oligopotent HSCs, while the bottom tier contains unipotent progenitors.

1.1.2: The role of transcription factors, extracellular signals and cell cycle proteins in the maintenance of HSC compartment

While giving a complete review of all factors involved in HSC maintenance are beyond the scope of this thesis, it is important to discuss some of the well-established players to understand the complexity and importance of the hematopoietic system homeostasis. Several transcription factors (Figure 1), extracellular signals and cell cycle proteins have been found crucial for HSC production, self-renewal and survival. Here, I will summarize some of the major players in HSC maintenance.

Transcription factors involved in HSC production and self-renewal: Basic-helix-loop-helix transcription factor SCL/tal1 and its associated partner LIM-finger protein LMO2 are necessary for development of all hematopoietic lineages (Porcher et al., 1996; Yamada et al., 1998). Even embryonic red blood cells are not produced in the absence of these transcription factors. Mice deficient in these proteins die around embryonic day (E) 9-10. Embryos deficient in GATA-2, a zinc-finger transcription factor, die around E10.5 with severe anemia and absence of GATA-2 also leads to severe defects in definitive hematopoiesis as evidenced in studies using chimeric embryos (Tsai et al., 1994). SET-domain containing histone methyltransferase MLL is also necessary for definitive hematopoiesis as AGM cells from MLL-deficient embryos lacked HSC activity and MLL-deficient cells did not contribute to fetal liver hematopoiesis in

chimeric embryos (Ernst et al., 2004). Meanwhile, RUNX1, the most common target of chromosomal rearrangements in human leukemia, is a Runt domain containing transcription factor and essential for fetal liver hematopoiesis. Embryos with homozygous mutations in RUNX1 die around E12.5 (Okuda et al., 1996). TEL/ETV6 gene, a transcription factor belonging to Ets family, is necessary specifically for the hematopoiesis in the bone marrow and also contributes to HSC survival in the adult bone marrow (Hock et al., 2004b; Wang et al., 1998). Mice deficient in Bmi1, a member of Polycomb group transcription repressors, are viable but develop hypocellular bone marrows and die in 2 months after birth (Park et al., 2003). It has been shown that Bmi1 is necessary for efficient self-renewal of HSCs. It is important to note that many of these transcription factors are associated with different types of leukemia.

Transcription factors involved in differentiation: Another set of transcription factors plays a critical role in the differentiation of mature blood cells (Figure 1). While HSCs usually express multiple transcription factors associated with different lineages at low levels, transcription factors associated with one lineage become dominant along the maturation of blood cells and others are silenced (Orkin and Zon, 2008). For example, C/EBPα and PU.1 are highly expressed in GMPs while MEPs exhibit high expression of GATA-1. Coexpression of two transcription factors affiliated with different lineages is thought to enable the cell to crosstalk between different cellular fates at the molecular level. PU.1 has been shown to inhibit erythroid differentiation by blocking GATA-1 binding to DNA (Zhang et al., 2000). Likewise, GATA-1 has the capacity to suppress PU.1-dependent myeloid gene expression program (Nerlov et al., 2000; Zhang et al., 1999). Even more intriguingly, introduction of a transcription factor could drive a

progenitor cell into another lineage. Forced expression of GATA-1 in GMPs and CLPs resulted in their conversion to MEPs or commitment to erythroid cells, mast cells and basophils (Iwasaki et al., 2006; Iwasaki et al., 2003). As another example, C/EBPα expression can drive CLPs into myeloid lineage (Hsu et al., 2006). Although specific lineage programs are transiently repressed, these results suggest that a certain level of plasticity exists in progenitor cells.

Niche-derived signals involved in HSC quiescence and self-renewal: After the initial observation that HSC pool is depleted as a consequence of serial transplantation experiments, it has been realized that HSCs have a finite lifespan and excessive proliferation can lead to stem cell exhaustion (Ross et al., 1982; Siminovitch et al., 1964). HSCs mostly reside in a quiescent state to prevent losing their ability to self-renew and generate mature daughter cells. Bone marrow niche-derived TGFβ and ANG-1 are critical to to maintain HSC quiescence through Smad and TIE-2 signaling, respectively (Arai et al., 2004; Yamazaki et al., 2009). On the other hand, bone marrow niche-derived Jagged-1 and Wnt can promote self-renewal and expansion of HSCs via Notch and β-catenin, respectively (Karanu et al., 2000; Reya et al., 2003).

Transcription factors that regulate cell cycle: Multiple intrinsic factors have been shown to regulate cell cycle in HSCs. Hoxb4 belongs to the homeobox family of developmental-regulatory transcription factors and regulates the expression of cyclin D2, cyclin D3 and cyclin E (Satoh et al., 2004). Hoxb4 promotes expansion of functional HSCs as evidenced by *in vitro* and *in vivo* studies (Antonchuk et al., 2002; Brun et al., 2004). A critical regulator of G1-S transition in cell cycle, c-Myc, is also induced downstream of Notch and Hoxb4 (Satoh et al., 2004). While the latter study suggested

that c-Myc overexpression enhances HSC numbers and activity *ex vivo*, another study identified that conditional deletion of c-Myc leads to accumulation of HSCs and decreased number of progenitors (Wilson et al., 2004). Hence, Wilson et al. proposed that c-Myc plays a critical role in the regulation of HSC differentiation vs. self-renewal.

Foxo family of transcription factors are known to inhibit cell cycle by repressing the transcription of cyclins and enhancing the expression of cyclin-dependent kinase inhibitors (Medema et al., 2000; Schmidt et al., 2002). Conditional deletion of Foxo1, 3 and 4 leads to reduced numbers of HSCs in spite of increased cycling suggesting that Foxo proteins prevent stem cell exhaustion (Tothova et al., 2007). Gfi-1 is a zinc finger transcriptional repressor and has been shown to restrict proliferation of HSCs in a manner similar to Foxo proteins. Although the number of Gfi-1-deficient HSCs is expanded due to an elevated proliferation rate, Gfi-1-deficient HSCs exhibit severe defects in competitive bone marrow reconstitution assays (Hock et al., 2004a).

Mef is an ETS-related transcription factor. While Mef promotes HSCs to exit quiescence and enter cell cycle, conditional deletion of Mef actually leads to expansion of HSC numbers due to reduced stem cell exhaustion (Lacorazza et al., 2006). PTEN, which is a negative regulator of phosphatidylinositol 3-kinase (PI3K) signaling, has also been shown to maintain the quiescence of HSCs. Conditional deletion of PTEN results in a short term increase in HSC number due to increased proliferation. Yet, HSCs are more rapidly exhausted in the long term (Zhang et al., 2006). Previously mentioned Foxo transcription factors have been suggested to be the critical effectors downstream of PTEN (Nakamura et al., 2000).

Cell cycle inhibitors: $p16^{INK4A}$, $p18^{INK4C}$, $p21^{CIP1/WAF1}$ and $p57^{KIP2}$ are cell cycle inhibitors. HSCs from mice deficient in each of these proteins exhibit increased rates of proliferation, albeit with unique properties. Of note, INK4 family members of cyclin-dependent kinase inhibitors inhibit the activity of cyclin D-CDK4/6 complex while CIP/KIP family members antagnozie cyclin E-Cdk2 complex, thereby blocking entry of cells into S phase. $p16^{INK4A}$-deficient HSCs from young mice are more rapidly exhausted in serial transplantation experiments (Janzen et al., 2006). Intriguingly, $p16^{INK4A}$-deficient HSCs from aged mice exhibit increased number and self-renewal function suggesting that $p16^{INK4A}$ also functions in the terminal exit of aged HSCs from cell cycle. Mice deficient in $p18^{INK4C}$ have increased numbers of HSCs as expected. Surprisingly, these HSCs are not exhausted as evidenced by enhanced chimerism even in secondary transplants (Yuan et al., 2004). $p21^{CIP1/WAF1}$ and $p57^{KIP2}$ function similar to $p16^{INK4A}$ in the sense that HSCs deficient in these proteins are rapidly exhausted (Cheng et al., 2000; Matsumoto et al., 2011).

Hematopoietic cytokines: The final set of proteins that regulate HSC compartment is extracellular cytokines. Of note, this group of proteins has been extensively studied for their therapeutic potential regarding bone marrow transplantation. Many studies utilize a combination of cytokines to promote the ex vivo expansion of stem cells although there is no consensus on a perfect cytokine cocktail that can maintain HSCs without differentiation in culture (Henschler et al., 1994; Ueda et al., 2000). Stem cell factor (SCF), which is the ligand for c-Kit, and thrombopoietin (TPO), which is the ligand for c-Mpl, are two of the most common cytokines used to maintain and expand HSCs (Brandt et al., 1992; Yagi et al., 1999). Cytokines that have

been shown to promote the growth of HSCs and downstream progenitor cells include Flt3L (the ligand for Flt3 receptor), IL-3, IL-6, IL-11 and erythropoietin among others (Bernad et al., 1994; Bryder and Jacobsen, 2000; Grover et al., 2014; Holyoake et al., 1996; Kikushige et al., 2008; Miller and Eaves, 1997).

1.1.3: The role of pro- and anti-apoptotic proteins in the maintenance of HSC compartment

Although the previously mentioned mechanisms involving HSC quiescence, self-renewal and proliferation are well-established, mechanisms involving apoptosis in HSC compartment are poorly understood. To date, there have been only a few studies that investigated the contribution of pro- and anti-apoptotic proteins to HSC pool and lifespan.

Bcl-2 belongs to a family of proteins that can prevent apoptosis, such as Bcl-2 and Bcl-xl, or induce apoptosis, such as Bim, Bid and Bad. The first study that suggested apoptosis plays a role in the maintenance of HSCs utilized a mouse model overexpressing Bcl-2. Bcl-2 inhibits apoptosis by sequestering the pro-apoptotic Bcl-2 family members such as Bim and Bad, which can form pores in the mitochondrial membrane and promote the efflux of cytochrome c from the mitochondria into cytosol (Cheng et al., 2001; Shimizu et al., 1996; Swanton et al., 1999; Yang et al., 1997). This in turn prevents the activation of caspase 3 (Shimizu et al., 1996; Swanton et al., 1999) and the downstream caspase activated DNAse that causes DNA fragmentation in nucleus (Enari et al., 1998; Wolf et al., 1999). Mice overexpressing Bcl-2 contain a higher number of HSCs that exhibit a competitive advantage over wild-type HSCs in

competitive reconstitution assays (Domen et al., 2000). They also display increased plating efficiency as evidenced by colony-forming cell (CFC) assays and are resistant to apoptosis induced by growth factor deprivation.

Mcl-1 is another anti-apoptotic protein. It has been shown to inhibit apoptosis by sequestering pro-apoptotic Bak, which can also form pores in the mitochondrial membrane (Willis et al., 2005). Conditional deletion of Mcl-1 causes severe anemia, reduced bone marrow cellularity and lethality in mice (Opferman et al., 2005). CFC assays revealed a severe reduction in the number of generated colonies and HSC numbers were greatly reduced. The mechanism for these phenotypes was explained by the high levels of HSC death observed after conditional deletion of Mcl-1 in sorted HSCs.

As mentioned previously, caspase 3 is a major component of the apoptotic machinery. Mice deficient in caspase 3 die around 4-5 weeks of age and exhibit severe neurological abnormalities (Woo et al., 1998). Caspase 3 deficiency in mice also leads to an increase in the number of HSCs (Janzen et al., 2008). While no difference in HSC apoptosis is seen *in vivo*, culturing sorted LSK cells in the presence or absence of recombinant cytokines reveals enhanced survival of caspase 3-deficient cells. The larger pool of caspase 3-deficient LSK cells can be observed even after the fourth serial transplant along with higher peripheral blood chimerism in the recipient mice as assayed by competitive reconstitution assays. Intriguingly, an increased rate of proliferation is also seen in caspase 3-deficient HSCs as a consequence of hyperactive cytokine signaling and Janzen et al. attributed the expanded HSC pool in caspase 3-deficient mice mainly to increased proliferation rather than decreased cell death.

In another study, injecting either donor or recipient mice with the pan-caspase inhibitor z-VAD-fmk led to a higher number of colony-forming units of spleen and better reconstitution of recipient mice with donor cells in an allogeneic bone marrow transplantation model (Imai et al., 2010). This effect is attributed to reduced apoptosis of donor-derived stem cells as they observed a reduction in the apoptosis of LSK compartment when bone marrow cells were cultured with z-VAD-fmk. This effect was specific to LSK cells as z-VAD-fmk treatment did not affect the apoptosis of total bone marrow cells.

In an effort to overcome the limiting numbers of hematopoietic stem and progenitor cells that can be obtained from cord blood for transplantation purposes, V. et al. investigated the therapeutic potential of z-VAD-fmk in the expansion of cord blood cells in addition to a cocktail of recombinant cytokines (V et al., 2010). The authors showed that inhibition of caspase activity improved the cell yield including immature CD34+ cells and reduced apoptosis during ex vivo expansion of cord blood cells. Cells expanded in the presence of z-VAD-fmk gave rise to a higher number of colonies in CFC assays and contained a higher number of long-term culture initiating cells. Finally, caspase inhibiton resulted in elevated engraftment in the bone marrow of recipient NOD/SCID mice.

Collectively, these results suggest that apoptosis machinery plays an important role in regulating HSC number and activity.

1.1.4: Age-triggered changes in the HSC compartment

Several changes occur in the hematopoietic system in the elderly. For instance, humans become more susceptible to infections and vaccine failure while the incidences of anemia, myeloid leukemia and myelodysplastic syndrome increase as they age. Since mature blood cells are generated from HSCs, it has been proposed that ageing of HSCs might be the driving force behind these changes. Indeed, growing evidence point to an increasing number of phenotypes associated with the physiological ageing of HSCs and the underlying mechanisms for HSC ageing.

The first major phenotype identified was an increase in HSC numbers due to elevated cycling activity (Morrison et al., 1996). Since transplantation of HSCs from aged donors into young recipients recapitulated the higher HSC numbers, it was suggested that HSC ageing was mostly due to HSC-intrinsic changes (Rossi et al., 2005). While intrinsic factors involved in HSC ageing are much better understood, it is important to note that recent studies also point to the partial contribution of bone marrow niche to HSC ageing (Ergen et al., 2012; Vas et al., 2012). Here, I will outline the major features of aged HSCs and factors known to exacerbate ageing.

Diminished regenerative potential: In spite of the higher HSC numbers as assayed by the immunophenotypic cell surface markers, aged HSCs display reduced regenerative potential. Aged HSCs exhibit diminished reconstitution capacity in transplantation studies *in vivo* and defective colony generation *in vitro* (Dykstra et al., 2011; Rossi et al., 2005; Sudo et al., 2000).

Myeloid skewing: One of the most striking features of aged HSCs is myeloid skewing. HSCs from aged mice and humans have diminished capacity to generate cells in lymphoid lineage (B and T cells) and differentiate to predominantly cells of myeloid origin (neutrophils and monocytes) (Pang et al., 2011; Rossi et al., 2005; Sudo et al., 2000). Aged mice have higher numbers of CMP cells and lower numbers of CLP cells. Genes involved in mediating lymphoid specification and function have been shown to be downregulated while myeloid genes were upregulated in HSCs from aged mice suggesting the contribution of an altered gene program to HSC ageing (Rossi et al., 2005). A clonal diversity model, in which myeloid-biased HSCs in young mice expand during the course of ageing, has then been proposed. This model was based on the observations that functionally distinct HSC subpopulations, which were prospectively isolated based on the expression of cell surface markers, exhibited different capacities in giving rise to lymphoid and myeloid cells (Beerman et al., 2010; Challen et al., 2010). Also, HSCs from aged mice also have a reduced output of cells in erythroid lineages (Florian et al., 2012).

Defects in homing and engraftment: Aged HSCs also exhibit severe defects in homing and engraftment, which also explain the reduced success rate of bone marrow transplants using elderly donors and recipients (Liang et al., 2005). Meanwhile, aged HSCs are more easily mobilized from the bone marrow in response to G-SCF, in a manner independent of the bone marrow microenvironment (Xing et al., 2006).

DNA damage: Various factors have been suggested to underlie HSC ageing. One of the most extensively studied mechanisms is DNA damage. While all cells are susceptible to DNA damage, somatic cells have a shorter lifespan and accumulation of

DNA damage in mostly quiescent stem cells can have detrimental outcomes due to the propagation of DNA damage into daughter cells. Indeed, accumulation of γH2AX foci, a marker of DNA damage has been shown in aged HSCs from mice and humans (Rossi et al., 2007a; Rube et al., 2011). Mice deficient in components of genomic maintenance pathways such as nucleotide excision repair (XPD^{TTD}), telomere maintenance ($mTR^{-/-}$) and non-homologous end joining ($mTR^{-/-}$and $Lig4^{Y288C}$) exhibited exacerbated features of HSC ageing (Nijnik et al., 2007; Rossi et al., 2007a). These results suggested that DNA repair mechanisms might be limiting during the course of ageing. Later studies identified that several genes in DNA damage response and repair pathways were attenuated in aged HSCs and could be reexpressed after stimulation of HSCs into cell cycle (Beerman et al., 2014; Flach et al., 2014). These studies pointed out the role of stem cell cell quiescence in accumulation of γH2AX foci.

Epigenetic dysregulation: Another well-established mechanism that underlies HSC ageing is epigenetic dysregulation, which can also be propagated into short-lived daughter cells. In the first study that analyzed epigenetic changes in aged HSCs, a global loss of transcriptional regulation was observed (Chambers et al., 2007b). Chromatin remodeling genes (Smarca4 and Smarcb1), histone deacetylases (Hdac1, Hdac5 and Hdac6) and a DNA methyltransferase (Dnmt3b) were downregulated while genes involved in stress response and inflammation were expressed at higher levels. Specific epigenetic modifications in aged HSCs have been later identified. Acetylation of lysine 16 on the tail of histone H4 (H4K16ac) is reduced in aged HSCs and has been suggested to play a causative role in HSC ageing (Florian et al., 2012). Changes in

global DNA methylation patterns in aged HSCs have also been identified (Beerman et al., 2013).

Senescence: Senescence is another feature associated with HSC ageing. Aged cells are thought to permanently exit from the cell cycle so that deleterious events are not passed to the subsequent generation of cells. While mechanisms that may clear senescent cells might also become defective during the course of ageing, $p16^{INK4A}$ has been established as an important intrinsic regulator of HSC senescence. $p16^{INK4A}$ is expressed in various aged tissues along with senescence-associated β-galactosidase activity (Dimri et al., 1995; Krishnamurthy et al., 2004). Clearance of p16 –positive senescent cells extends lifespan and improves functions of vital organs such as heart and kidney (Baker et al., 2016). $p16^{INK4A}$ expression also increases with age in HSCs and aged HSCs from mice deficient in $p16^{INK4A}$ exhibit improved reconstitution capacity (Janzen et al., 2006). A recent study identified that a selective inhibitor of the anti-apoptotic proteins Bcl-2 and Bcl-xl, ABT263, could selectively kill senescent cells (Chang et al., 2016). Treatment of mice with ABT263 could rejuvenate HSC activity in aged mice as evidenced by improved regenerative potential and lymphoid cell generation in transplantation studies.

Reduced cell polarity: Aged HSCs also exhibit reduced cell polarity, which has been suggested to regulate asymmetric cell division in HSCs. Various proteins such as Tubulin, Actin and Cdc42 were found to be distributed in a polarized fashion in young HSCs and this phenotype was reduced during the course of ageing (Florian et al., 2012; Kohler et al., 2009). Cdc42 is a member of Rho-GTPases and its expression increases with age. A crucial role for Cdc42 in HSC ageing was established using mice with a

constitutively active form of Cdc42 (Florian et al., 2012). HSCs from these mice were depolarized at a higher frequency and displayed defects in reconstitution capacity. Using a selective inhibitor of Cdc42 rejuvenated HSC activity in these mice and improved repopulation activity in aged wild-type HSCs.

ROS: The free radical theory of ageing suggests a central role for reactive oxygen species (ROS) in ageing. Although HSCs maintain low levels of ROS due to their low metabolic activity and preferential use of glycolysis in the hypoxic bone marrow microenvironment (Simsek et al., 2010), ROS plays a significant role in several exacerbated mouse models of ageing. HSCs from ATM-deficient mice are rapidly exhausted (Ito et al., 2006). In this study, authors found that ATM-/- HSCs had higher levels of intracellular ROS, which activated the p38-MAPK signaling pathway and led to elevated proliferation rates. Treatment of mice with an antioxidant (N-acetyl-L-cysteine, NAC) or a p38 MAPK inhibitor prevented the exhaustion of ATM-/- HSCs. Moreover, NAC treatment prolonged the lifespan of wild-type HSCs as assayed in a serial transplantation experiment. A similar outcome was also observed in FoxO-deficient mice as the defective long-term reconstitution capacity of FoxO-deficient HSCs could be rescued by NAC treatment (Tothova et al., 2007). ROS also contributes to the defective hematopoiesis seen in Tsc1-deficient HSCs (Chen et al., 2008). Similarly, self-renewal and hematopoietic potential of wild-type HSCs from aged mice were restored by pharmaceutical inhibition of downstream mTOR via rapamycin (Chen et al., 2009). While ROS might play an important role in the last two studies, alterations in protein homeostasis could also contribute to the observed results as mTOR regulates

autophagy, which is essential for HSC maintenance (Kim et al., 2011; Mortensen et al., 2011).

1.2: Proteinase 3

Neutrophils are the first cells to arrive at sites of inflammation and provide the first line of defense against infections. Mechanisms of ROS production and the central role of ROS in bacterial killing have been well-established. Later studies identified that neutrophil serine proteases could also contribute to bacterial killing as mice lacking neutrophil serine proteases were deficient in clearance of certain pathogens (Belaaouaj et al., 1998). To date, four active neutrophil serine proteases have been identified: proteinase 3 (PR3), neutrophil elastase (NE), cathepsin G and recently identified NSP4 (Perera et al., 2012; Pham, 2006).

The gene for PR3 is located on chromosome 19 in human cells and on chromosome 10 in mouse cells in the same cluster with NE and azurocidin, a closely-linked family member that lost its catalytic activity (Sturrock et al., 1998; Zimmer et al., 1992). *Pr3* expression has been reported exclusively in myeloid progenitors and mature myeloid cells but not in other cell types.

Pr3 expression is controlled transcriptionally and post-translationally. Its promoter region contains a PU.1 regulatory element, a CG-element, a TATA-box as well as potential binding sites for C/EBP and c-Myb (Sturrock et al., 1996; Sturrock et al., 1993; Zimmer et al., 1992). PR3 is synthesized as a prepropeptide. First, the signal peptide is removed after the transportation of the prepropetide into endoplasmic reticulum. Next, PR3 is glycosylated on two N-glycosylation sites. Then, the N-terminal dipeptide is

excised by DPPI, a tetrameric cysteine protease. Finally, an unknown protease cleaves the C-terminal propetide to generate the mature form of PR3 (Garwicz et al., 1997; Rao et al., 1996). Mature PR3 exists as 29-32 kD isoforms depending on the carbohydrate content. The catalytic triad required for serine protease activity consists of His57-Asp102-Ser195 residues. Major endogenous inhibitors of PR3 are Serpina1 (also known as α1-antitrypsin) and Serpinb1 (also known as leukocyte elastase inhibitor) (Rao et al., 1991; Sugimori et al., 1995).

While other members of neutrophil serine protease family are primarily located in azurophilic granules, PR3 is located in azurophilic, specific and gelatinase granules, secretory vesicles and surprisingly on the cell membrane (Campbell et al., 2000; Loison et al., 2014; Witko-Sarsat et al., 1999). Neutrophil serine proteases can act intracellularly within phagolysosomes to digest phagocytosed pathogens and act extracellularly after secretion. The acidic pH environment in lysosomes and granules contributes to keep PR3 inactive as the protease activity requires neutral pH (Baici et al., 1996).

Of note, PR3 is expressed on the surface of human neutrophils but not mouse neutrophils since the crucial hydrophobic patch consisting of six amino acids is not present in mouse PR3 (Korkmaz et al., 2008). The function of PR3 on the cell membrane in resting human neutrophils is not clear as it has been shown that PR3 on the cell surface is unable to cleave a PR3-specific FRET substrate suggesting that it is either enzymatically inactive or cannot interact with the substrate (Korkmaz et al., 2009). Regardless, PR3 on the cell membrane has been suggested to exacerbate Wegener's granulomatosis (WG) (Rarok et al., 2002). WG is a chronic inflammatory disorder

characterized by necrotizing granulomatous inflammation and vasculitis. The most commonly affected sites are the respiratory tract and kidneys. It is caused by antineutrophil cytoplasmic antibodies (ANCA) and PR3 has been identified as the major target antigen for ANCAs in WG (Jenne et al., 1990). ANCA binding to PR3 leads to activation of neutrophils.

1.2.1: Better-established functions of Proteinase 3 in neutrophils

Microbicidal activity: Early *in vitro* studies showed the microbicidal activities of PR3. *In vitro*, PR3 kills Gram-negative *Escherichia coli*, Gram-positive *Streptococcus faecalis* and the fungus *Candida albicans* (Campanelli et al., 1990). Although later studies showed that other neutrophil serine proteases could cleave *Escherichia coli* outer membrane protein A and *Pseudomonas aeruginosa* flagellin, such a bacterial target has not been found for PR3 (Belaaouaj et al., 2000; Lopez-Boado et al., 2004). One of the mechanisms that can explain microbicidal activities of neutrophil serine proteases suggests that these highly cationic proteins can interact with the bacterial membrane simply because of their charge. This in turn can lead to membrane depolarization and disruption thereby killing pathogens (Pham, 2006; Zasloff, 2002).

Modulation of cytokines: In addition to its direct role in bacterial killing, PR3 also regulates several pathways involved in inflammation. PR3 cleaves precursors of TNFα and IL-1β to generate the active forms of these cytokines (Coeshott et al., 1999). Indeed, IL-1β production in neutrophils is independent of caspase 1, the essential regulator of IL-1β production in macrophages (Greten et al., 2007). Similar to the previous proinflammatory cytokines, proforms of IL-8, a major neutrophil chemotactic

factor, and IL-18 are also converted into their active state after proteolytic cleavage by PR3 (Padrines et al., 1994; Robertson et al., 2006; Sugawara et al., 2001). On the other hand, PR3 can also cleave and inactivate IL-6, thereby providing a feedback mechanism to downregulate IL-6 mediated neutrophil activation (Bank et al., 1999).

Generation of antimicrobial peptides: Granulin peptides possess proinflammatory features and can promote IL-8 release from epithelial cells (Zhu et al., 2002). Another key role for PR3 in inflammatory processes is its capability to cleave the anti-inflammatory progranulin into proinflammatory granulin peptides (Kessenbrock et al., 2008). Importantly, this study utilized the first mouse model that was deficient in PR3. However, mice used in this study were deficient for both NE and PR3 and the results were compared to mice deficient in only NE. Using a non-infectious immune complex-mediated neutrophil infiltration model, the authors showed that mice lacking both NE and PR3 had significantly reduced neutrophil recruitment and activation due to the inability of neutrophils to cleave progranulin into granulin peptides. Additionally, human cathelicidin, hCAP-18, is processed by PR3 to generate the antimicrobial peptide LL-37 in the extracellular environment after exocytosis (Sorensen et al., 2001).

Transmigration and chemotaxis: Because of its protease activity, PR3 can degrade various extracellular matrix and basement membrane proteins such as elastin, fibronectin, laminin, vitronectin, collagen type IV and fibrinogen (Ludemann et al., 1990; Rao et al., 1991; Wiesner et al., 2005). Serpina1, an endogenous inhibitor of serine proteases, can inhibit neutrophil migration to fMLP in a transwell assay (Stockley et al., 1990). This *in vitro* finding suggests a potential role for neutrophil serine proteases in chemotaxis. Yet, *in vivo* deficiency in NE, cathepsin G or DPPI (required for activation of

all neutrophil serine proteases) did not alter neutrophil migration characteristics (Adkison et al., 2002; Allport et al., 2002; MacIvor et al., 1999).

While there may be a redundancy between serine proteases in promoting neutrophil transmigration, PR3, NE and cathepsin G have been shown to cleave and shed CD11b, a critical adhesion molecule on neutrophil cell surface (Zen et al., 2011). In this study, the authors suggested that CD11b shedding by serine proteases may be a critical step in detachment from the endothelial cells during transmigration as they observed migration defects of neutrophils from mice deficient in both cathepsin G and NE. A recent study suggested that PR3 functions in the transendothelial migration of a specific subset of human neutrophils, which have a surface marker phenotype of $NB1^{+}$ (Kuckleburg et al., 2012). NB1 is a binding partner for PR3 on the neutrophil cell surface and PECAM-1, which is expressed on both leukocytes and endothelial cells (von Vietinghoff et al., 2007). Kuckleburg et al. showed that transmigration increased the cell surface expression of PR3 on NB1+ cells. Pharmacological inhibition of PR3, treating neutrophils with a blocking antibody against NB1 and treating endothelial cells with a blocking antibody against PECAM led to defective neutrophil transmigration under static and flow conditions.

ROS production: Intriguingly, one study identified that a specific PR3-containing fraction in the supernatant of stimulated-neutrophils and recombinant PR3 could block NADPH oxidase activation (Tal et al., 1998). The physiological relevance of the latter study is not well-established.

Regulation of apoptosis: A newly established physiological function of PR3 is regulation of apoptosis. After the initial observation that PR3 internalization could lead to

apoptosis of endothelial cells (Yang et al., 2001), two different studies identified a role for PR3-mediated NF-kB and $p21^{CIP1/WAF1}$ cleavage resulting in the induction of apoptosis in endothelial cells due to their inactivation (Pendergraft et al., 2004; Preston et al., 2002). Of note, $p21^{CIP1/WAF1}$ can function as an inhibitor of cell proliferation or apoptosis in different settings. For instance, overexpression or knock-down studies using transfected rat (RBL) and human (HMC1) mast cell lines showed that PR3-mediated $p21^{CIP1/WAF1}$ cleavage increased cell proliferation (Witko-Sarsat et al., 2002). In this setting, PR3 can modulate cell proliferation by releasing the inhibitory effect of p21 on the cell cycle. Interestingly, using the same cell lines, another study showed that PR3 could cleave procaspase 3 to generate caspase 3 although this did not affect the viability of cells (Pederzoli et al., 2005). In a physiological model, a recent study published by Loison et al. showed that PR3 could cleave procaspase 3 to generate mature caspase 3 in ageing neutrophils from mice and humans (Loison et al., 2014). Importantly, this process involved caspase 8- and caspase 9-independent mechanisms and was essential in the regulation of neutrophil viability.

1.2.2: Lesser-known roles of Proteinase 3 in regulation of hematopoiesis

PR3 is the only neutrophil serine protease that has been shown to function in the regulation of hematopoietic progenitor cells. To date, its expression has been reported exclusively in mature myeloid cells and myeloid progenitor cells. Results from *in vitro* differentiation studies using promyelocytic cell line HL-60 showed that PR3 expression is downregulated as cells become more mature (Bories et al., 1989; Lutz et al., 2000). The downregulation pattern was observed for the first time after HL-60 cells were

treated with dimethylsulfoxide (DMSO) and retinoic acid to induce granulocyte differentiation or when cells were stimulated with 1,25-dihidroxyvitamin D3 or phorbol myristate acetate (PMA) to induce monocyte differentiation. Bories et al. observed that inhibition of PR3 with knock-down studies led to growth arrest and monocytic maturation of a specific clone derived from HL-60 cells, which cannot normally differentiate into monocytes upon 1,25-dihidroxyvitamin D3 or PMA treatment. Hence, PR3 plays a role in the expansion of myeloid progenitor cells and keeps them in an undifferentiated state. This function of PR3 was reflected in the naming of the protein as “myeloblastin” at the time.

A similar pattern showing the downregulation of PR3 expression during myeloid differentiation program has been confirmed in another promyelocytic cell line NB4 (Labbaye et al., 1993) and a promonocytic cell line, U937 (Zimmer et al., 1992).

Various mechanisms have been suggested to act downstream of PR3 to regulate the expansion of undifferentiated progenitor cells. The first study identified that the 28 kD heat shock protein (Hsp28) expression negatively correlates with PR3 during the differentiation of promyelocytic NB4 cells (Spector et al., 1995). Spector et al. also observed that recombinant Hsp28 protein could be cleaved by PR3. Hence, the authors proposed that PR3-mediated Hsp28 downregulation might be involved in maintaining the leukemic cells in their undifferentiated and proliferating state.

Another group identified similar results for Sp1, a transcription factor that binds to GC-rich DNA elements also known as GC-box (Rao et al., 1998). A cleaved Sp1 fragment is found in undifferentiated promyelocytic HL-60 cells while the full length Sp1 persists in the differentiated HL-60 cells stimulated with 1,25-dihidroxyvitamin D3.

Purified recombinant PR3 has been shown to cleave Sp1 in assays using both the recombinant full length Sp1 and nuclear extracts.

In a later study, overexpression or knock-down studies using a promonocytic cell line, U937, suggested that PR3-mediated $p21^{CIP1/WAF1}$ cleavage could prevent monocytic differentiation of U937 cells (Dublet et al., 2005). Also, transfection of cells with a mutant p21 that was resistant to PR3 cleavage could lead to exit of cells from the cell cycle and promote differentiation of U937 cells into monocytes. Collectively, these data suggest that PR3-mediated cleavage and degradation of these proteins might play a role in keeping the myeloid progenitor cells in the cell cycle in their undifferentiated state.

A new layer of complexity in the regulation of hematopoiesis by PR3 came from observations that minor portions of the proenzyme form of PR3 could escape granular translocation, be secreted and negatively regulate the proliferation of granulopoietic cells. Conditioned mediums from normal bone marrow cells, leukemic cells and HL-60 cell line have been known to contain a large glycoprotein complex with suppressive activity on normal granulopoiesis (Olofsson et al., 1984; Olofsson and Olsson, 1980a, b). This complex could potentially serve as a negative feedback regulator of granulopoiesis in the basal state and favor the expansion of leukemic cells in the case of leukemia. A later study identified the proform of PR3 in these conditioned mediums (Skold et al., 1999). Immunoprecipitation of PR3 from condition medium neutralized the inhibitory effect of the conditioned medium on granulopoiesis of bone marrow $CD34^+$ cells. Culturing $CD34^+$ cells showed that the reduction in the frequency of granulocyte and monocyte colony-forming units in S phase of the cell cycle depended on PR3

proform in a dose-dependent manner and could be reversed by G-CSF, a potent stimulator of granulopoiesis.

An important study on human bone marrow CD34+ progenitor cells identified that PR3 expression is first enhanced in myeloid progenitor cells during the differentiation program before it is downregulated at the late stages of myeloid differentiation (Lutz et al., 2000). In the same study, it has been shown that G-CSF treatment of $CD34^+$ cells could upregulate PR3 expression and this effect was dependent on the C/EBP, c-Myb and most importantly PU.1 binding sites in the PR3 promoter region. Finally, using an IL-3 or G-CSF dependent pro-B cell line that constitutively expresses the receptor for G-CSF, Ba/F3/G-CSFR, the authors showed that transfection of PR3 into these cells rendered them growth factor-independent. The enzymatic activity of PR3 was essential in this finding. PR3-induced factor-independent growth was not seen in the parental Ba/F3 cell line showing the requirement for constitutive G-CSFR expression, which might provide enough G-CSF signaling in the absence of G-CSF. While the regulation of PR3 by G-CSF is an important observation, the physiological relevance of the latter findings in hematopoiesis is not clear due to the use of a pro-B cell line with constitutive G-CSFR expression.

1.2.3: Generation of Proteinase 3-deficient mice

Our lab generated mice deficient in PR3 to confirm the *in vivo* function of PR3 in neutrophils. We reported that PR3 could mediate the cleavage of procaspase 3 to active caspase 3 initiating the spontaneous death of ageing neutrophils (Loison et al., 2014).

PR3-deficient mice were generated on a pure C57BL/6 background using standard homologous recombination techniques (Figure 2A). Briefly, LoxP sites were inserted around exon 2 of the *Pr3* gene in the targeting vector. Gene targeting was achieved by electroporation of the targeting vector into C57BL/6 embryonic stem cell line Bruce 4. ES cells undergoing homologous recombination were identified by Southern blotting and injected into blastocysts of C57BL/6 mice. To generate whole-body knockout mice, the offspring was mated to C57BL/6-NCr mice to remove exon 2 flanked by LoxP sites in all tissues. Germline transmission of *Pr3* deletion was confirmed by PCR on genomic tail DNA and by Western blot analysis of bone marrow neutrophil lysates (Figure 2B-C).

So far, all of the studies that suggested a role for PR3 in hematopoiesis focused on either cell lines from various origins and at different maturation stages or the mixed $CD34^+$ progenitor cell population from human bone marrow. These studies utilized overexpression and knockdown of PR3 as well as using blocking antibodies. The generation of PR3-deficient mice prompted us to investigate how PR3 affects hematopoiesis *in vivo*. We asked which cells express PR3 and if PR3-deficiency leads to changes in the frequency and function of different hematopoietic cells along the blood cell development cascade.

Finally, although the function of PR3 has been extensively studied in neutrophils *in vitro*, little is known about its physiological roles. We asked how PR3 deficiency affects neutrophil functions such as bacterial killing, ROS production, adhesion dynamics, chemotaxis and posttranscriptional regulation of cytokines *in vivo*.

Figure 2

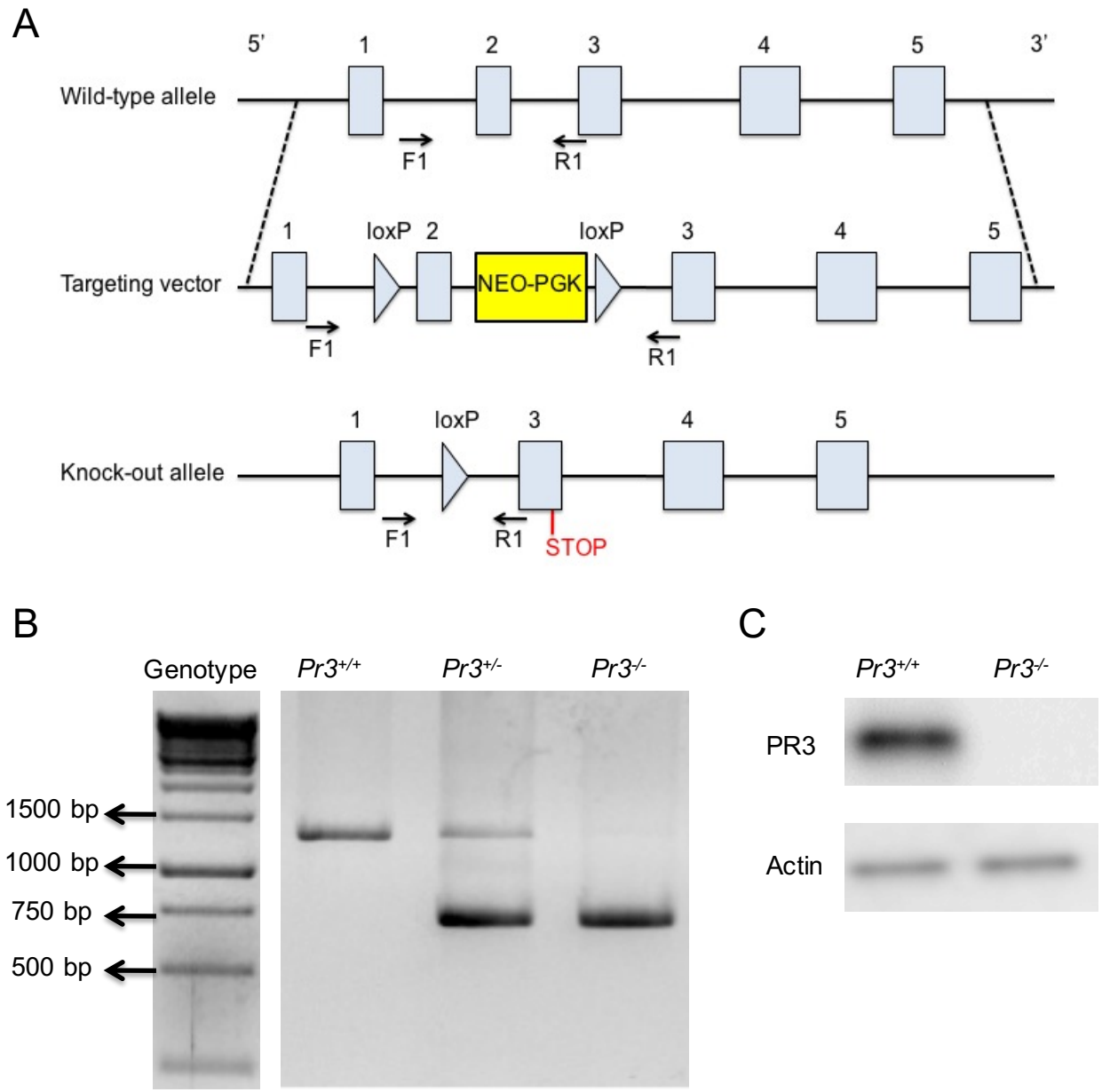

Figure 2. Generation of PR3-deficient mice
(A) Wild type allele, targeting vector and the knock-out allele for PR3. Numbers denote the exon number. The positions of the regions targeted by primers for genotyping are indicated. (B) Genotyping PCR of tail genomic DNA from *Pr3*$^{+/+}$, *Pr3*$^{+/-}$ and *Pr3*$^{-/-}$ mice using the indicated primers. (C) Western blotting analysis of bone marrow neutrophil lysates from *Pr3*$^{+/+}$ and *Pr3*$^{-/-}$ mice. This figure was prepared for a previous study and published in Loison et al., 2014.

Chapter 2: Role of Proteinase 3 in bone marrow hematopoiesis

HSCs are mostly quiescent with finite lifespan (Cheshier et al., 1999; Sieburg et al., 2011). Cell cycling and apoptosis in HSCs are dynamically regulated according to context (Takizawa et al., 2011). Deletion of anti-apoptotic Mcl-1 leads to HSC death (Opferman et al., 2005), while overexpression of anti-apoptotic Bcl-2 (Domen et al., 2000) or deficiency of pro-apoptotic caspase 3 (Janzen et al., 2008) enhances HSC survival. Inhibition of caspase activity facilitates engraftment of donor HSCs and accelerates donor hematopoiesis in a mouse intra-bone marrow-bone marrow transplantation model (Imai et al., 2010). Caspase inhibition in human $CD34^+$ cells results in higher engraftment in NOD/SCID mice and enhanced clonogenicity and long-term culture-initiating potential *in vitro* (V et al., 2010). However, the mechanisms that regulate apoptosis in HSCs are not as well understood as those regulating cell cycling.

PR3 is mainly expressed in granulocytes and myeloid progenitor cells. As reviewed in detail in the previous chapter, PR3 has a unique role among neutrophil serine protease family members in the regulation of hematopoiesis. We previously reported that PR3 regulates neutrophil spontaneous death by cleaving and activating pro-caspase 3 (Loison et al., 2014). In this study, we report that PR3 is also expressed in the HSC compartment and investigated how it regulates HSC function and lifespan.

The work presented in this chapter was performed in distinct collaboration with Haiyan Zhu in the laboratory of Tao Cheng at the Chinese Academy of Medical Sciences and Peking Union Medical College. Haiyan Zhu performed studies involving

recovery after sublethal irradiation, survival after lethal irradiation and transplantation studies with middle-aged (14 month old) mice.

2.1: Expression of Proteinase 3 in hematopoietic stem and progenitor cells

To address whether *Pr3* expression in the BM is restricted to neutrophils and myeloid progenitors, we assayed highly purified LSK cells ($Lin^-c\text{-}Kit^+Sca1^+$) and neutrophils from PR3-deficient ($Pr3^{-/-}$) and control wild-type (WT) mice. For this aim, we flushed bone marrow cells from femurs and tibias. For neutrophil purification, cells were stained with antibodies against Gr1 and CD11b after lysis of red blood cells. For purification of LSK cells, hematopoietic progenitor cells were first enriched with an immunomagnetic negative selective method using biotinylated antibodies against differentiated cells. Then, cells were stained with fluorophore conjugated Streptavidin and antibodies against c-Kit and Sca-1 before cell sorting. High *Pr3* transcript levels were detected in WT but not $Pr3^{-/-}$ LSK cells (Figure 3A-B). Quantification of mRNA revealed 2-fold higher *Pr3* mRNA expression in LSK cells compared to neutrophils (Figure 3C). Examination of two publicly available transcriptome databases of hematopoietic cells revealed high levels of *Pr3* expression in the most immature HSCs (Figure 3D-E) (Chambers et al., 2007a; Hyatt et al., 2006). PR3 was also detected at the protein level in LSK cells and lineage negative, c-Kit positive, and Sca-1 negative (LK) cells (which include myeloid progenitor cells) as assayed by western blotting and flow cytometry (Figure 3F-G). Comparison of PR3 expression among different LSK subsets by conventional flow cytometry revealed that $CD34^-Flk2^-$ long-term (LT) HSCs,

Figure 3. *Pr3* is expressed in hematopoietic stem and progenitor cells.
(A) Representative plots for *Pr3* and *GAPDH* mRNA expression in sorted WT and *Pr3*$^{-/-}$ (KO) LSK cells from three independent experiments. (B) *Pr3* mRNA expression in sorted BM stem (LSK) cell-containing populations in WT and *Pr3*$^{-/-}$ mice as determined by quantitative RT-PCR. Data shown are mean ± SEM (n=3 mice). **p < 0.01. (C) Comparison of *Pr3* mRNA expression in sorted LSK cells and neutrophils from WT mice. *Gapdh* was used as a housekeeping control (n=3 mice). *p < 0.05. (D) *Pr3* mRNA expression in hematopoietic stem cells and neutrophils from the ImmGen Database (Hyatt et al., 2006). HSC and neutrophil populations are highlighted in red. (E) *Pr3* mRNA expression in hematopoietic stem cells and neutrophils from the Gene Expression Across Multiple Hematopoietic Lineages Database (Chambers et al., 2007a). HSC and neutrophil populations are highlighted in red. (F) PR3 protein expression in sorted BM stem (LSK) and progenitor (LK) cell-containing populations and neutrophils as determined by western blotting. gp91phox was used to rule out neutrophil contamination in LSK and LK cells, and GAPDH was used as a loading control. Results are representative of three independent experiments. (G) Intracellular PR3 staining in LSK cells from WT and *Pr3*$^{-/-}$ BM by conventional flow cytometry. Results are representative of five independent experiments. (H) Intracellular PR3 staining in different cell populations as determined by conventional flow cytometry. Results are representative of five independent experiments.

Figure 3 continued

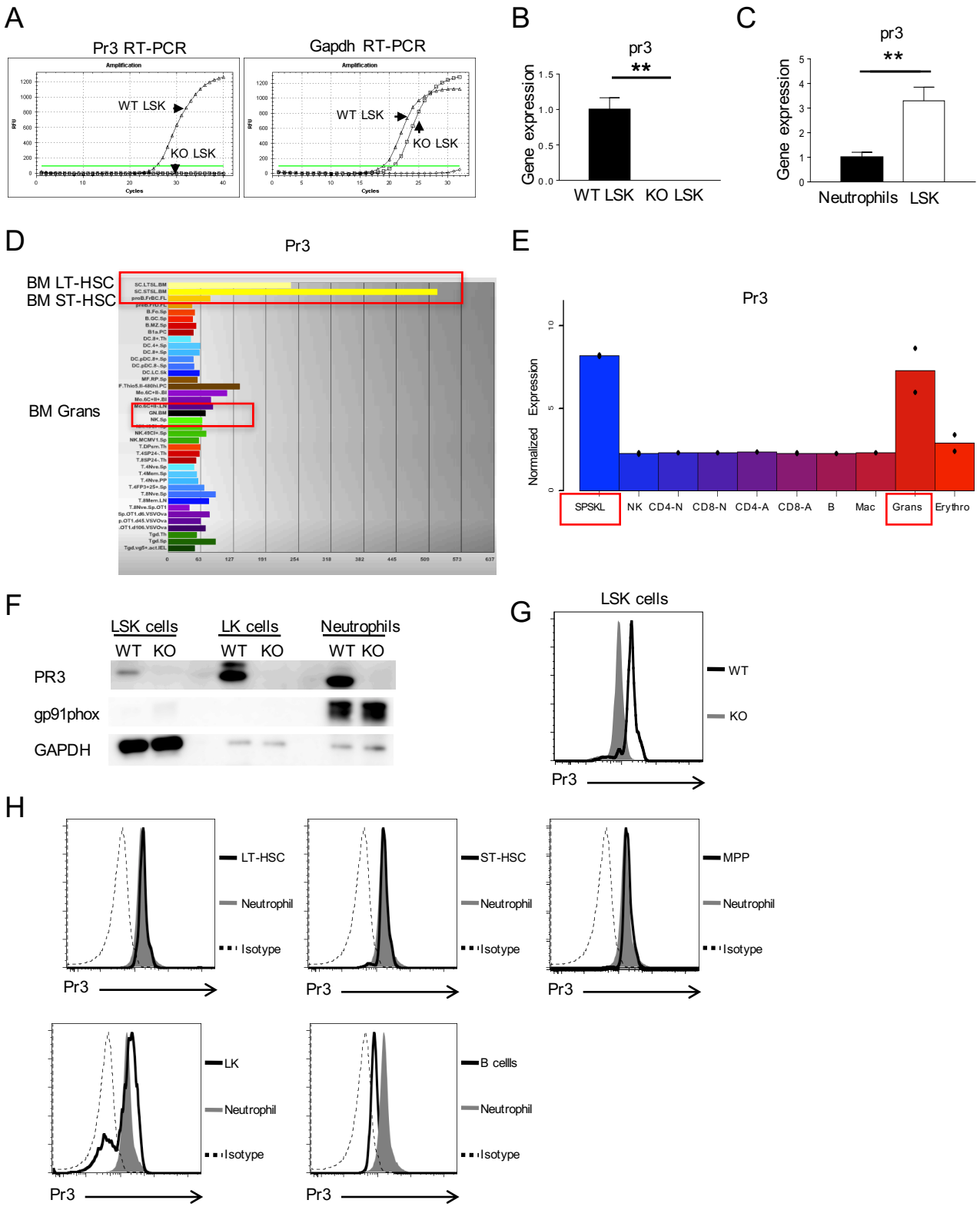

$CD34^+Flk2^-$ short-term (ST) HSCs, and $CD34^+Flk2^+$ multipotent progenitors (MPPs) expressed PR3 at levels comparable to neutrophils (Figure 3H).

2.2: Phenotypic and functional changes in the murine bone marrow in the absence of Proteinase 3

Due to high *Pr3* expression in HSCs, we explored whether PR3 modulates hematopoiesis *in vivo*. $Pr3^{-/-}$ spleens weighed less than those from WT mice despite no difference in body weights, BM cellularity, and total peripheral blood cell counts (Figure 4A-C). The peripheral blood contained a slightly higher percentage of neutrophils and monocytes and a slightly lower percentage of lymphoid cells in the $Pr3^{-/-}$ mice compared to WT mice, while eosinophil, basophil, red blood cell and hemoglobin levels were unchanged (Figure 4D).

We next examined the overall frequency and numbers of hematopoietic stem and progenitor cells (HSPCs) in the BM of WT and $Pr3^{-/-}$ mice and found that the frequency and absolute number of LSK cells in $Pr3^{-/-}$ mice was twice that of controls. Expansion of the LSK compartment was not restricted to a specific LSK subset: both the proportions and numbers of LT-HSCs, ST-HSCs, and MPPs were higher in $Pr3^{-/-}$ bone marrow (Figure 5A-B). The $CD150^+CD48^-$ LSK ($SLAM^+$ LSK) cell compartment was also enhanced in $Pr3^{-/-}$ mice (data not shown). The proportion and number of LK cells, the hematopoietic progenitor cells that can give rise to myeloid or erythroid lineages, was 50% higher in $Pr3^{-/-}$ BM. When the LK population was subfractionated into $CD34^-$ $CD16/32^-$ megakaryocyte/erythroid progenitors (MEPs), $CD34^+CD16/32^-$ common myeloid progenitors (CMPs), and $CD34^+CD16/32^+$ granulocyte/monocyte progenitors

Figure 4

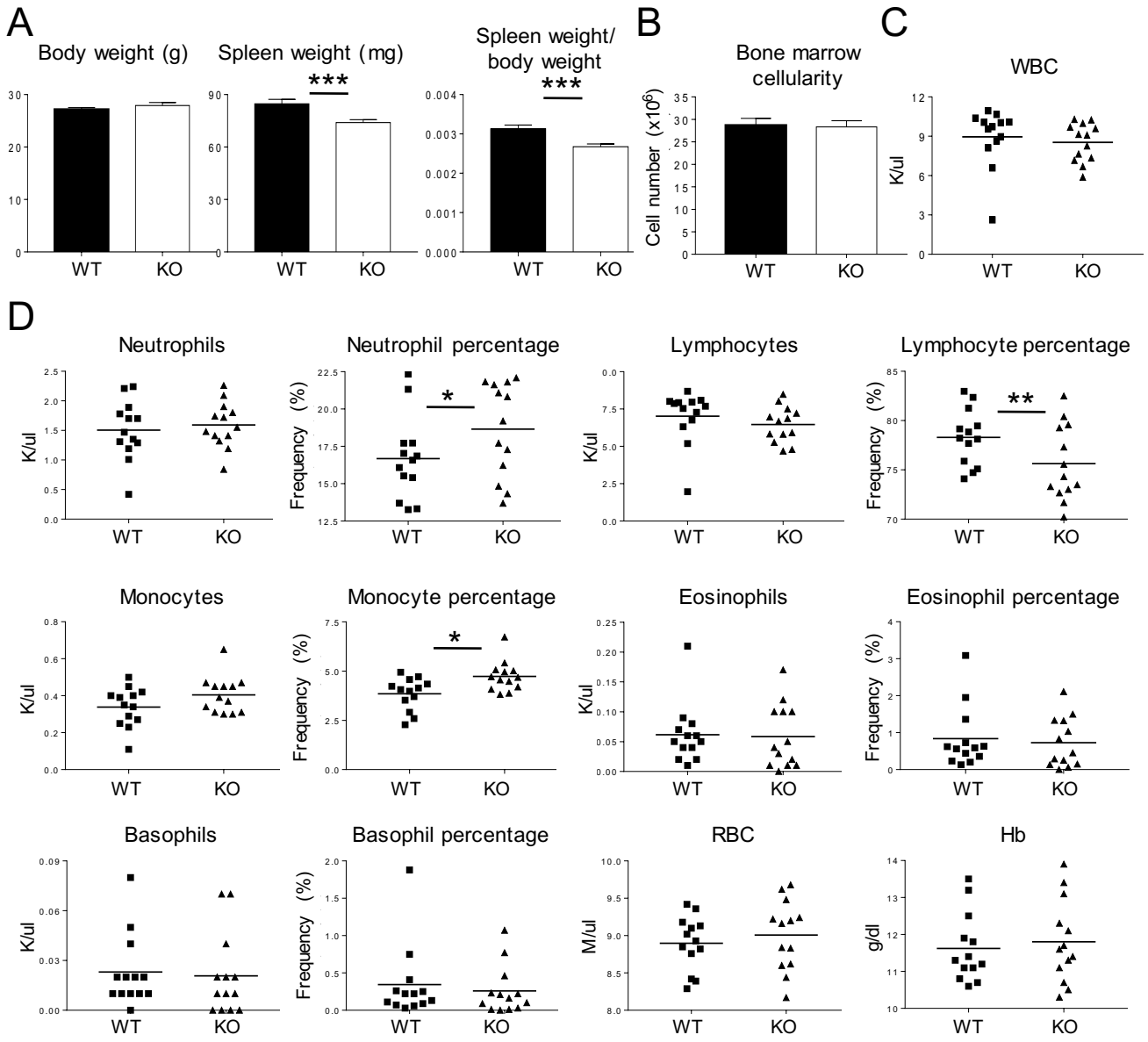

Figure 4. Pr3 deficiency leads to a slight reduction in spleen weight, reduced percentage of lymphoid cells and increased percentage of neutrophils and monocytes in peripheral blood. (A) Body weights, spleen weights, and spleen weight/body weight ratios of WT and *Pr3*$^{-/-}$ mice (n=28). ***p <0.001. (B) The number of BM mononuclear cells per one femur and one tibia in WT and *Pr3*$^{-/-}$ mice (n=18). Data in bar graphs are represented as mean ± SEM. (C) Total white blood cell counts in WT and *Pr3*$^{-/-}$ mice (n=13). (D) Numbers and percentages of different blood cell lineages and hemoglobin levels in WT and *Pr3*$^{-/-}$ mice (n=13). Blood parameters were analyzed by using Hemavet 950FS (Drew Scientific). *p < 0.05, **p < 0.01.

Figure 5

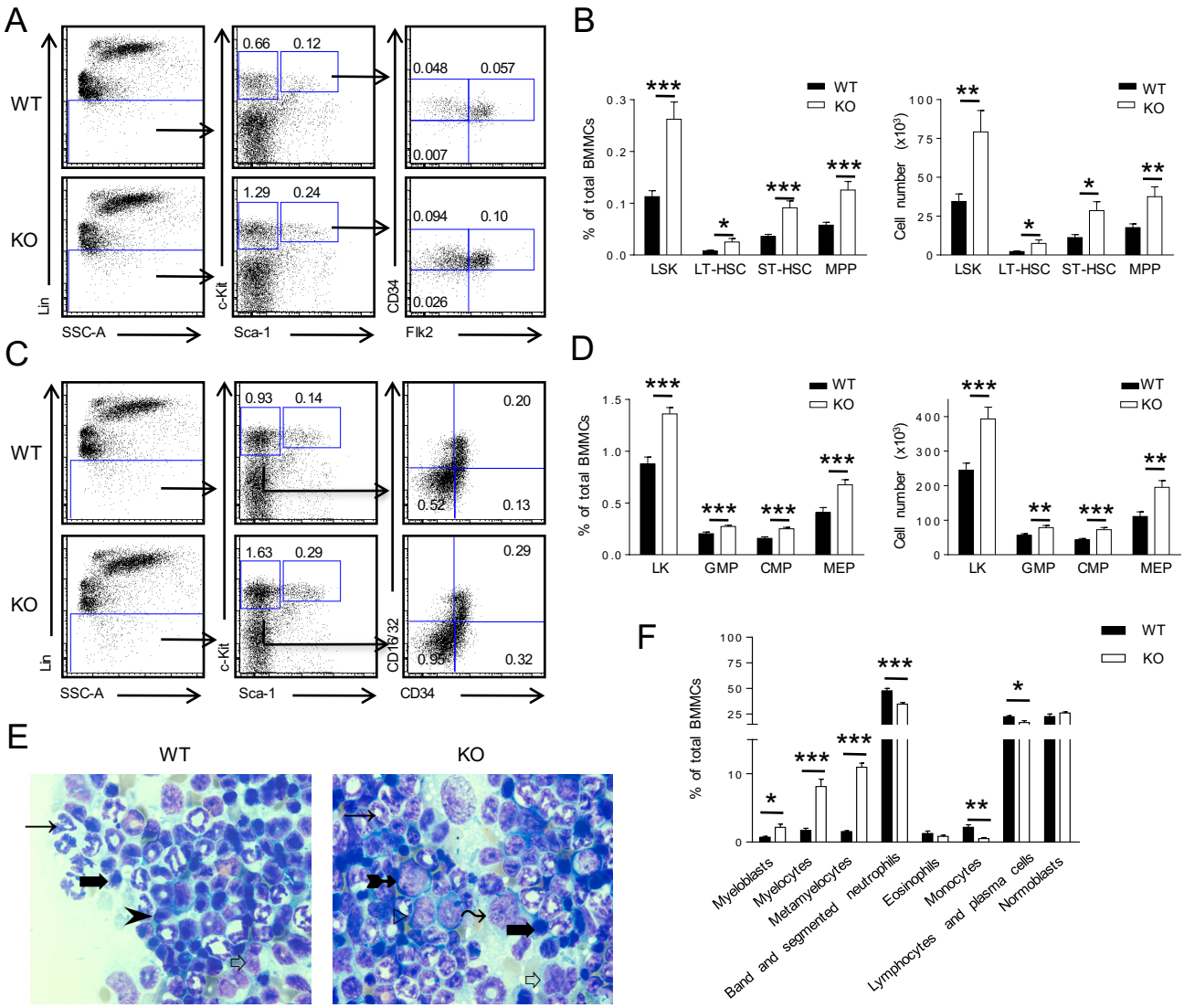

Figure 5. *Pr3* regulates the frequency and number of stem and progenitor cell subsets as well as immature neutrophils.

(A) Representative flow cytometry plots for LSK subsets in WT and *Pr3*$^{-/-}$ mice. Numbers denote the frequency of each population among live singlets. (B) Quantification of the frequency and number (per one femur and one tibia) of LSK subsets in WT and *Pr3*$^{-/-}$ mice (n=10). Results are pooled from four independent experiments. *p < 0.05, **p < 0.01, ***p < 0.001. (C) Representative flow cytometry plots for LK subsets in WT and *Pr3*$^{-/-}$ mice. Numbers denote the frequency of each population among live singlets. (D) Quantification of the frequency and number of LSK subsets in WT and *Pr3*$^{-/-}$ mice (n=16). Results are pooled from five independent experiments. **p < 0.01, ***p < 0.001. (E) Representative images of histological analysis of BM smears from WT and *Pr3*-/- mice. Arrowhead (➤): lymphocyte, long arrow (→): neutrophil, big arrow (➡): normoblast, white arrow (⇨): monocyte, tailed arrow (➳): myelocyte, right-pointing triangle (▷): myeloblast, wavy arrow (⇝): metamyelocyte. (K) Quantification of cells belonging to different lineages and maturation stages according to histological analysis of BM smears (n=6). *p < 0.05, **p < 0.01, ***p < 0.001

(GMPs), the frequency and number of all three subpopulations was increased in *Pr3*$^{-/-}$ BM (Figure 5C-D).

Given the increased number of stem and progenitor cells in *Pr3*$^{-/-}$ mice, we next determined the frequency of cells at different maturation stages of myeloid and lymphoid development. Histological analysis of BM smears was performed by a modified Wright-Giemsa stain that can differentiate cells by their intracytoplasmic content. Histological analysis of WT and *Pr3*$^{-/-}$ BM smears revealed an increased frequency of immature myeloid cells such as myeloblasts, myelocytes, and metamyelocytes in *Pr3*$^{-/-}$ BM and decreased frequencies of band and segmented neutrophils and lymphocytes (Figure 5E-F). Collectively, these results indicate that *Pr3* disruption expands HSPCs and enhances hematopoiesis, particularly myelopoiesis.

To test if the enhanced multilineage progenitor cell compartment in *Pr3*$^{-/-}$ mice is functional *in vitro*, we performed colony-forming cell (CFC) assays. CFC assays utilize recombinant cytokines to promote the growth of progenitor cells into single colonies representative of distinct lineages. Myeloid and erythroid CFC assays with total BM cells confirmed an increase in the number of functional progenitors in *Pr3*$^{-/-}$ mice *in vitro* (Figure 6A). Splenocytes from *Pr3*$^{-/-}$ mice also gave rise to more colonies than those from WT mice (Figure 6B), suggesting that the enhanced progenitor cell compartment in *Pr3*$^{-/-}$ mice is not BM-restricted. Of note, WT and *Pr3*$^{-/-}$ total BM-derived colonies were of similar size (Figure 6C-D). To examine whether early progenitor cells in *Pr3*$^{-/-}$ mice could compete with WT cells *in vivo*, we transplanted total BM cells from WT and *Pr3*$^{-/-}$ mice into lethally irradiated congenic recipients in a competitive BM transplantation

Figure 6. Expanded hematopoietic progenitor cells in *Pr3*$^{-/-}$ bone marrow are functionally active.
(A) Quantification of *in vitro* progenitor cell activity as evidenced by colony forming cell assays using BM cells (n=9 from three independent experiments). *p < 0.05, **p < 0.01. (B) Quantification of *in vitro* progenitor cell activity as evidenced by colony forming cell assays using splenocytes (n=3). *p < 0.05. (C) Representative images of WT and *Pr3*$^{-/-}$ colonies from colony forming cell assays. Scale bar = 100 μm. (D) Quantitative analysis of colony sizes from WT and *Pr3*$^{-/-}$ colonies. The sizes of at least 10 colonies were measured per sample (n=6 from two independent experiments). (E) Scheme of the experimental setup for the competitive bone marrow transplantation. (F) Representative FACS dot plots for myeloid cells, B cells, and T cells showing the reconstitution capacity of different donors in the recipient mice. (G) Quantitative analysis of the distribution of cells in the recipient mice at 8 weeks post-transplantation (n=4). The experiment was repeated twice with a cohort of four mice per group. Data shown are means ± SEM. *p < 0.05, ***p < 0.001.

Figure 6 continued

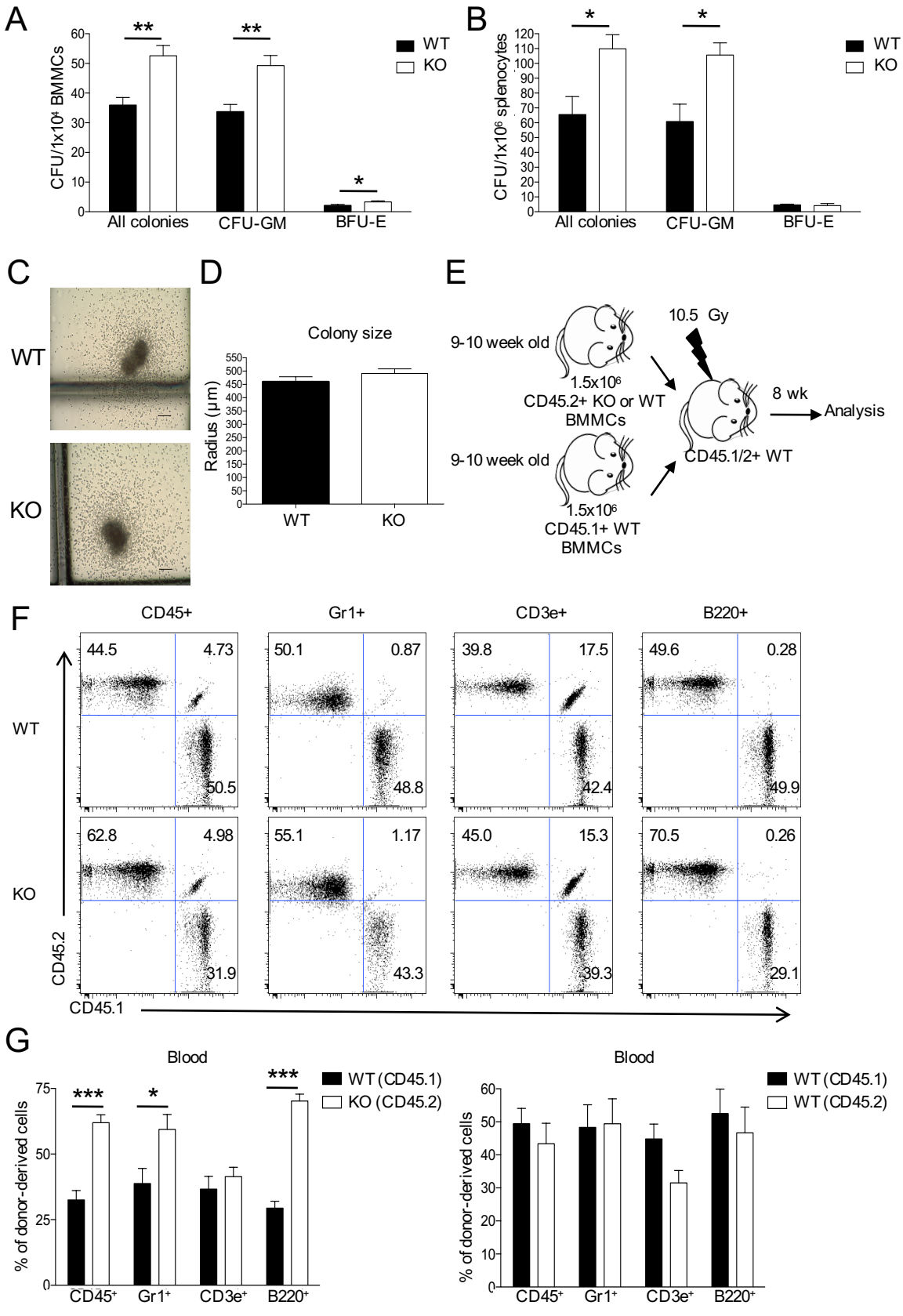

setting (Figure 6E). At 8 weeks post-transplant, peripheral blood cells were analyzed for donor contribution by lineage analysis. *Pr3*$^{-/-}$ mice gave rise to more total white blood, myeloid, and B cells, but not T cells, than the WT donor (Figure 6F-G). Taken together, these results confirm that *Pr3* disruption does indeed expand functionally active HSPCs.

Accelerated expansion of HSPCs often improves BM recovery after damage, so we investigated whether *Pr3* disruption improves BM recovery in irradiated mice. WT and *Pr3*$^{-/-}$ mice were sublethally irradiated (4 Gy) and hematopoietic recovery assessed by analyzing peripheral blood, BM, and spleen at various time points (Figure 7A). Starting at 7 days post-irradiation, *Pr3*$^{-/-}$ mice had higher numbers of total white blood cells in the peripheral blood (Figure 7B). Various lineages in the peripheral blood including neutrophils, monocytes, lymphocytes, and eosinophils exhibited faster recovery in *Pr3*$^{-/-}$ mice (Figure 7C). *Pr3*$^{-/-}$ mice had higher body weights after irradiation, suggesting that *Pr3*$^{-/-}$ mice were more resistant to hematopoietic injury (Figure 7D). *Pr3*$^{-/-}$ mice also had higher BM cellularity 7 days post-irradiation (Figure 8A), with BM analysis showing that neutrophil, T cell, B cell, and LK cell recovery was more rapid in the BM of *Pr3*$^{-/-}$ mice (Figure 8B-D). Although the spleen weights of *Pr3*$^{-/-}$ mice were slightly higher in the early stages after sublethal irradiation, the results were not statistically significant (Figure 9A). Yet, analysis of spleen cellularity and the numbers of different cell lineages in the spleen revealed an enhanced ability of *Pr3*$^{-/-}$ mice to cope with hematopoietic injury similar to peripheral blood cells and bone marrow cells (Figure 9B-C).

Figure 7

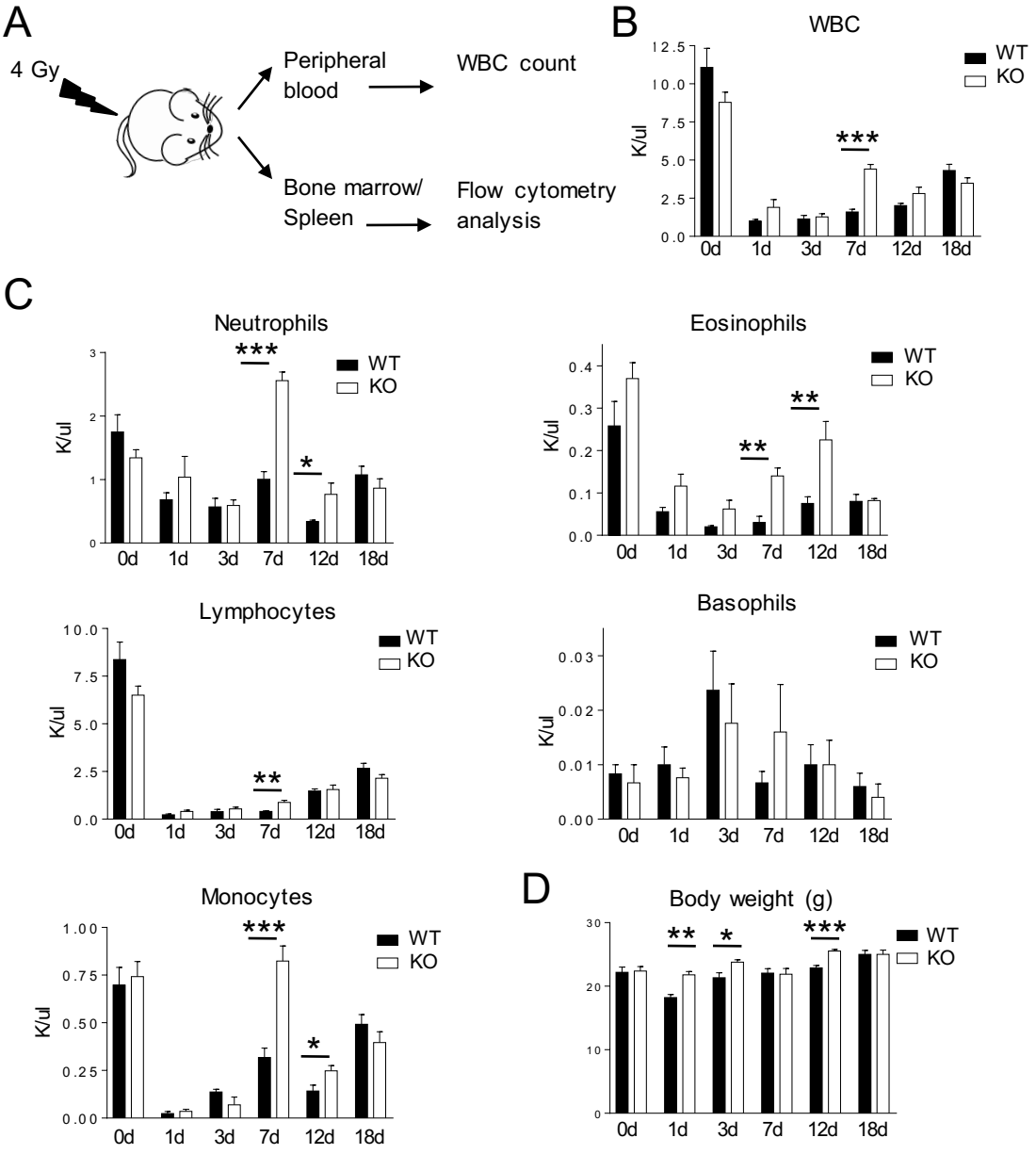

Figure 7. Expanded hematopoietic progenitor cell population in *Pr3*$^{-/-}$ bone marrow provides faster recovery of mature blood cells and resistance to reduction in body weight after sublethal irradiation.

(A) The experimental setup used to analyze hematopoietic recovery after challenge with sublethal irradiation (4 Gy). (B-C) Peripheral blood cell counts in WT and *Pr3*$^{-/-}$ mice before and after sublethal irradiation (n=5-9 mice per genotype). *p < 0.05, **p < 0.01, ***p < 0.001. (D) Body weights of WT and *Pr3*$^{-/-}$ mice before and after sublethal irradiation (n=5-9 mice per genotype). *p < 0.05, **p < 0.01, ***p < 0.001.

Figure 8

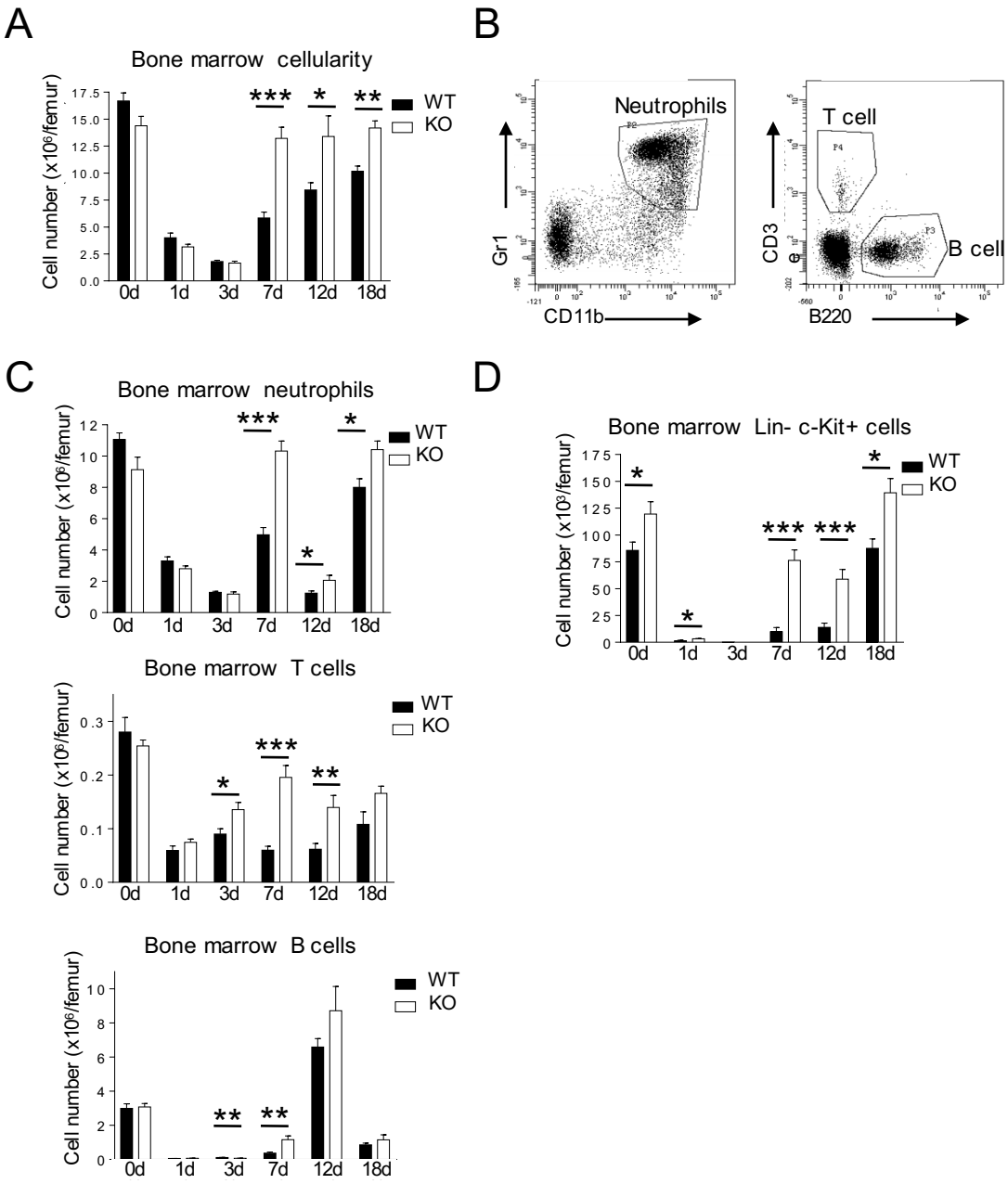

Figure 8. Bone marrow cellularity, mature bone marrow cells and hematopoietic progenitor cells recover faster in *Pr3*$^{-/-}$ mice after sublethal irradiation.

(A) The number BM mononuclear cells per one femur in WT and *Pr3*$^{-/-}$ mice before and after sublethal irradiation (n=5-9 mice per genotype). *p < 0.05, **p < 0.01, ***p < 0.001. (B) Representative FACS dot plots for identifying the frequencies of neutrophils, T cells and B cells in the BM. (C-D) Quantitative analysis of neutrophils, T cells, B cells and LK cells per one femur in WT and *Pr3*$^{-/-}$ mice before and after sublethal irradiation (n=5-9 mice per genotype). *p < 0.05, **p < 0.01, ***p < 0.001.

Figure 9

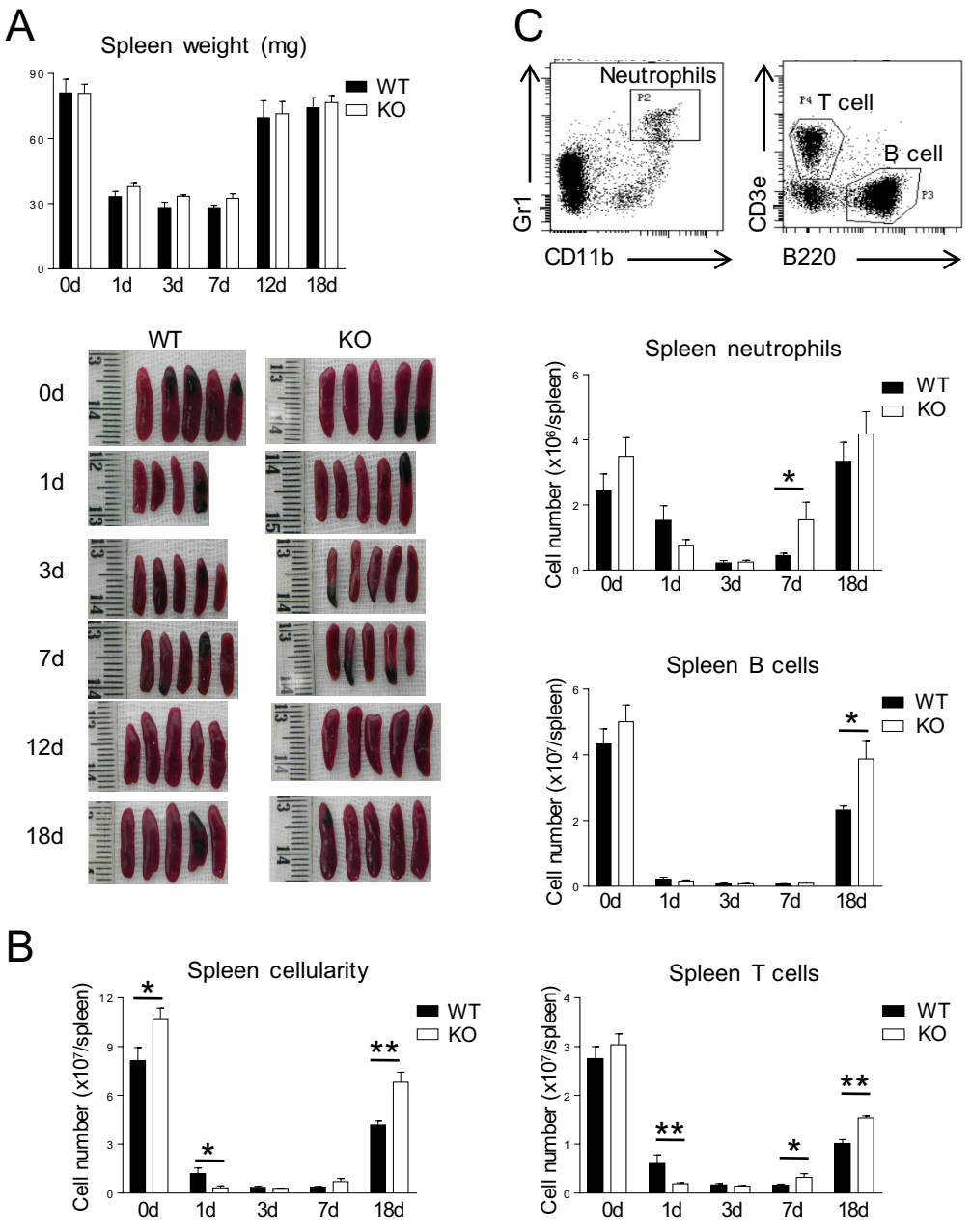

Figure 9. Spleen cellularity and mature splenocytes recover faster in *Pr3*$^{-/-}$ mice after sublethal irradiation.

(A) Spleen weights of WT and *Pr3*$^{-/-}$ mice before and after sublethal irradiation (n=5-9 mice per genotype). *p < 0.05, **p < 0.01, ***p < 0.001. (B-C) Quantitative analysis of total mononuclear cells, neutrophils, B cells, and T cells in the spleen before and after sublethal irradiation (n=5-9 mice per genotype). *p < 0.05, **p < 0.01, ***p < 0.001.

To assess if the quicker hematopoietic recovery in *Pr3*$^{-/-}$ mice translated into survival, WT and *Pr3*$^{-/-}$ mice were lethally irradiated (6 Gy) and survival rates were monitored for 30 days (Figure 10). WT mice started dying around day 10 and had a survival rate of about 10% on day 20 post-irradiation. In contrast, *Pr3*$^{-/-}$ mice had a survival rate of 50% on day 20 post-irradiation. Collectively, CFC assays, competitive BM reconstitution, and sublethal and lethal irradiation experiments all show that the enhanced early progenitor cell compartment in *Pr3*$^{-/-}$ BM is functional *in vitro* and *in vivo*.

2.3: Stem cells as the source for elevated hematopoiesis in the absence of Proteinase 3

To further delineate whether the enhanced hematopoiesis in *Pr3*$^{-/-}$ mice is an intrinsic feature of HSCs, we competitively transplanted LSK cells from WT or *Pr3*$^{-/-}$ mice carrying CD45.2 allele in with LSK cells from WT mice carrying CD45.1 allele into lethally irradiated WT congenic recipients carrying both CD45.1 and CD45.2 alleles. Total bone marrow cells from mice carrying both CD45.1 and CD45.2 alleles were also injected as supporting cells (Figure 11A).

BM and peripheral blood compartments were examined at 16 weeks post-transplant to assess the long-term reconstitution efficiency of stem cells. Peripheral blood cell counts were similar in mice injected with either WT or *Pr3*$^{-/-}$ LSK cells (Figure 11B). However, in mice injected with *Pr3*$^{-/-}$ donor LSK cells competing against WT donor LSK cells, we noted a dramatic increase in Pr3$^{-/-}$ donor-derived chimerism in LSK and LK cells in the BM (Figure 11C). There was also a higher frequency of *Pr3*$^{-/-}$ donor-derived myeloid and B cells in the BM (Figure 11D). Similar to BM cells, the *Pr3*$^{-/-}$ LSK

Figure 10

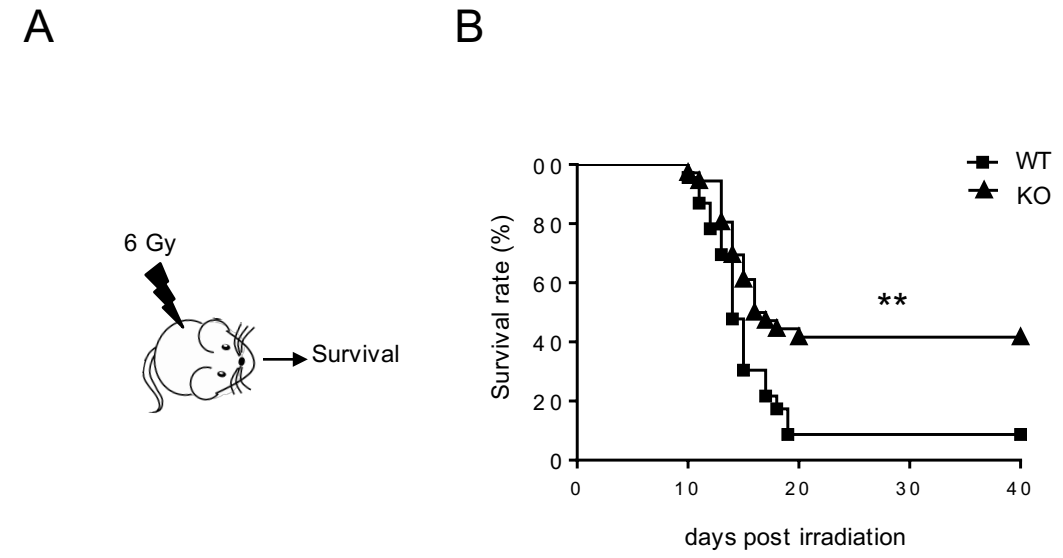

Figure 10. *Pr3*$^{-/-}$ mice exhibit increased survival after hematopoietic injury. (A) Scheme of the experimental setup for survival analysis after irradiation. (B) Analysis of the survival curves of WT and *Pr3*$^{-/-}$ mice receiving 6 Gy irradiation (n=23 for WT and n=36 for *Pr3*$^{-/-}$). **p < 0.01.

Figure 11. Elevated hematopoiesis caused by *Pr3* deficiency is an intrinsic feature of LSK cells.
(A) Scheme of the experimental setup used to compare WT and *Pr3*$^{-/-}$ LSK cells by competitive transplantation. (B) Peripheral blood cell counts (n=4). (C) Representative FACS plots showing WT and *Pr3*$^{-/-}$ donor-derived LSK and LK cells in recipient mice are shown in the top panels. Numbers denote the frequency of specific cell populations among the parent gate. The frequency of WT and *Pr3*$^{-/-}$ donor-derived LSK and LK cells among total BM cells is shown in the middle panels. The percentage of LSK and LK cells from individual donors is shown in the bottom panels (n=4). $^{**}p < 0.01$. (D-E) Quantitative analysis of the origin of cells in recipient mice at 16 weeks post-transplantation in the BM and peripheral blood (n=4-7 mice). $^{*}p < 0.05$, $^{**}p < 0.01$, $^{***}p < 0.001$.

Figure 11 continued

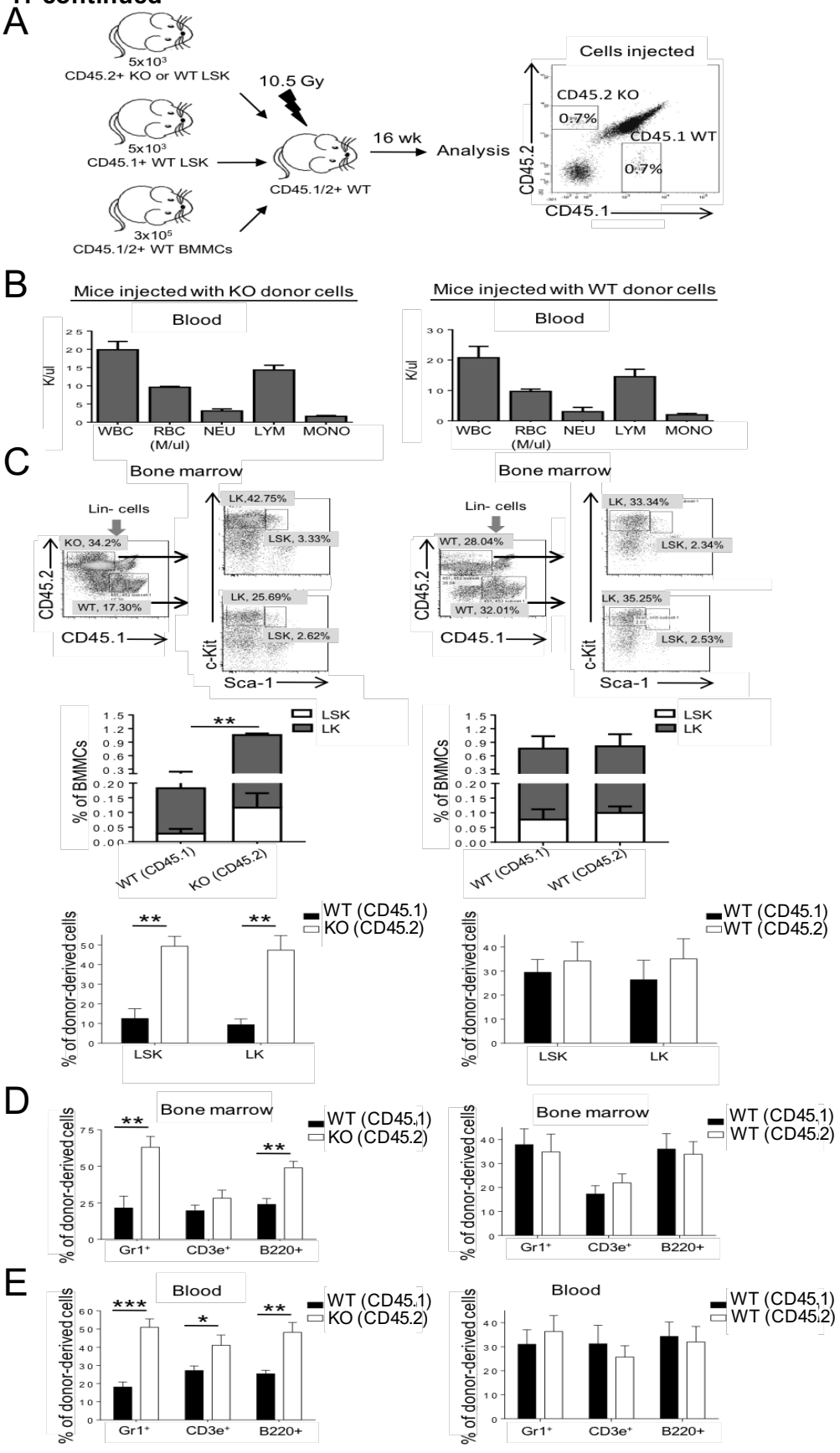

cell chimerism outcompeted that of WT LSK cells in different lineages in peripheral blood (Figure 11E). Control mice reconstituted with competing congenic WT (CD45.2) and WT (CD45.1) LSK cells did not show any difference in chimerism pattern between the two congenic groups (Figure 11C-E). In this setup, reconstitution efficiency of WT and *Pr3*$^{-/}$- LSK cells was assessed in the same BM environment. Thus, the higher reconstitution efficiency observed in *Pr3*$^{-/-}$ LSK recipients suggests that the augmented hematopoiesis induced by PR3 disruption is an intrinsic feature of PR3-deficient HSCs.

2.4: The mechanism for dysregulated hematopoietic stem cell compartment in Proteinase 3-deficient mice

The enhanced stem and progenitor cell compartments in *Pr3*$^{-/-}$ mice prompted us to investigate the underlying mechanism. We first explored progenitor cell proliferation using a bromodeoxyuridine (BrdU) incorporation assay and DNA staining with 7-AAD to analyze the frequency of LSK cells at different stages of the cell cycle in WT and *Pr3*$^{-/-}$ mice. BrdU is a thymidine analog and incorporated into newly synthesized DNA during the S phase of cell cycle. It can be detected by fluorophore-conjugated anti-BrdU antibodies after the permeabilization of cells. At the end of the S phase, DNA levels reach 2-fold the original DNA level. Staining with 7-AAD, a fluorescent intercalator that undergoes a spectral shift when it forms a complex with DNA, permits the identification of cells that have completed S phase and are in G2/M phases of the cell cycle. The percentage of cells at different cell cycle phases (S/G2/M) was similar in WT and *Pr3*$^{-/-}$ mice at 24 or 72 h post-BrdU injection (Figure 12A-C). Although *Pr3*$^{-/-}$ mice had a higher

Figure 12

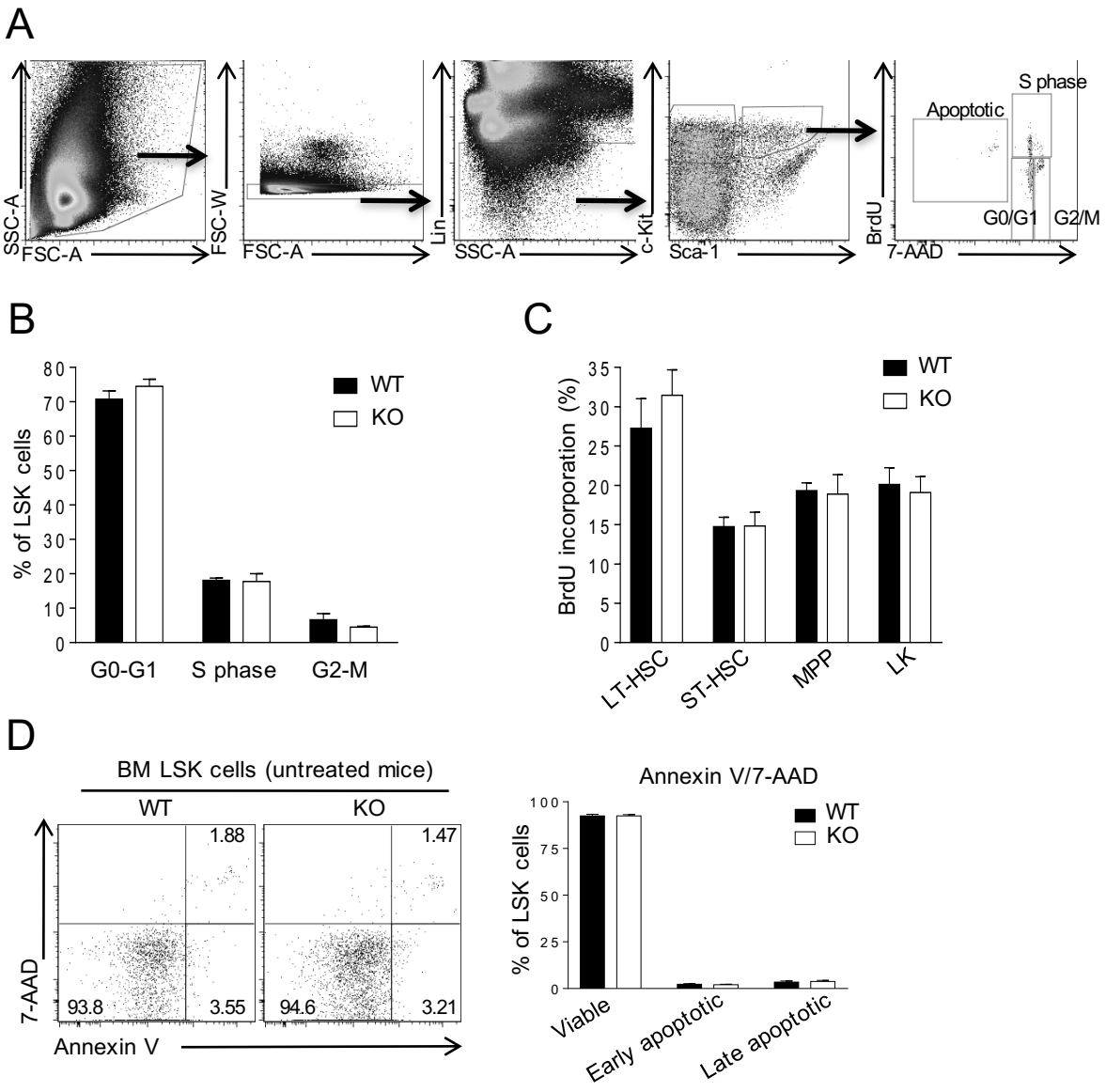

Figure 12. Pr3 deficiency does not affect proliferation or viability of LSK cells in untreated mice.

(A) Gating strategy to analyze the cell cycle status of BM LSK cells by BrdU incorporation. (B) Cell cycle analysis of LSK cells (n=4 from two independent experiments). (C) The rate of BrdU incorporation in LSK subsets (n=4 from two independent experiments). (D) Analysis of the frequency of viable (Annexin V^- 7-AAD^-), early apoptotic (Annexin V^+ 7-AAD^-), and late apoptotic (Annexin V^+ 7-AAD^+) LSK cells in untreated WT and *Pr3*$^{-/-}$ mice (n=12-15 from four independent experiments).

number of $BrdU^+$ cells in the BM (data not shown), this is due to the increased number of HSPCs. The proportions of $BrdU^+$ cells in the LSK subsets were also similar in the BM of WT and *Pr3*$^{-/-}$ mice. These data exclude the possibility that altered proliferation is responsible for the enhanced stem cell population seen in *Pr3*$^{-/-}$ mice.

We recently reported that PR3 can regulate neutrophil spontaneous death by cleaving and activating pro-caspase 3 (Loison et al., 2014). We therefore wondered whether PR3 regulated HSC and HPC numbers by modulating their survival. To test this possibility, we first assessed spontaneous stem cell death using annexin V/7-AAD staining with freshly isolated BM cells from WT and *Pr3*$^{-/-}$ mice. Annexin V binds to phosphatidlyserine, which is normally located on the cytoplasmic surface on the cell membrane but exposed to the outer leaflet of the cell membrane in dying cells. As previously mentioned, 7-AAD can be used to detect DNA levels but cannot pass through the cell membrane unless cells have lost their membrane integrity. Of note, loss of membrane integrity happens in the later stages of cell death compared to phosphatidlyserine exposure. Hence, cells in a specific population can be differentiated into three groups according to their viability as viable (Annexin V^- 7-AAD^-), early apoptotic (Annexin V^+ 7-AAD^-) and late apoptotic (Annexin V^+ 7-AAD^+). The frequencies of viable, early apoptotic, and late apoptotic cells in the stem and progenitor cell-containing populations were comparable between WT and *Pr3*$^{-/-}$ bone marrow (Figure 12D).

We also cultured freshly isolated total BM cells and measured apoptosis rates and caspase 3 activation in LSK cells at various time points. Since caspase 3 activation is one of the earliest events in apoptosis, we used caspase 3 activity as a viability

readout. The proportions of apoptotic and caspase 3^+ LSK cells in the total LSK cell populations were similar after culture (Figure 13A-B).

In another set of experiments, sorted LSK cells from WT or *Pr3*$^{-/-}$ mice were cultured in a stem cell maintenance medium containing various recombinant cytokines as previously described in (Janzen et al., 2008). LSK cells undergo rapid cell death in the absence of these cytokines (data not shown). Annexin V/7-AAD staining was performed on day 6 to detect early apoptotic events and terminal deoxynucleotidyl transferase dUTP nick end labeling (TUNEL) was used to detect late stages of apoptosis on day 7. TUNEL assay relies on the presence of exposed 3' hydroxyl ends due to DNA fragmentation. dUTP nucleotide can be incorporated into these exposed 3' hydroxyl ends by the enzymatic activity of terminal dexoynucleotidyl transferase. Regardless of the assay used, there were no observable differences in apoptotic cell frequency in *Pr3*$^{-/-}$ and WT LSK cultures (Figure 13C-D). We also compared the frequency of apoptotic cells derived from colonies on methylcellulose medium in CFC assays; again, no differences were observed (Figure 13E). Of note, cells were cultured for more than 6 days. Also, these culture conditions contained cytokines such as SCF that can promote the expansion of stem and progenitor cells and IL-3, which can support myeloid differentiation. Hence, the expansion of HSPCs and differentiation into mature cell might be a confounding factor in these experiments. Indeed, we noticed expansion and differentiation of HSPCs into more mature cells in these assays (data not shown).

Figure 13. Culture of total bone marrow cells, sorted LSK cells and CFC assays reveal similar levels of viability between WT and *Pr3*$^{-/-}$ HSPCs.
(A) Quantification of LSK cell viability at the indicated time points in cultured total BM cells (n=4). (B) Analysis of caspase 3 activation in LSK cells at the indicated time points in cultured total BM cells. Results are representative of three independent experiments. (C) Analysis of LSK cell viability at the indicated time points in sorted LSK cell culture (n=3 from three independent experiments). (D) Analysis of late apoptotic events using TUNEL at the indicated time points in sorted LSK cells (n=3 from three independent experiments). (E) Representative FACS plots demonstrating the viability of cells obtained from colony-forming assays and the corresponding quantitative analysis (n=3 from three independent experiments).

Figure 13 continued

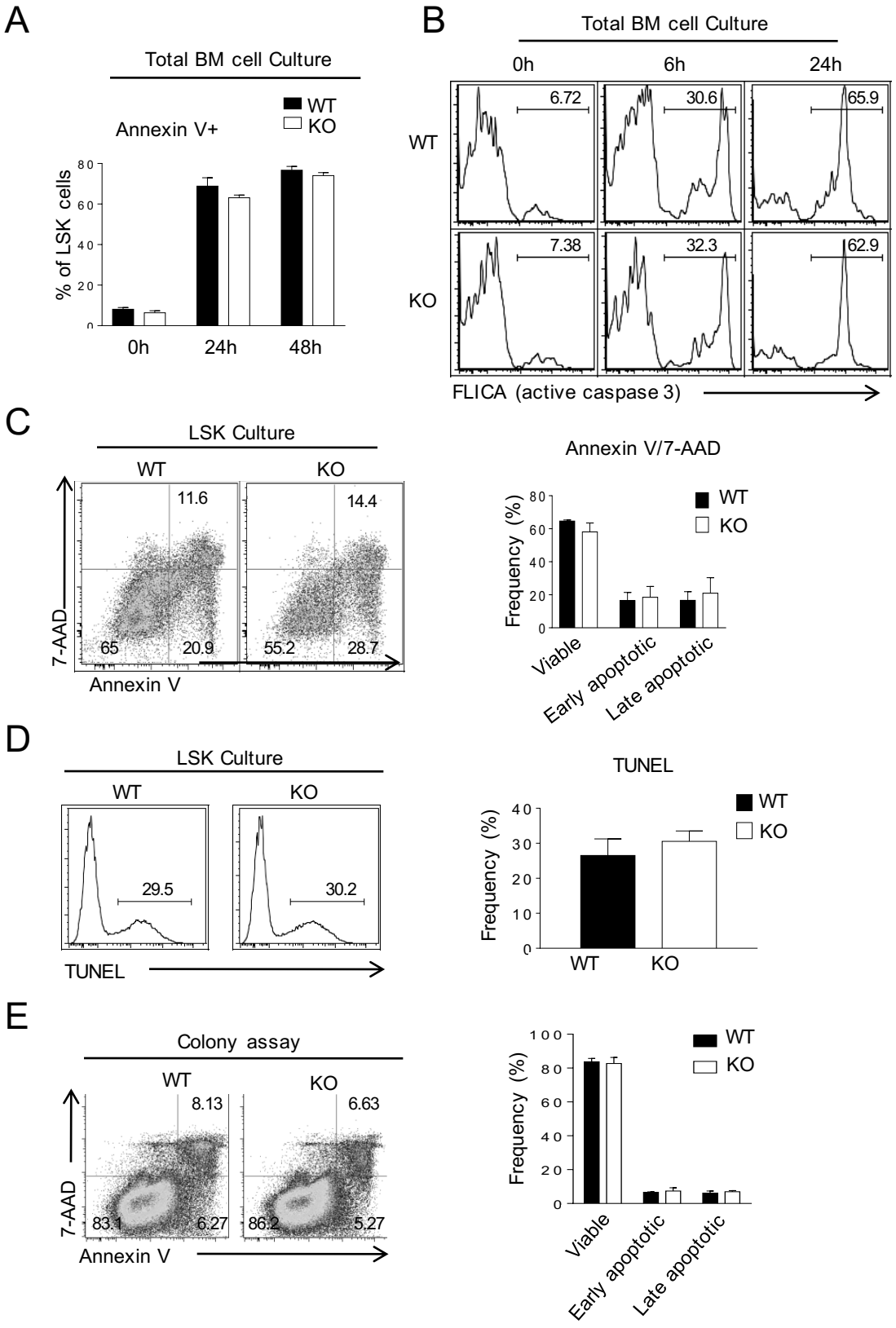

Since macrophages rapidly clear apoptotic cells, we decided to deplete BM macrophages using clodronate liposomes and then examine LSK cell viability (Giuliani et al., 2001). BM macrophages remain markedly depleted for up to 2 weeks following clodronate liposome injection (Chow et al., 2011). At 9 days after injection, clodronate liposomes depleted 80% of $Gr1^{-}CD115^{-}F4/80^{+}$ $SSC\text{-}A^{normal}$ BM macrophages in both WT and *Pr3*$^{-/-}$ mice, with no difference in the proportion of BM macrophages observed between clodronate or PBS liposome-treated WT and *Pr3*$^{-/-}$ mice (Figure 14A-B). On day 9 post-clodronate liposome injection, the frequency of viable LSK cells (Annexin V^{-} $7\text{-}ADD^{-}$) increased and the frequency of late apoptotic LSK cells (Annexin $V^{+}7\text{-}ADD^{+}$) decreased in *Pr3*$^{-/-}$ compared to WT BM (Figure 14C). Of note, both WT and *Pr3*$^{-/-}$ BM contained very few early apoptotic LSK cells (Annexin $V^{-}7\text{-}ADD^{-}$), suggesting that early apoptotic LSK cells might be quickly converted to Annexin $V^{+}7\text{-}ADD^{+}$ cells in the BM.

PR3 regulates neutrophil spontaneous death by cleaving and activating pro-caspase 3 (Loison et al., 2014). We tested if this mechanism also explained the reduced spontaneous death of LSK cells in *Pr3*$^{-/-}$ mice after depletion of macrophages. Using a fluorescent probe, we stained for active caspase 3 in LSK cells following macrophage depletion in the BM. Indeed, *Pr3*$^{-/-}$ LSK cells exhibited significantly less active caspase 3, suggesting that the delayed spontaneous death may well be due to a defect in pro-caspase 3 cleavage by PR3 (Figure 14D). Finally, performing a luminescence-based caspase 3 activity assay after a short-term culture of sorted LSK cells as previously described (Flach et al., 2014) revealed a 40% and 50% reduction in caspase 3 activity in *Pr3*$^{-/-}$ LSK cells at 12 hours and 36 hours post-culture, respectively (Figure 14E).

Figure 14. *Pr3* deletion leads to enhanced viability and reduced caspase 3 activity of LSK cells after macrophage depletion as well as short term culture of LSK cells.

(A) Gating strategy to identify macrophage frequency in BM after treatment with PBS or clodronate liposomes. Numbers denote the frequency of specific cell subsets among live singlets. (B) Quantification of BM macrophage frequency in WT and *Pr3*$^{-/-}$ mice after PBS and clodronate liposome injection (n=13-18 mice from four independent experiments). (C) Analysis of the frequency of viable (Annexin V^{-} 7-AAD^{-}), early apoptotic (Annexin V^{+} 7-AAD^{-}), and late apoptotic (Annexin V^{+} 7-AAD^{+}) LSK cells in WT and *Pr3*$^{-/-}$ mice after BM macrophage depletion. Numbers denote the frequency of cells among LSK cells (upper panel). Quantification of LSK viability is shown in the bottom panel (n=12-13 from three independent experiments). *$p < 0.05$. (D) Analysis of caspase 3 activation in LSK cells using a cell-permeable, fluorescent caspase 3 substrate (upper panel). Numbers denote the frequency of LSK cells with active caspase 3. Quantitative analysis of the frequency of LSK cells with active caspase 3 is shown in the bottom panel (n=5). *$p < 0.05$. (E) Analysis of caspase 3 activity in sorted LSK cells using a luminescence-based assay at 12 or 36 hours post-culture (n=11 for 12h culture from 5 independent experiments and n=7 for 36h culture from 3 independent experiments). Data were normalized to the average luminescence value of WT cells for each independent experiment.

Figure 14 continued

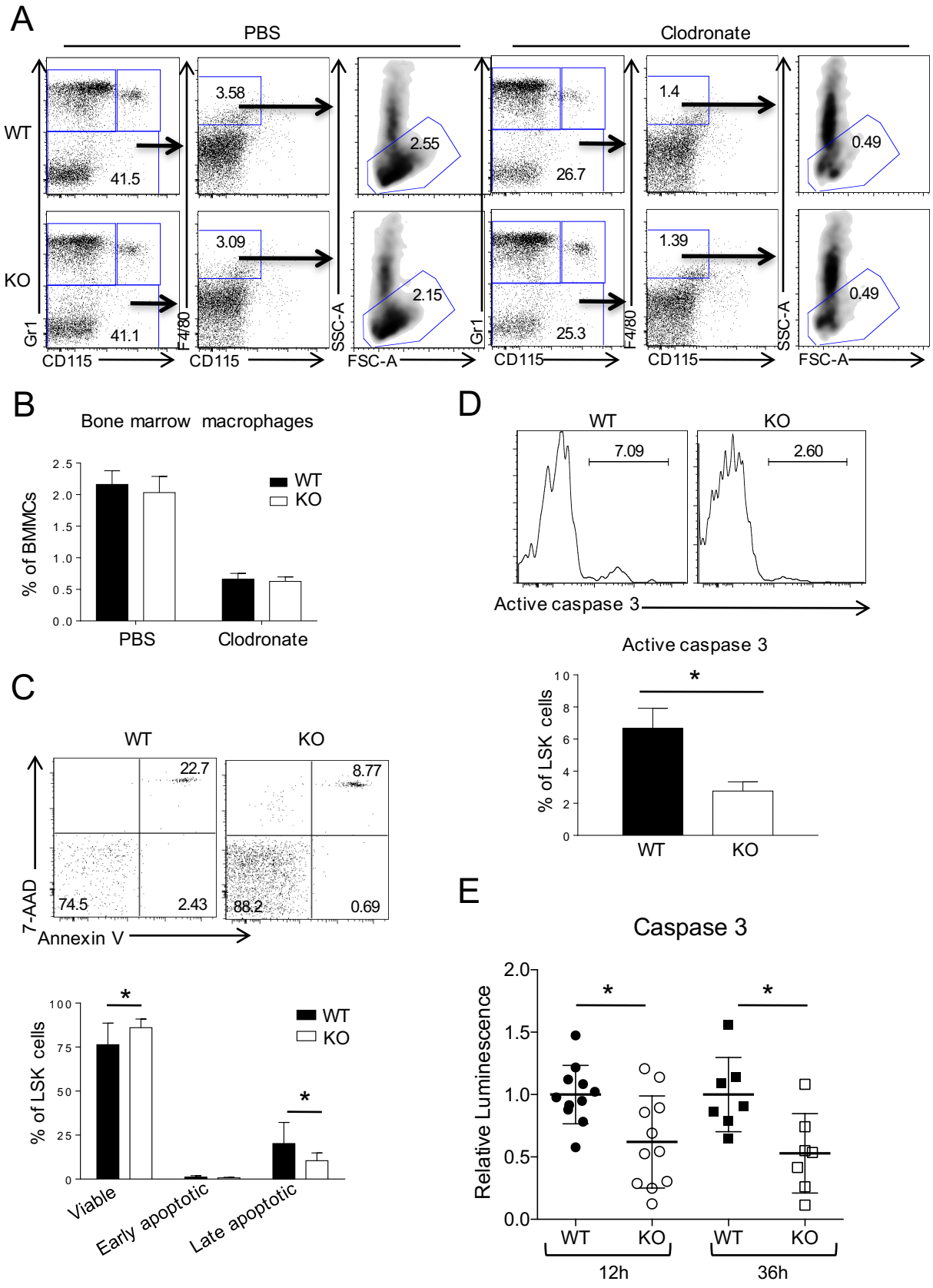

The apoptosis and caspase 3 activation rates were similar between WT and *Pr3*$^{-/-}$ mice when mice were treated with PBS liposomes, confirming that the difference was macrophage-dependent (Figure 15A-B). Collectively, these data demonstrate that *Pr3*$^{-/-}$ LSK cells exhibit a reduced rate of apoptosis that is best observed after depletion of BM macrophages *in vivo* and reduced caspase 3 activation under these conditions as well as in short term culture culture conditions *ex vivo*.

2.5: Investigation of features associated with aged HSCs

HSC ageing is tightly regulated to ensure that stem cells that have exhausted their proliferative potential or accumulated dangerous mutations undergo apoptosis. The reduced rate of apoptosis in *Pr3*$^{-/-}$ LSK cells encouraged us to investigate if *Pr3*$^{-/-}$ HSCs undergo aberrant ageing. Aged HSCs exhibit markers associated with DNA damage (Rossi et al., 2007a), reduced cell polarity (Florian et al., 2012), and increased senescence (Chang et al., 2016; Flach et al., 2014). Thus, we explored these features in *Pr3*$^{-/-}$ HSCs.

Sorted Lin^{-} Sca-1^{+} c-Kit^{+} CD135^{-} CD48^{-} CD150^{+} HSCs from 12-16 week-old *Pr3*$^{-/-}$ mice contained more DNA damage-associated γH2AX foci than their WT counterparts as assayed by immunofluorescence microscopy (Figure 16A). Quantification showed that the *Pr3*$^{-/-}$ HSC population contained fewer cells with no γH2AX foci and more cells with two or more γH2AX foci (Figure 16B). DNA damage in HSCs from 22-26 month-old WT and *Pr3*$^{-/-}$ mice was comparable, both showing higher levels than their young counterparts (Figure 17A-B).

Figure 15

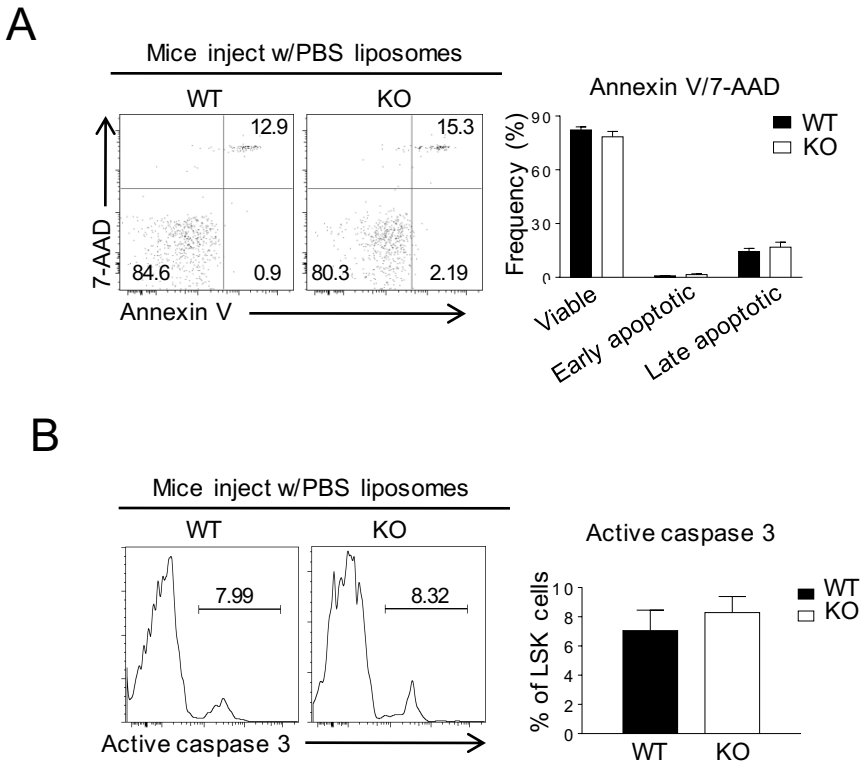

Figure 15. LSK cells from WT and *Pr3*$^{-/-}$ mice treated with PBS liposomes exhibit similar viability profiles and caspase 3 activation.
(A) Analysis of the frequency of viable (Annexin V^{-} 7-AAD^{-}), early apoptotic (Annexin V^{+} 7-AAD^{-}), and late apoptotic (Annexin V^{+} 7-AAD^{+}) BM LSK cells in WT and *Pr3*$^{-/-}$ mice after injection of PBS liposomes. Numbers denote the frequency of cells among LSK cells (left panel). Quantification of LSK viability is shown in the right panel (n=5). (B) Representative FACS plots showing the frequency of BM LSK cells with active caspase 3 after treatment with PBS liposomes (left panel). Quantitative analysis of the frequency of LSK cells with active caspase 3 is shown in the right panel (n=5).

Figure 16

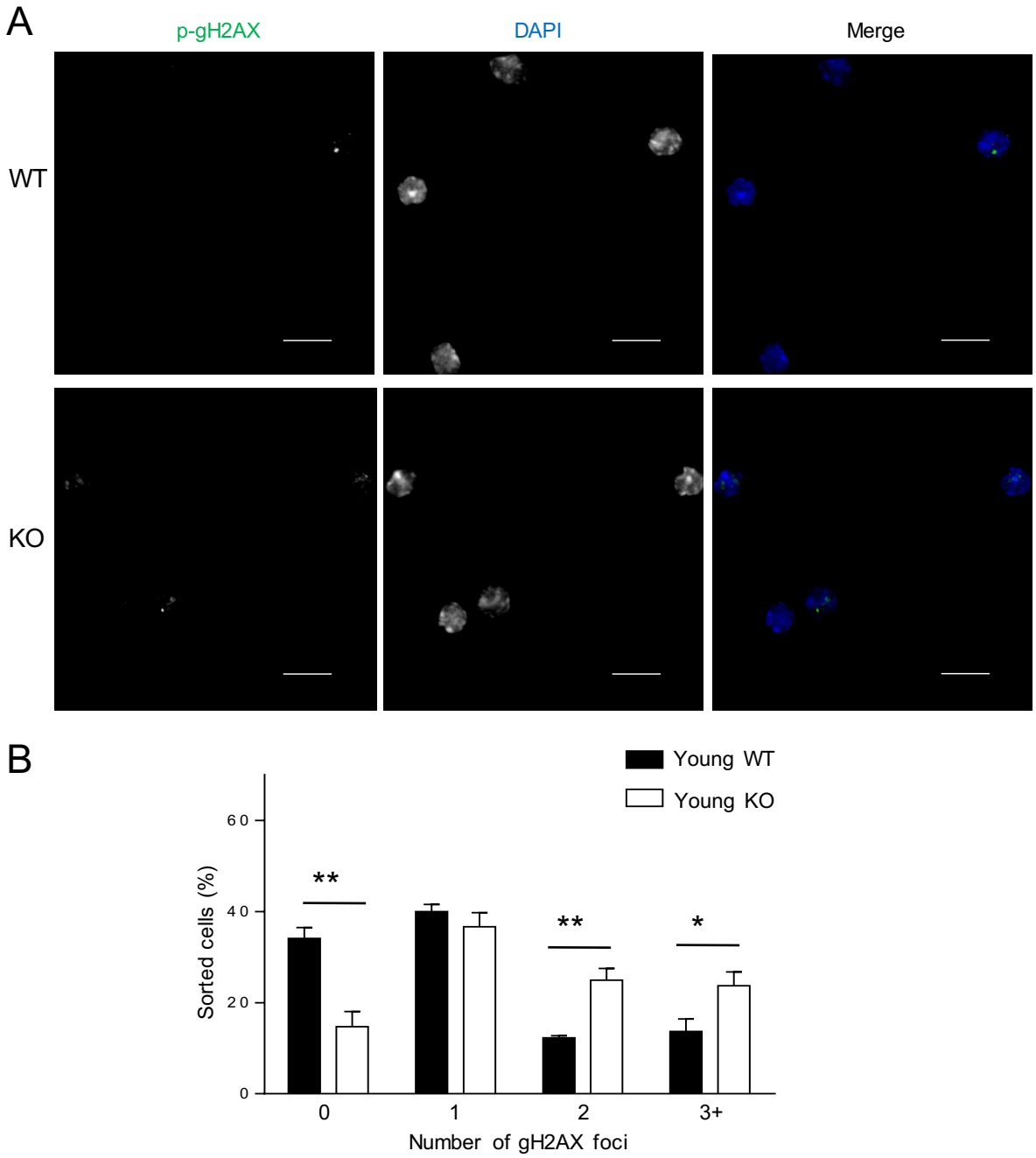

Figure 16. *Pr3*$^{-/-}$ HSCs from young mice display higher levels of γ-H2AX foci, a marker of DNA damage.
(A) Representative γ-H2AX images in young WT and *Pr3*$^{-/-}$ HSCs as determined by immunofluorescence (IF) microscopy. (B) Quantification of γ-H2AX foci in young WT and *Pr3*$^{-/-}$ HSCs (n=5 from five independent experiments). Scale bar = 10 μm. *$p < 0.05$, **$p < 0.01$.

Figure 17

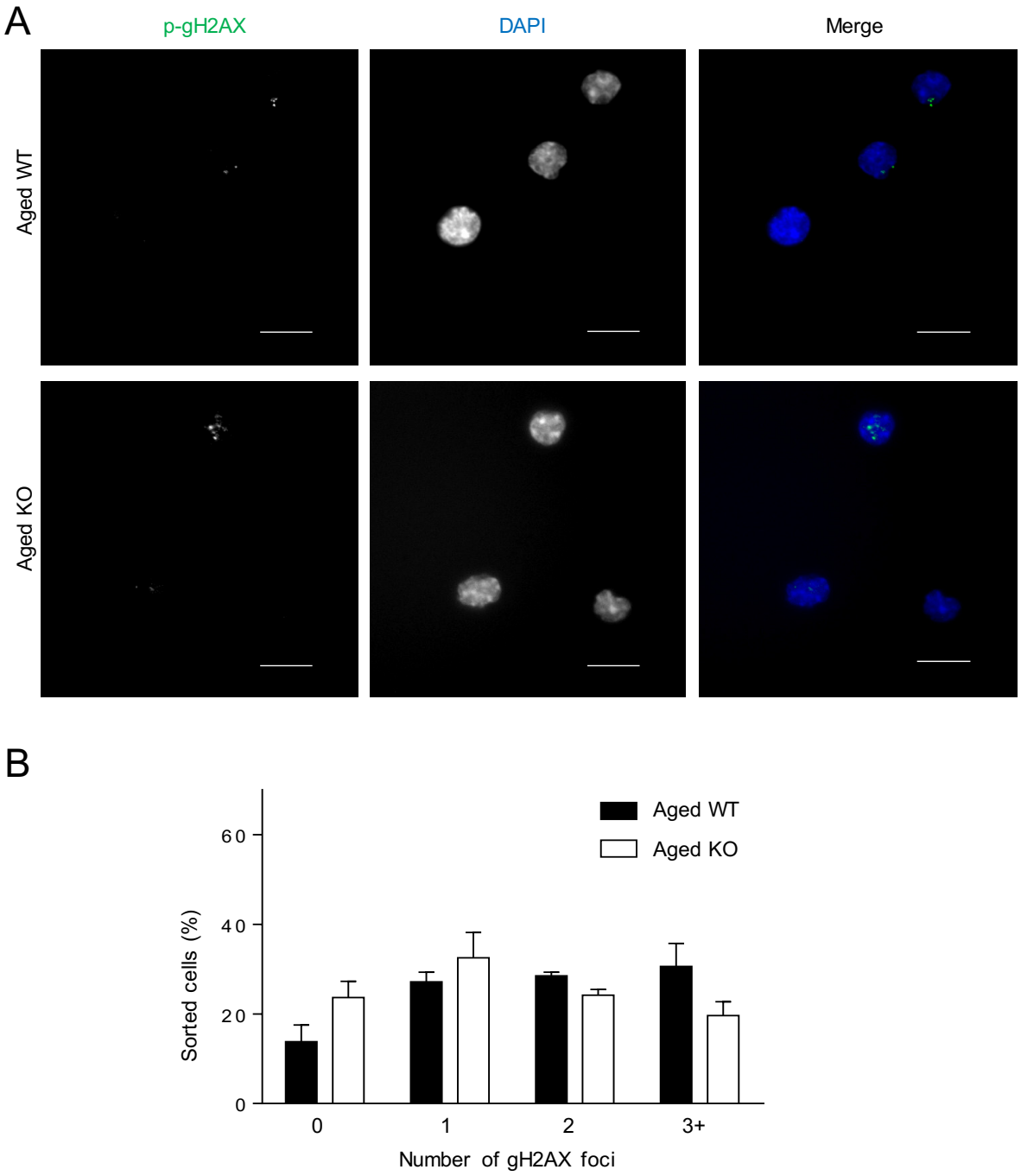

Figure 17. Aged WT and *Pr3*$^{-/-}$ HSCs exhibit similar levels of γ-H2AX foci. (A) Representative γ-H2AX images in aged WT and *Pr3*$^{-/-}$ HSCs as determined by immunofluorescence (IF) microscopy. (B) Quantification of γ-H2AX foci in young WT and *Pr3*$^{-/-}$ HSCs (n=3 from three independent experiments). Scale bar = 10 μm.

The majority of Lin^- $Sca\text{-}1^+$ $c\text{-}Kit^+$ $CD34^-$ $CD135^-$ LT-HSCs from young WT mice showed a polarized α-tubulin and Cdc42 distribution, but both markers were evenly distributed throughout the cell body at a higher frequency in *Pr3*$^{-/-}$ LT-HSCs, similar to aged LT-HSCs (Figure 18A-B). We did not observe a difference in the frequency of polarized LT-HSCs from old WT and old *Pr3*$^{-/-}$ mice, both showing highly diminished polarized distribution of these proteins compared to young WT and *Pr3*$^{-/-}$ LT-HSCs (Figure 19A-B).

We also assessed senescence using a substrate of senescence-associated β-galactosidase (SA-β-gal), C12FDG. C12FDG is cell-permeable but does not fluorescence until it is hydrolyzed by the enzyme, which is highly active in senescent cells (Dimri et al., 1995). Intriguingly, LSK cells from aged *Pr3*$^{-/-}$ mice showed higher SA-β-gal activity as assayed by conventional flow cytometry compared to aged WT mice (Figure 20A). In contrast, LSK cells from young WT and *Pr3*$^{-/-}$ mice showed similar SA-β-gal activity, suggesting that senescence-associated alterations in β-galactosidase activity might be a relatively late event compared to DNA damage and cell depolarization (Figure 20B). Taken together, these results indicate that the ageing phenotype is promoted in HSCs from *Pr3*$^{-/-}$ mice.

2.6: Competitive transplantation experiments using aged donor mice

PR3 appears to play a role in HSC aging. Aged HSCs have defects in their repopulation ability and are skewed toward myeloid differentiation with diminished lymphoid potential (Rossi et al., 2005). Accordingly, total BM cells from aged mice were skewed toward myeloid differentiation compared to young mice (Figure 21A-D). The

Figure 18

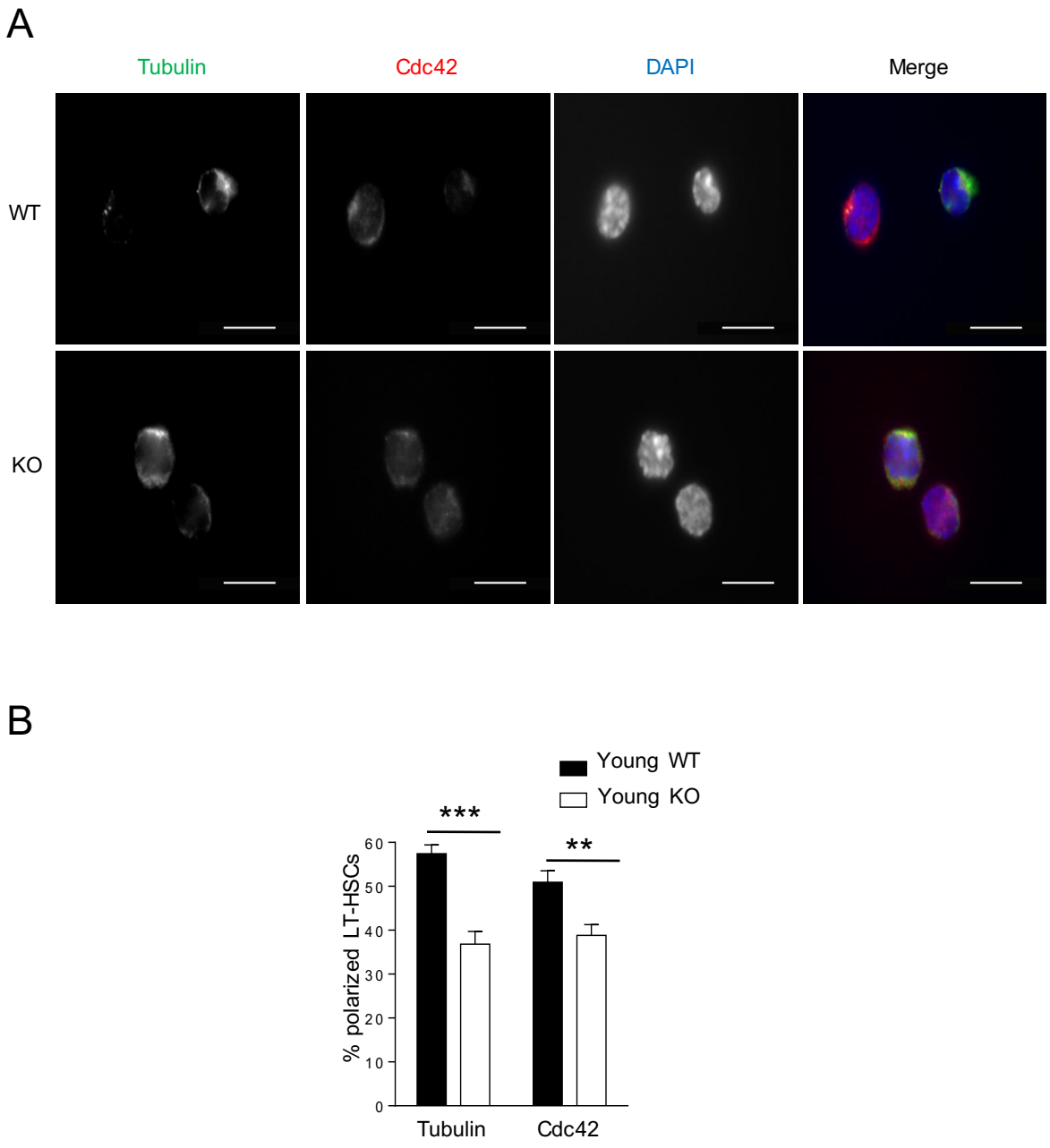

Figure 18. *Pr3*$^{-/-}$ HSCs from young mice display reduced cell polarity. (A) Representative localization of tubulin and Cdc42 in young WT and *Pr3*$^{-/-}$ HSCs as determined by IF microscopy. (B) The percentage of HSCs with a polarized distribution in young WT and *Pr3*$^{-/-}$ HSCs (n=7-8 from eight independent experiments). Scale bar = 10 μm. **p < 0.01, ***p < 0.001.

Figure 19

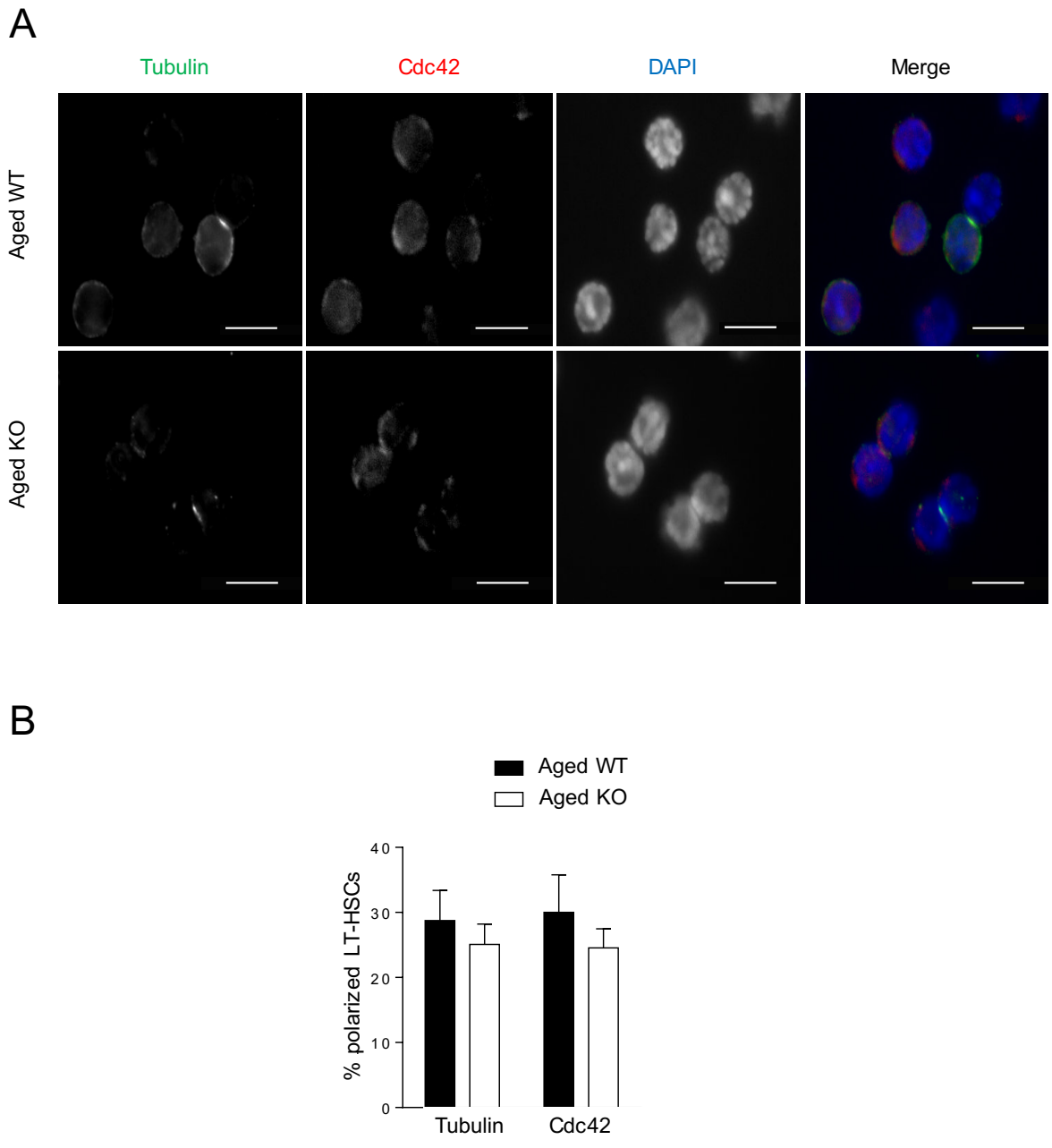

Figure 19. Frequencies of aged WT and *Pr3*$^{-/-}$ HSCs with polarized distribution of tubulin and Cdc42 are similar.
(A) Representative localization of tubulin and Cdc42 in aged WT and *Pr3*$^{-/-}$ HSCs as determined by IF microscopy. (B) The percentage of HSCs with a polarized distribution in aged WT and *Pr3*$^{-/-}$ HSCs (n=3 from three independent experiments). Scale bar = 10 μm.

Figure 20

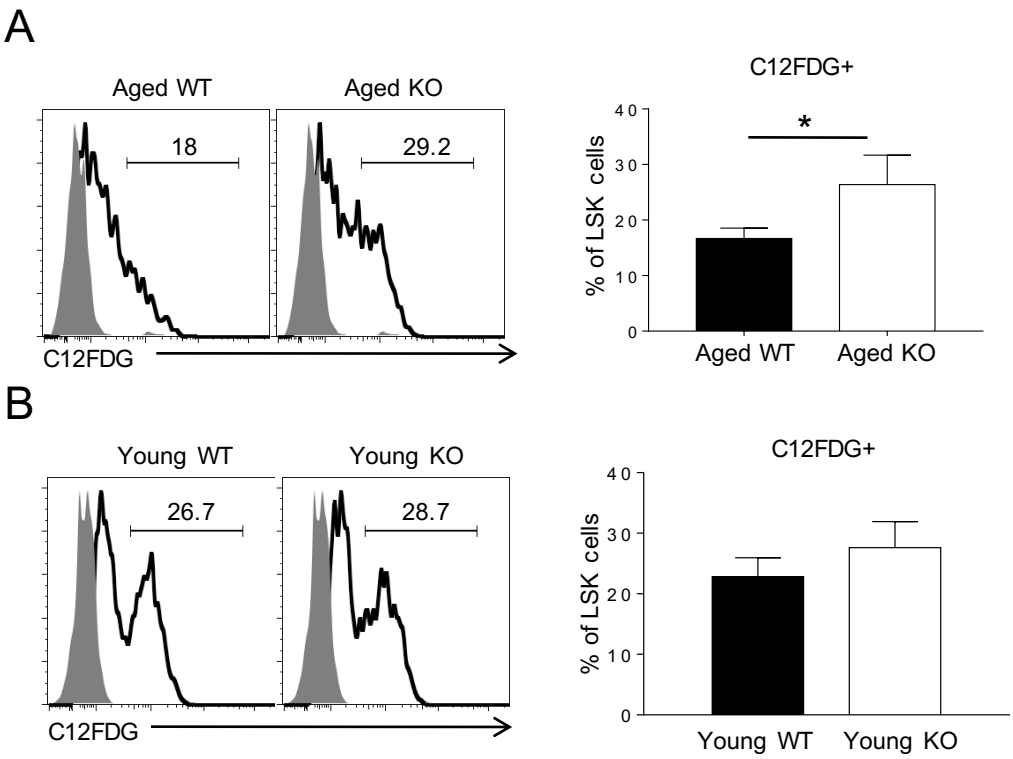

Figure 20. *Pr3*$^{-/-}$ HSCs from aged mice exhibit higher SA-β-gal activity. (A) Representative histograms of SA-β-gal activity in gated LSK cells (left panel) and quantification of the percentage of SA-β-gal^{+} LSK cells (right panel) from aged WT and *Pr3*$^{-/-}$ mice. Numbers denote the frequency of SA-β-gal^{+} LSK cells (n=4 from four independent experiments). *$p < 0.05$. (B) Representative histograms of SA-β-gal activity in gated LSK cells (left panel) and quantification of the percentage of SA-β-gal^{+} LSK cells (right panel) from young WT and *Pr3*$^{-/-}$ mice. Numbers denote the frequency of SA-β-gal^{+} LSK cells (n=8 from three independent experiments).

Figure 21. Aged total bone marrow cells are skewed toward myeloid lineage.

(A) Scheme of the experimental setup to compare 12-14-month-old and young total BM cells using competitive transplantation. (B) Gating strategy to analyze lineage bias (myeloid vs. lymphoid) of aged and young donor-derived cells. (C) Quantification of the lineage potential of aged and young total BM cells (n=8). **p < 0.01. (D) Quantification of the myeloid to lymphoid ratio of donor-derived cells in recipient mice at 20 weeks post-transplantation. For each donor-derived population, the frequency of $Gr1^+$ cells among cells in the indicated population is divided by the sum of the frequencies of $CD3e^+$ and $B220^+$ cells (n=8). **p < 0.01.

Figure 21 continued

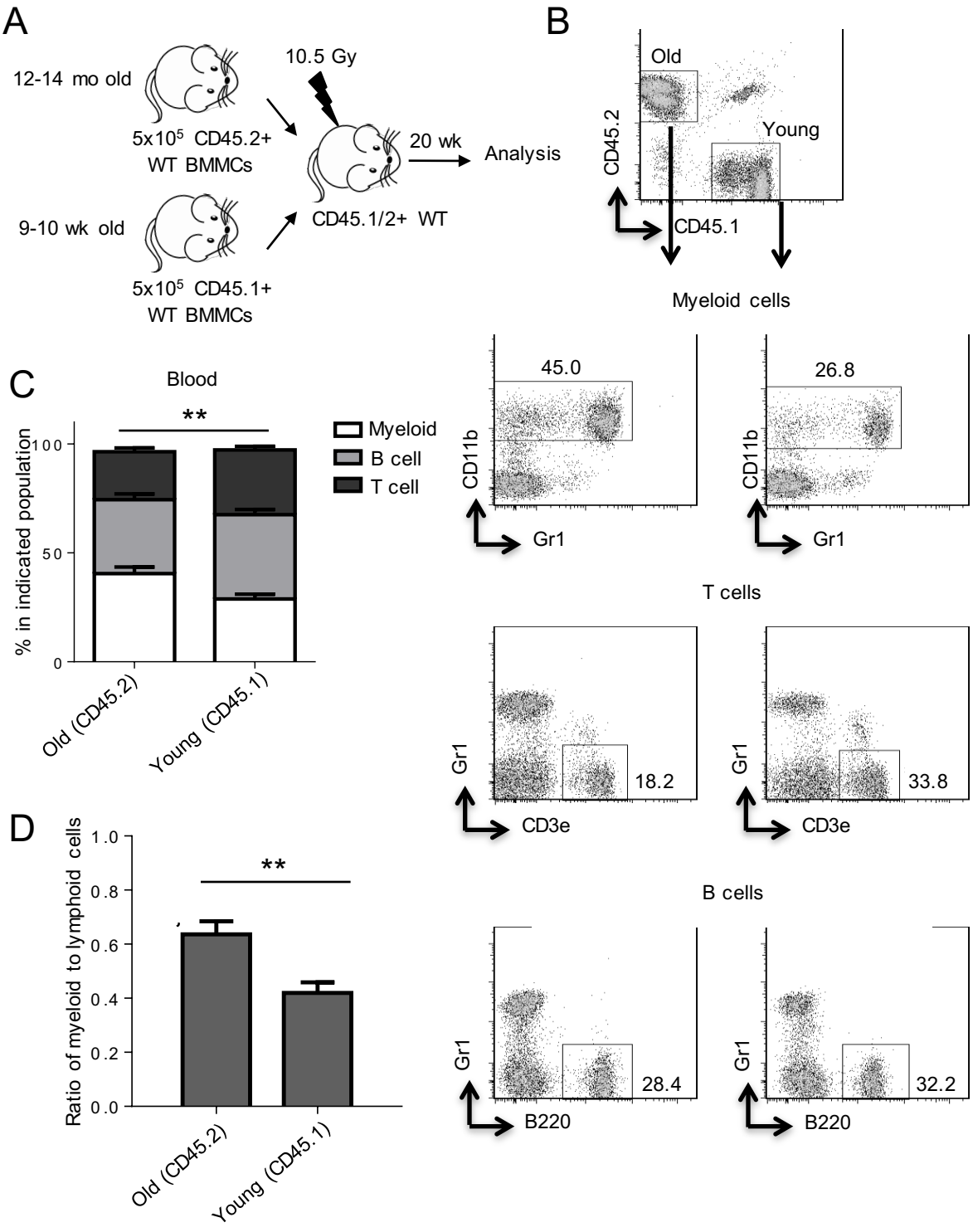

ratio of myeloid to lymphoid cells was determined as follows. The frequency of $Gr1^+$ cells among cells in the indicated population was divided by the sum of the frequencies of $CD3e^+$ and $B220^+$ cells to determine the myeloid to lymphoid ratio.

We next investigated whether PR3 disruption altered the repopulation ability of aged HSCs and myeloid skewing. We first set up a competitive BM reconstitution experiment using WT and *Pr3*$^{-/-}$ total BM cells isolated from 14-month-old mice (Figure 22A) and assessed chimerism in the peripheral blood (Figure 22B). At 28 weeks post-reconstitution, the myeloid to lymphoid ratio was significantly higher in the *Pr3*$^{-/-}$ donor-derived cell population compared to WT counterparts (Figure 22C-D). While chimerism of *Pr3*$^{-/-}$ donor-derived cells outcompeted that of WT donor-derived cells at early time points, WT donor-derived cells became more dominant after 20 weeks post-reconstitution, demonstrating that the long-term repopulation ability of PR3 deficient HSCs was defective (Figure 22E). The augmented reconstitution of the *Pr3*$^{-/-}$ population at early time points was likely due to augmented expansion of HSPCs and the enhanced myeloid reconstitution capacity of *Pr3*$^{-/-}$ BM cells. There were no differences in chimerism patterns in control mice reconstituted with competing congenic WT (CD45.2) and WT (CD45.1) cells (Figure 22B-F).

Next, we transplanted total BM cells from 2-year-old WT or *Pr3*$^{-/-}$ mice into lethally irradiated congenic recipients in a competitive setting with young total BM cells (Figure 23A). At 24 weeks post-reconstitution, mice reconstituted with aged *Pr3*$^{-/-}$ donor cells had a higher percentage of neutrophils and eosinophils and a reduced percentage of lymphocytes in the peripheral blood (Figure 23B). As expected, in mice reconstituted with aged and young WT donor cells, aged WT cells gave rise to a higher frequency of

Figure 22. *Pr3*$^{-/-}$ total bone marrow cells from middle-aged mice exhibit more pronounced myeloid skewing and reduced repopulation ability compared to WT total bone marrow cells.
(A) Scheme of the experimental setup to compare 14-month-old WT and *Pr3*$^{-/-}$ total BM cells using competitive transplantation. (B) Gating strategy to analyze lineage bias (myeloid vs. lymphoid) of donor-derived cells. (C) Quantification of the lineage potential of 14-month-old WT and *Pr3*$^{-/-}$ total BM cells (n=4-5 mice). *$p < 0.05$. (D) Quantification of the myeloid to lymphoid ratio of donor-derived cells in the recipient mice at 28 weeks post-transplantation. For each donor-derived population, the frequency of $Gr1^+$ cells among cells in the indicated population is divided by the sum of the frequencies of $CD3e^+$ and $B220^+$ cells (n=4-5 mice). *$p < 0.05$. (E-F) Quantitative analysis of the origin of total $CD45^+$ cells in the recipient mice at 4, 8, 20, and 28 weeks post-transplantation in the peripheral blood (n=4-5 mice). The ratio of CD45.2 donor-derived total cells to CD45.1 donor-derived total cells at the indicated time points is given in the bottom panel. **$p < 0.01$, ***$p < 0.001$.

Figure 22 continued

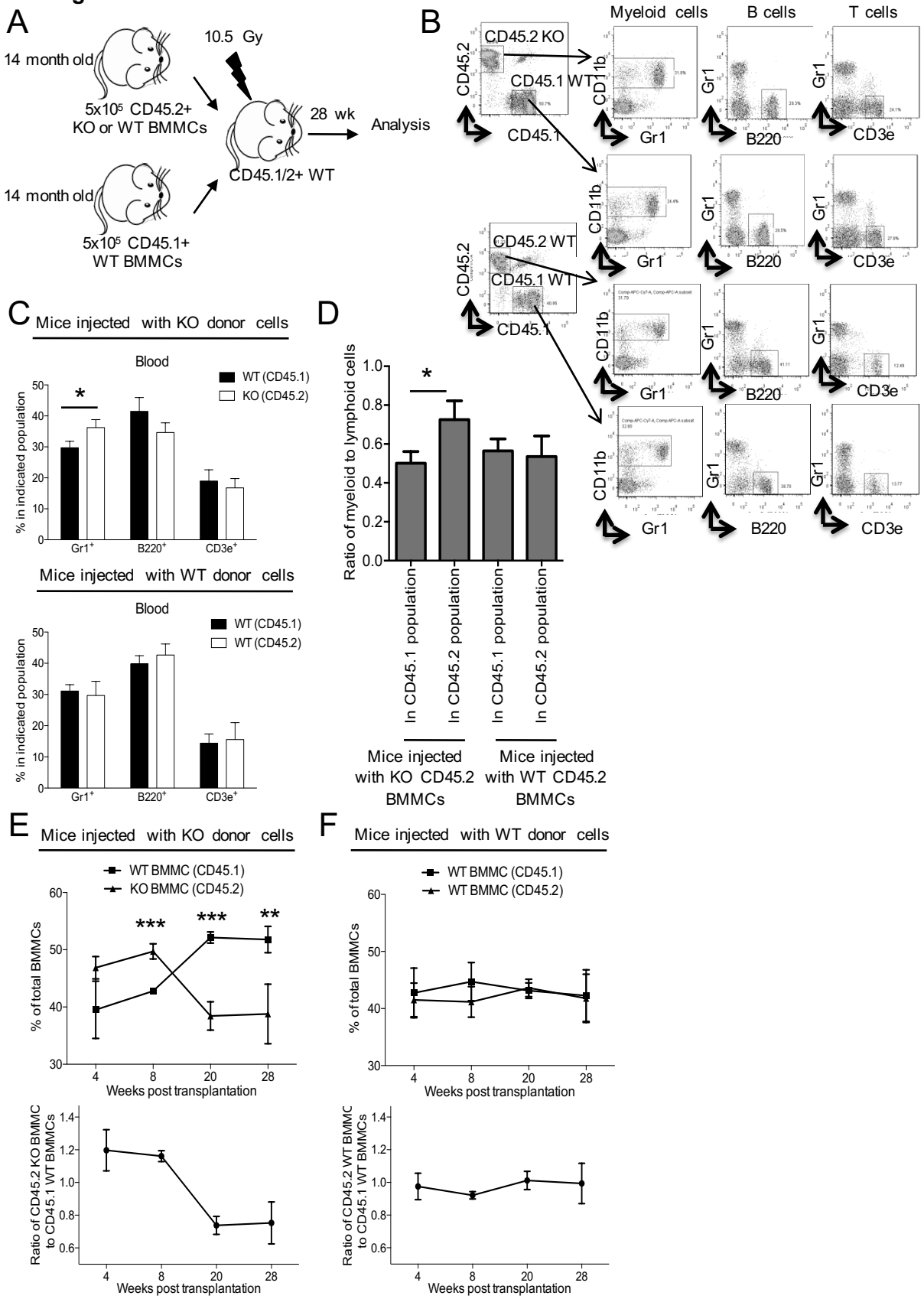

Figure 23. *Pr3*$^{-/-}$ total bone marrow cells from aged mice exhibit more pronounced myeloid skewing than their WT counterparts

(A) Scheme of the experimental setup to compare aged WT and *Pr3*$^{-/-}$ total bone marrow cells using competitive transplantation. (B) Percentages of different blood cell lineages in recipients reconstituted with total BM cells from aged WT and *Pr3*$^{-/-}$ mice at 24 weeks post-transplantation (n=6). *$p < 0.05$, **$p < 0.01$. (C) Quantitative analysis of the lineage potential of donor-derived cells at 24 weeks post-transplantation in the peripheral blood (n=6). *$p < 0.05$, ***$p < 0.001$. (D) Quantification of the myeloid to lymphoid ratio of donor-derived cells in recipient mice at 24 weeks post-transplantation. For each donor-derived population, the frequency of $Gr1^+$ cells among cells in the indicated population is divided by the sum of the frequencies of $CD3e^+$ and $B220^+$ cells (n=6). *$p < 0.05$. (E-F) Quantitative analysis of the origin of $Gr1^+$, $B220^+$, $CD3e^+$, and total $CD45^+$ cells in recipient mice at 4, 8, 20, and 24 weeks post-transplantation in the peripheral blood (n=6-7 mice).

Figure 23 continued

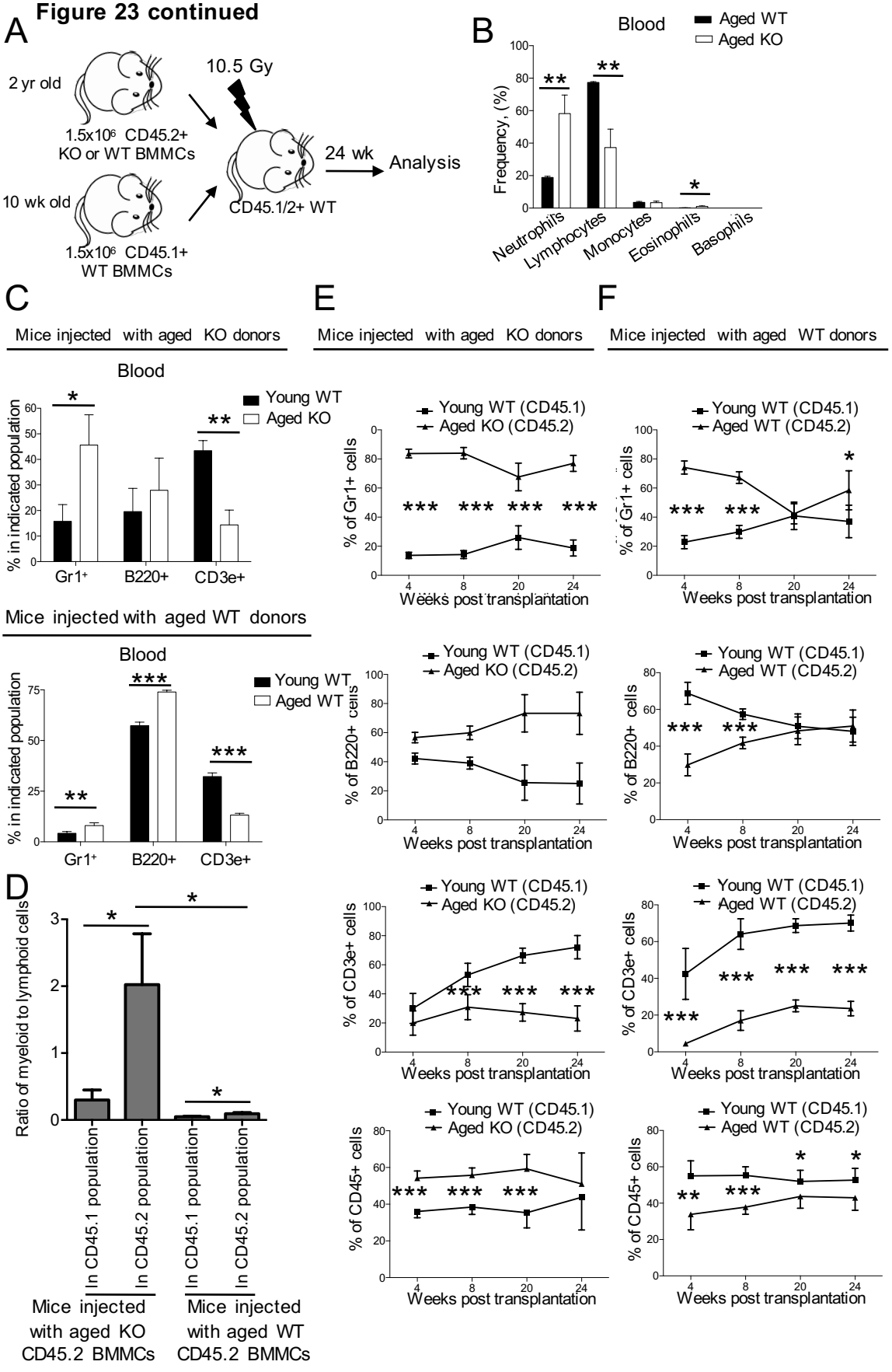

myeloid cells and a lower frequency of T cells (Figure 23C-D). In mice reconstituted with aged *Pr3*$^{-/-}$ and young WT donor cells, aged *Pr3*$^{-/-}$ donor cells gave rise to a much higher frequency of myeloid cells than young WT donor cells (Figure 23C). Importantly, the myeloid skewing of aged *Pr3*$^{-/-}$ donor cells was more dominant than aged WT donor cells, as assessed by the ratio of myeloid to lymphoid cells (Figure 23D). Taken together, these results suggest that the aged *Pr3*$^{-/-}$ hematopoietic compartment is skewed toward the myeloid lineage and resembles an exacerbated ageing phenotype.

In this experiment, there was an unexpected, dramatic increase in aged *Pr3*$^{-/-}$ donor-derived chimerism (CD45+ cells) at 4, 8, and 20 weeks post-reconstitution compared to young WT cells, primarily due to the higher frequency of myeloid cells in the early stages after transplantation (Figure 23E). This phenotype was abolished at 24 weeks post-reconstitution in line with the development and maturation of T cells, confirming that PR3 deficient HSCs had long-term repopulation defects. In spite of the higher myeloid reconstitution capacity of aged donor-derived cells, control mice reconstituted with competing congenic aged WT (CD45.2) and young WT (CD45.1) cells revealed consistently reduced chimerism in total white blood cells (CD45^{+} cells) from aged WT donors compared to young WT donors at all time points (Figure 23F).

These results suggest that *Pr3*$^{-/-}$ donor-derived cells can outcompete even young WT cells at early time points due to the expanded HSPC population in *Pr3*$^{-/-}$ donor mice. PR3-deficient HSCs are also defective in long-term repopulation ability and, along with the development of lymphoid cells (particularly T cells), aged *Pr3*$^{-/-}$ donors lose enhanced chimerism in the recipients.

2.7: Lifespan analysis

Finally, to understand if the HSC ageing phenotype affected lifespan, we examined the longevity of *Pr3*$^{-/-}$ mice. In agreement with the accelerated ageing phenotype, *Pr3*$^{-/-}$ mice had an approximately 25% decrease in median lifespan (Figure 24). This finding will be elaborated in detail in the discussion.

Figure 24

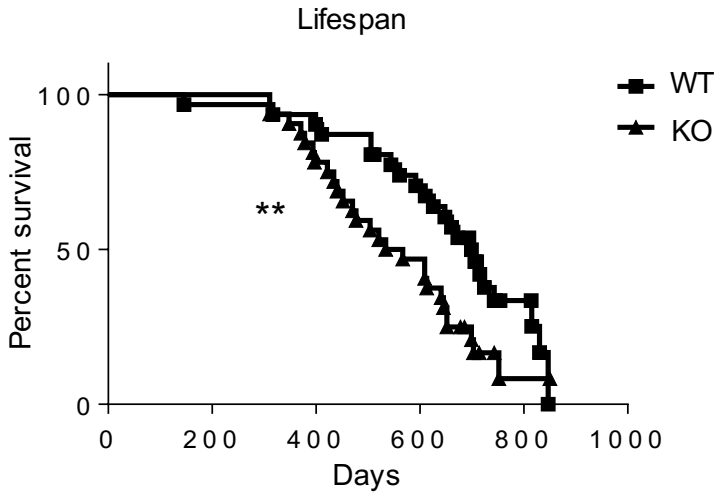

Figure 24. *Pr3*$^{-/-}$ mice have a shorter lifespan.
The survival curves of unchallenged WT and *Pr3*$^{-/-}$ mice kept in specific pathogen-free conditions (n=29-31). **p < 0.01.

Chapter 3: Role of Proteinase 3 in neutrophil function

This chapter focuses on the roles of PR3 in neutrophil function. As previously mentioned, PR3 has been suggested to play a role in the regulation of ROS production (Tal et al., 1998), transmigration (Kuckleburg et al., 2012), bacterial killing (Campanelli et al., 1990) and modulation of cytokine activity (Coeshott et al., 1999). We investigated the effects of PR3 deficiency in these processes using *in vitro* and *in vivo* assays. We found that PR3 deficiency in neutrophils does not lead to defects in microbicidal activities, ROS production, chemotaxis, cell adhesion or detachment. However, PR3 plays an important role in IL1β processing.

The work presented in this chapter benefited from collaborative studies with Dr. Hiroto Kambara in our lab, who performed the detection of secreted IL1β levels in PR3-deficient mouse bone marrow neutrophils.

3.1: Production of reaction oxygen species

Previous work has suggested that a PR3-containing fraction in the supernatant of stimulated neutrophils and recombinant PR3 could inhibit NADPH oxidase activity in unstimulated neutrophils (Tal et al., 1998). To test the ability of intrinsic PR3 regulating ROS production, we isolated bone marrow neutrophils from WT and *Pr3*$^{-/-}$ mice using an immunomagnetic negative selection kit. We stimulated neutrophils with fMLP and measured extracellular ROS production using an isoluminol-enhanced chemilluminescence assay (Lundqvist and Dahlgren, 1996). We did not observe any difference in ROS production levels between WT and *Pr3*$^{-/-}$ neutrophils (Figure 25A).

3.2: Dynamics of cell adhesion and detachment under shear flow

Recruitment of neutrophils to sites of infection can be mimicked *in vitro* by two assays: (1) adhesion to and detachment from an extracellular matrix molecule (or an endothelial cell surface molecule), and (2) chemotaxis towards a chemoattractant. Serpina1, an endogenous inhibitor of neutrophil serine proteases, has been shown to inhibit chemotaxis of neutrophils in a transwell assay (Stockley et al., 1990). In an *in vitro* setting, we tested the ability of fMLP-stimulated bone marrow neutrophils from WT and *Pr3*$^{-/-}$ mice to adhere to a microchannel coated with fibronectin under shear flow. The ability of WT and neutrophils to adhere to the fibronectin-channel microchannel under shear flow was similar (Figure 25B, left panel). We also measured the strength of adhesion in this assay. After the adhesion of neutrophils, reverse shear flow was applied and the number of cells that detached from the fibronectin-coated surface were counted. Neutrophils from WT and *Pr3*$^{-/-}$ mice detached at similar rates under reverse shear flow (Figure 25B, right panel).

3.3: Chemotaxis

The ability of unstimulated WT and *Pr3*$^{-/-}$ neutrophils from mouse bone marrow to migrate towards fMLP was compared using the EZ-taxiscan chamber (Effector Cell Institute, Tokyo, Japan). In this experiment, cells are loaded into a reservoir. After the loading of the chemoattractant into another reservoir, cells are recorded sequentially as

Figure 25. *Pr3*$^{-/-}$ neutrophils exhibit normal ROS production, cell adhesion and chemotactic properties.
(A) Extracellular ROS production of bone marrow derived neutrophils from WT and *Pr3*$^{-/-}$ mice after stimulation with 1 uM fMLP using an isoluminol-based chemiluminescent assay. Data are representative of 5 independent experiments. (B) The number of fMLP-stimulated neutrophils adhered to a microchannel coated with fibronectin under shear flow (left panel). After the adhesion of neutrophils, shear flow was applied in the opposite direction to investigate the frequency of cells detached (right panel). (n=3 from three independent experiments) (C) Cell tracks of neutrophils migrating towards fMLP (n=20). (D) Quantification of the speed and directionality of neutrophils migrating towards fMLP (n=20). Data are representative of four independent experiments.

Figure 25 continued

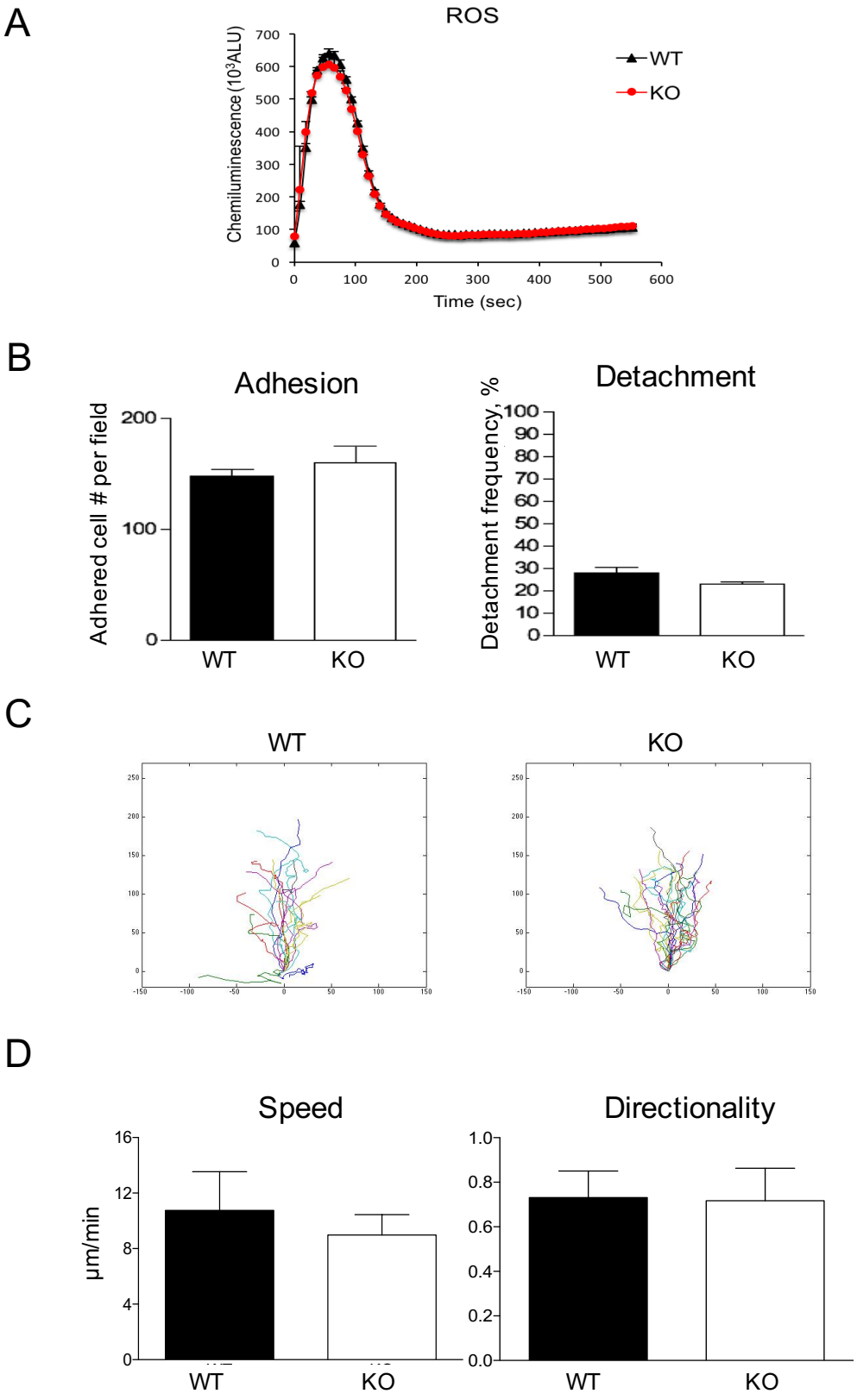

they migrate and their tracks are analyzed (Figure 25C). Speed and directionality of *Pr3*$^{-/-}$ neutrophils migrating towards fMLP was comparable to those of WT neutrophils (Figure 25D).

3.4: Microbicidal activity

We employed two strategies to look at the effects of PR3 deficiency in bacterial killing ability. In *in vitro* bacterial killing studies, we used mouse bone marrow neutrophils and co-incubated them with *Escherichia coli*, a Gram-negative bacteria, or *Staphylococcus aureus*, a Gram-positive bacteria. Incubation of opsonized *E. coli* or *S. aureus* with purified neutrophils for different periods of time revealed no defect in the ability of *Pr3*$^{-/-}$ neutrophils to kill bacteria (Figure 26A-B).

In *in vivo* bacteria-induced peritonitis models, mice were injected intraperitoneally with *E. coli* and *S. aureus*. We collected peritoneal lavage fluid at 4 hours post-injection to minimize the contribution of inflammatory monocytes that are recruited at later stages. Viable bacteria were counted by plating serial dilutions from the peritoneal lavage fluid. It is important to note that both doses used in these studies (2×10^6 for *E. coli* and 1×10^8 for *S. aureus*) were known to be self-limited in WT mice. At these conditions, *Pr3*$^{-/-}$ mice could clear bacteria as efficiently as WT mice (Figure 26C-D). In these experiments, similar numbers of neutrophils were recruited to the peritoneal cavity (data not shown). These results also suggest that PR3 deficiency does not lead to a defect in the recruitment of neutrophils to sites of infection confirming the results obtained from *in vitro* cell adhesion and chemotaxis assays.

Figure 26

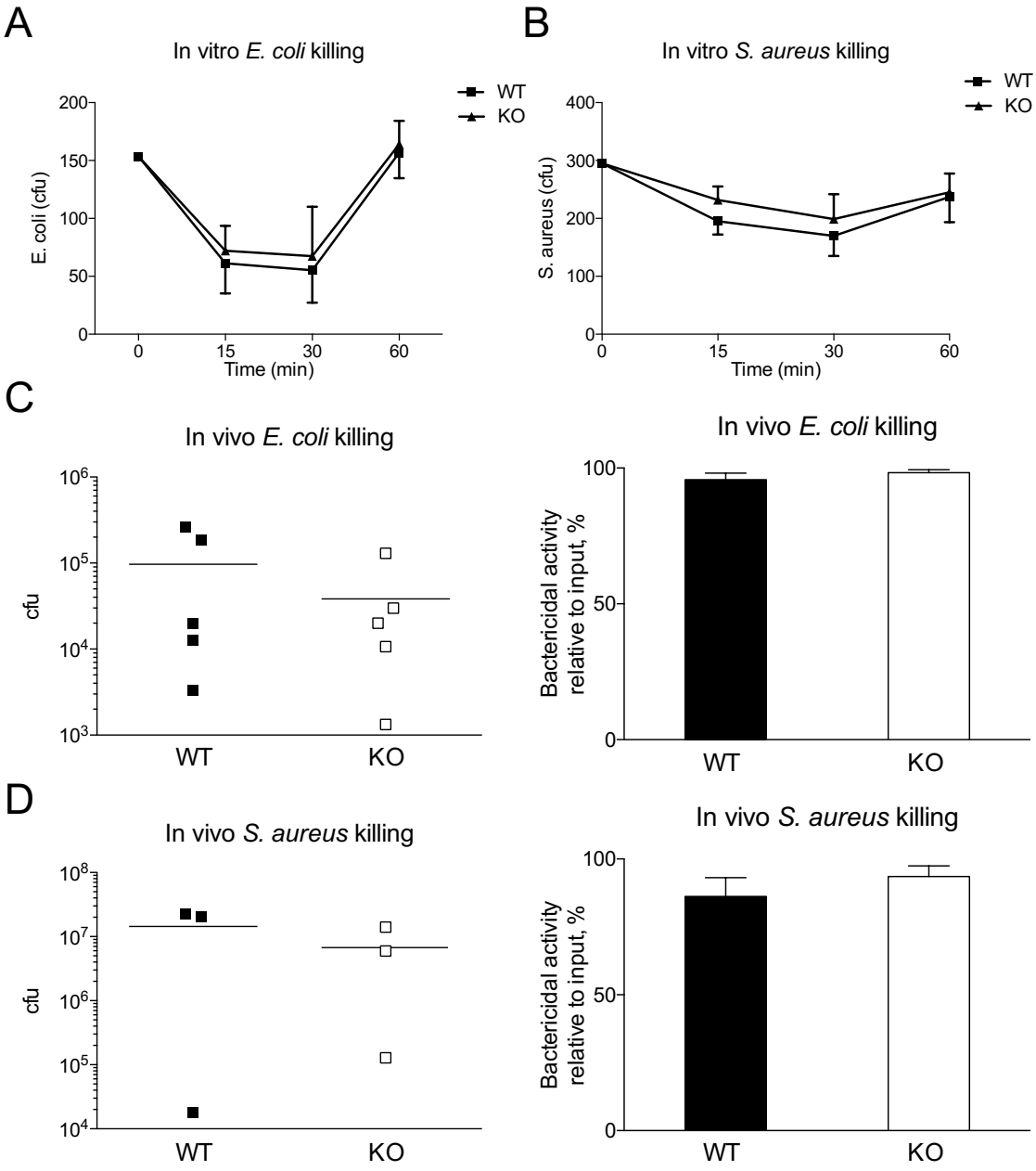

Figure 26. *Pr3* deficiency does not lead to a major defect in microbicidal activity. (A) Quantification of viable *E. coli* at indicated time points post-incubation with WT and *Pr3*$^{-/-}$ neutrophils at a 5:1 ratio. (B) Quantification of viable *S. aureus* at indicated time points post-incubation with WT and *Pr3*$^{-/-}$ neutrophils at a 10:1 ratio. (C) 8-10 week old WT and *Pr3*$^{-/-}$ mice were injected with $2x10^6$ E. coli. Peritoneal lavage was collected at 4 hours post bacteria injection. The number of viable bacteria was determined after plating dilutions on LB agar plates (left panel) (n=5). Bactericidal activity was determined as follows: Bactericidal activity = 100-[(Input-viable bacteria)/Input] (D) WT and *Pr3*$^{-/-}$ mice were injected with $1x10^8$ S. aureus. Sample collection and analysis are same as Figure (C). Results are representative of two independent experiments. (n=3)

3.5: Regulation of IL1β processing

To assess the role of PR3 in IL1β processing as previously described (Coeshott et al., 1999), we first incubated recombinant human pro-IL1β with recombinant human PR3, ran the samples on SDS-PAGE gel and performed Coomassie Blue staining to visualize the proteins. Co-incubation with PR3 led to cleavage of pro-IL1β into two fragments suggesting the generation of mature forms (Figure 27A). Next, we wanted to confirm the activity of generated fragments by looking at IκBα degradation in HeLa cells as previously described (Alkalay et al., 1995). We added aliquots from the co-incubated recombinant proteins and controls into HeLa cells. While addition of mature form of IL1β and pro-IL1β incubated with PR3 led to degradation of IκBα, PR3 or IL1β alone had no effect (Figure 27B). This finding shows that PR3-mediated pro-IL1β cleavage leads to generation of functionally active mature IL1β.

Finally, we looked at the ability of mouse bone marrow neutrophils from WT and *Pr3*$^{-/-}$ mice to secrete IL1β. Neutrophils were stimulated with LPS for 4 hours and IL1β levels were measured by ELISA. Indeed, we observed a 40% reduction in IL1β secretion levels in *Pr3*$^{-/-}$ neutrophils in response to LPS (Figure 27C).

Figure 27

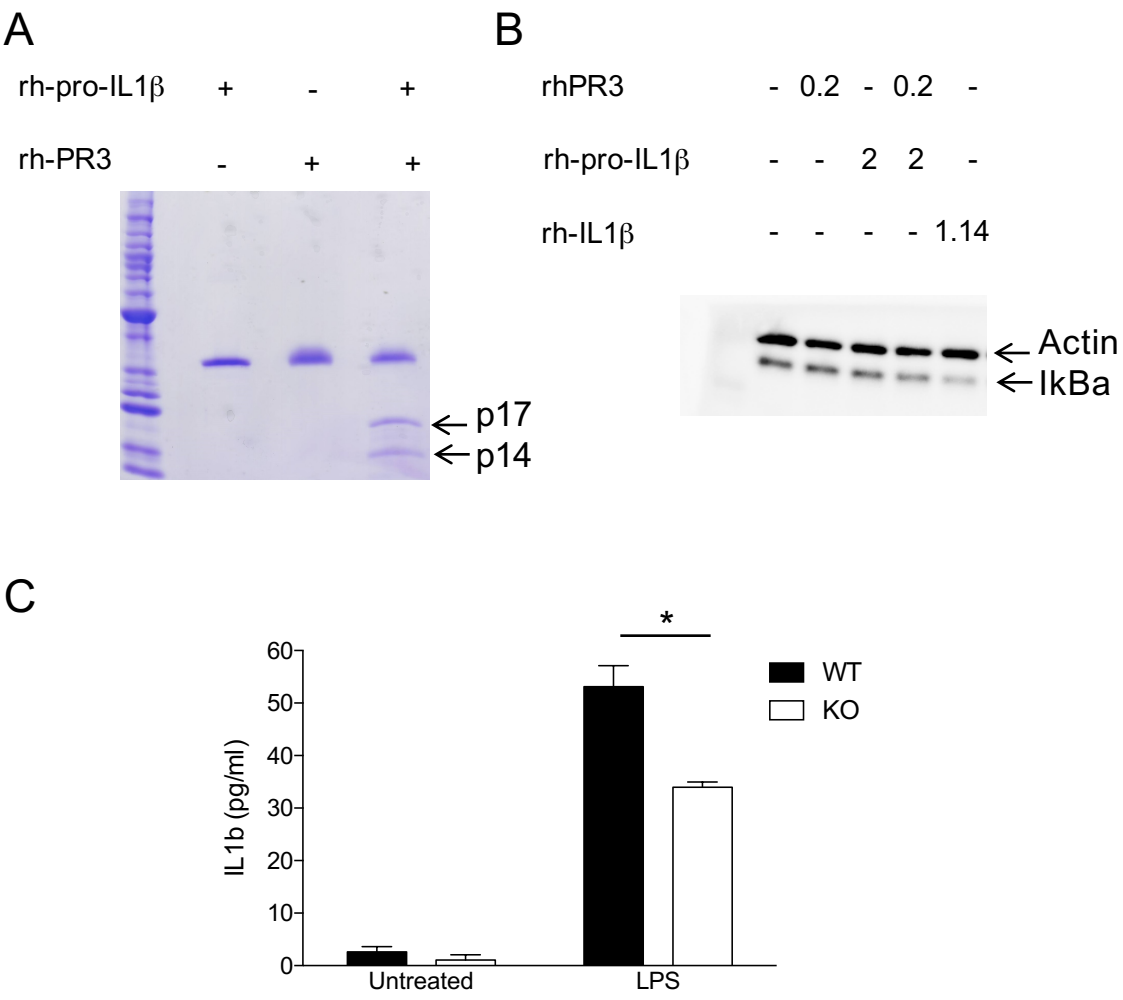

Figure 27. *Pr3* cleaves pro-IL1β to generate the mature active form. (A) Coomassie Blue-stained SDS-PAGE gels for lysates containing rh-pro-IL1β, rh-PR3 or both. (B) Analysis of IL1β activity as determined by IκBα degradation in HeLa cells as assayed by Western blotting for IκBα. Actin is used as a loading control. Numbers denote ng/ml final concentration in the medium. (C) IL1β secretion levels in mouse bone marrow neutrophils from WT and Pr3-/- mice after stimulation with LPS for 4 hours as determined by ELISA (n=3).

Chapter 4: Materials and Methods

4.1: Mice

All experiments, unless otherwise noted, were performed on eight to twelve-week old male mice. C57BL/6 wild-type and Pr3-/- mice were bred in-house in specific pathogen-free animal facilities at Boston Children's Hospital. Pr3-/- mice were generated as previously described (Loison et al., 2014) and backcrossed to C57BL/6 mice for eight generations. B6.SJL-Ptprca Pepcb/BoyJ mice carrying CD45.1 allele were purchased from Jackson Laboratories and acclimated for 2 weeks prior to start of the experiment. B6.SJL-Ptprca Pepcb/BoyJ mice and C57BL/6 mice were bred in-house to generate mice carrying CD45.1 and CD45.2 alleles. In all experiments performed with knockout mice, we always used corresponding littermates as WT controls. All procedures involving mice were approved and monitored by the Children's Hospital Animal Care and Use Committee.

For complete blood count, orbital peripheral blood (150 μl) was collected by heparinized capillary tubes (Fisher Scientific, 22-362-566) and transferred into K2-EDTA-coated tubes (Becton Dickinson, 365974). Blood parameters were analyzed by using Hemavet 950FS (Drew Scientific).

For BrdU incorporation assays, 2 μg BrdU was injected in 200 μl DPBS intrapertioneally 24-72 hours before sacrifice.

For macrophage depletion assays, mice were injected with 250 μl of clodronate or PBS liposomes (ClodLip BV) intravenously at 8 days before tissue collection.

4.2: Lifespan analysis

For lifespan analysis, age and sex-matched male and female mice were housed in specific pathogen-free animal facilities at Boston Children's Hospital. All groups had *ad libitum* access to water and regular diet. Most of the mice were kept until natural death. Some mice were euthanized for humane reasons due to their poor prognosis because of various reasons including head tilt, severe dermatitis, tumor formation and severe lethargy.

4.3: Competitive bone marrow transplantation studies

Transplantation was conducted using lethally irradiated mice carrying CD45.1 and CD45.2 alleles as recipients. Mice were γ-irradiated with two doses of 5.25 Gy at a 4 hour interval. Total bone marrow cells and LSK cells from age and sex-matched donors were prepared as previously described. For total bone marrow transplantation, recipients were injected with equal numbers of total bone marrow cells from each recipient via tail vein injection. For LSK transplantation, $5x10^3$ sorted LSK cells from each donor (CD45.1 or CD45.2) were injected along with $3x10^5$ supporting total bone marrow cells (CD45.1/2). Retroorbital bleeding was performed every 4 weeks to analyze peripheral blood chimerism. Bone marrow chimerism was analyzed at the end of each experiment.

4.4: Hematopoietic recovery after sublethal and lethal irradiation experiments

To analyze hematopoietic recovery after sublethal irradiation mice were γ-irradiated with one dose of 4 Gy and euthanized at the indicated time points. Peripheral

blood was used for complete blood counts while bone marrow and spleen were harvested for analyisis of different cell populations using conventional flow cytometry methods.

To analyze survival after lethal irradiation, mice were irradiated with 6 Gy and their survival was monitored up to 40 days.

4.5: Bacteria-induced peritonitis models

Mice were injected intraperitoneally with $2x10^6$ of *E. coli* (strain 19138, ATCC) or $1x10^8$ *S. aureus* (strain 10390, ATCC) in DPBS (Life Technologies, 14190-250). At 4 hours post-injection, mice were euthanized and peritoneal exudates were harvested in 2 successive washes with 5 ml of DPBS supplemented with 2 mM EDTA (Thermo Fisher Scientific, 15575-020). Diluted aliquots from the lavaged fluid were spread on LB agar plates for *E. coli* and blood agar plates for *S. aureus*. CFU were counted after incubating the plates overnight at 37^oC. Injected bacteria were used as input control. The number of neutrophils recruited were quantified by counting the cells in the peritoneal exudate with a hematocytometer and analyzing the frequency of $Gr1^+$ $CD11b^+$ cells in the exudate by conventional flow cytometry methods.

4.6: Colony forming cell assays

Bone marrow cells ($2x10^4$) and splenocytes ($1x10^6$) from WT and *Pr3*$^{-/-}$ mice were seeded in semisolid Methocult GF M3434 medium containing rmSCF, rmIL-3, rhIL-6 and rhEpo for detection of CFU-GM and BFU-E (Stem Cell Technologies,

03434). Colony numbers were counted on day 7, images for colony sizes were obtained on day 8 and annexin V/7-AAD staining was performed on day 9 post-plating.

4.7: Flow cytometry

Bone marrow cells from two femurs and two tibias were flushed into DPBS supplemented with 2% FBS (Atlanta Biologicals, S11150H). Red blood cells were lysed by incubation with 2 ml of ACK buffer (Life Technologies, A10492-01) at room temperature for 5 min. For sample analysis, five million bone marrow cells were incubated with an antibody mixture including antibodies for lineage markers CD3e-APC (Biolegend, 100312), CD4-APC (Biolegend, 100516), CD8a-APC (Biolegend, 100712), CD11b-APC (Biolegend, 101212), CD45R/B220-APC (Biolegend, 103212), Gr1-APC (Biolegend, 108412), Ter119-APC (Biolegend, 116212) as well as Sca1-PE/Cy7 (Biolegend, 108114) and c-Kit-APC/Cy7 (Biolegend, 105826) in DMEM (Life Technologies, 31053-028) supplemented with 2% FBS. For LSK subset analysis, CD34-FITC (eBioscience, 11-0341-85) and CD135-PE (Biolegend, 135306) were used in addition to these stains. Alternatively, CD48-PE (Biolegend, 103405) and CD150-PerCp/Cy5.5 (Biolegend, 115921) were used for LSK subset analysis. For LK subset analysis, CD34-FITC and and CD16/32-PE (Biolegend, 101308) were used in addition to the former stains. Samples were incubated on ice for 15 minutes, washed and filtered before FACS analysis.

For the intracellular detection of PR3, bone marrow cells were fixed and permeabilized using eBioscience Intracellular Fixation & Permeabilization Buffer Set

(eBioscience, 88-8824-00) according to the manufacturer's recommendations. The anti-mouse PR3 (D-20) antibody was purchased from Santa Cruz.

In competitive transplantation experiments, Gr1-FITC (Biolegend, 108406), CD45.1-PE (Biolegend, 110708), CD45.2-APC (Biolegend, 109814), CD3e-PE/Cy7 (Biolegend, 100320) and CD45R/B220-APC/Cy7 (Biolegend, 103224) antibodies were used to assess chimerism of mature cells. To assess stem and progenitor cell populations, CD3e-FITC (Biolegend, 100306), CD4-FITC (Biolegend, 100510), CD8a-FITC (Biolegend, 100706), CD11b-FITC (Biolegend, 101206), CD45R/B220-FITC (Biolegend, 103206), Ter119-FITC (Biolegend, 116205) along with the previously mentioned Gr1-FITC, CD45.1-PE, CD45.2-APC, Sca1-PE/Cy7 and c-Kit-APC/Cy7 antibodies were used.

Cell proliferation was assessed using a BrdU labeling kit (BD Biosciences, 559619) according to the manufacturer's instructions. Twenty-four to seventy-two hours before sacrifice, 2 μg BrdU was injected i.p. in 200 μl DPBS. At indicated time points, the frequencies of LSK, LT-HSC, ST-HSC, MPP and LK cells in different stages of cell cycle were determined.

For detection of apoptotic events, cells were first stained with antibodies against various cell surface markers and then stained with annexin V-FITC (BD Biosciences, 556420) and 7-AAD (BD Biosciences, 559925) in annexin V binding buffer (BD Biosciences, 556454).

To detect active caspase 3 by flow cytometry, Vybrant FAM Caspase Assay Kit (Thermo Fisher Scientific, V35118) was used according to the manufacturer's instructions.

In vivo macrophage depletion was performed by injecting mice with 250 µl of clodronate or PBS liposomes (ClodLip BV) i.v. at 9 days before tissue collection. To confirm depletion of macrophages, F4/80-FITC (Biolegend, 123108), Gr1-PE (Biolegend, 108408) and CD115-APC (Biolegend, 17-1152-82) antibodies were used.

β-galactosidase activity was determined using Imagene Green C_{12}FDG lacZ gene expression kit (Thermo Fisher Scientific, I2904) according to the manufacturer's instructions. Briefly, total bone marrow cells were stained with Lin-APC, Sca-1-PE/Cy7 and c-Kit-APC/Cy7 antibodies. Then, cells were incubated with 25 μM chloroquine for 30 minutes at 37°C in RPMI+10% FBS to induce lysosomal alkalinization and inhibit basal endogenous β-galactosidase activity. After being washed, cells were incubated with 16µM 5-dodecanoylaminofluorescein di-β-D-galactopyranoside C_{12}FDG for 10 minutes at 37°C in RPMI supplemented with 10% FBS. Cells were washed again and analyzed using flow cytometry.

All data were collected on FACSCanto II or LSR II flow cytometers (Becton Dickinson). Data analysis was performed by using FlowJo software (Tree Star, Inc.).

For sorting highly purified stem cell populations, EasySep mouse hematopoietic progenitor cell enrichment kit that relies on immunomagnetic negative selection was used (Stem Cell Technologies, 19756). After enrichment, cells were stained with Streptavidin-FITC (Biolegend, 405202), c-Kit-PE (Biolegend, 105808) and Sca1-APC (Biolegend, 108112) to sort LSK and LK cells. To sort HSCs, enriched cells were stained with Streptavidin-APC/Cy7 (Biolegend, 405208), Sca1-PE/Cy7 (Biolegend, 108114), c-Kit-PE/Dazzle 594 (Biolegend, 105834), CD48-FITC (Biolegend, 103404), CD135-PE (Biolegend, 135306), CD150-APC (Biolegend, 115909) or Streptavidin-

APC/Cy7, Sca1-PE/Cy7, c-Kit-PE/Dazzle 594, CD34-FITC and CD135-PE for foci and polarity assays, respectively. DAPI (BD Biosciences, 564907) was added to exclude dead cells. Cells were sorted on Aria cell sorter (Becton Dickinson) or MoFlo cell sorter (Dako).

4.8: Cell culture

Total bone marrow cells were cultured in RPMI (Life Technologies, 11875-093) supplemented with 10% FBS and 1 mM sodium pyruvate (Life Technologies, 11360-070) for indicated time points prior to annexin V/7-AAD staining.

LSK cells were directly sorted into 96-well round bottom plates (or solid white luminescence plates). For short-term cultures, sorted LSK cells were cultured in IMDM (Life Technologies, 12440-053) supplemented with 5% FBS (Stem Cell Technologies, 06200), 100 U/ml penicillin, 100 μg/ml streptomycin (Life Technologies, 15140-122), 0.1 mM non-essential amino acids (Life Technologies, 11140-050), 1 mM sodium pyruvate (Life Technologies, 11360-070), 2 mM L-glutamine (Life Technologies, 25030-081), 50 μM β-mercaptoethanol (Life Technologies, 21985-023), rmSCF (25 ng/ml), rmTPO (25 ng/ml), rmFlt-3L (25 ng/ml), rmIL-3 (10 ng/ml), rmIL-11 (25 ng/ml), rmGM-CSF (10 ng/ml) and rmEpo (4 U/ml) as described previously (Flach et al., 2014). All recombinant cytokines were purchased from Peprotech. After 12-36 hour culture, caspase 3 activity was detected by using luminescence based Caspase-Glo 3/7 assay (Promega, G8090) according to the manufacturer's instructions.

For longer cultures of LSK cells, a slightly different culture condition was used as previously described (Janzen et al., 2008). LSK cells were cultured in X-Vivo 15 (Lonza,

04-744Q) supplemented with 10% endotoxin-free BSA (EMD Millipore, 126579), 1X penicillin/streptomycin, 2 mM L-glutamine, 100 μM β-mercaptoethanol, rmSCF (50 ng/ml), rmTPO (50 ng/ml), rmFlt-3L (50 ng/ml) and rmIL-3 (20 ng/ml). After 48 hours, cells were cultured in the presence of 10 ng/ml rmSCF and 10 ng/ml rmTPO. After total culture time of 96 hours, medium was replaced by fresh medium. Annexin V/7-AAD staining was performed on day 6 and TUNEL assay was performed using APO-BrdU TUNEL Assay kit (Thermo Fisher Scientific, A23210) on day 7 post-initiation of cell culture.

HeLa cells used in IL1β activity assay were grown in DMEM (Life Technologies, 11965-092) supplemented with 10% FBS.

4.9: Histological analysis and immunofluorescent microscopy

Bone marrow smears were prepared by squeezing the cells from femurs and tibias of mice directly onto slides. Cells were stained by Diff-Quik Stain Kit (Siemens, B41312-1A) according to the to the manufacturer's instructions. At least 400 cells were counted to identify the lineage and maturation stage of bone marrow cells.

For immunofluorescent microscopy studies, freshly sorted LT-HSCs were seeded in 100 μl HBSS (Life Technologies, 14025-134) supplemented with 10% FBS on poly-L-lysine coated slides (VWR, 16002-116). Lin^- c-Kit^+ $Sca1^+$ $CD135^-$ $CD48^-$ $CD150^+$ cells were analyzed in foci assays and Lin^- c-Kit^+ $Sca1^+$ $CD34^-$ $CD135^-$ cells were used in polarity assays as previously described (Flach et al., 2014; Florian et al., 2012).

For analysis of γH2AX foci, cells were incubated on slides for 15 minutes and fixed in 4% PFA for 10 minutes at room temperature. Cells were permeabilized with ice

cold 90% methanol for 10 minutes at -20°C, washed with PBS and blocked in 1% BSA in PBS containing 0.15% Triton X 100 (PBST) for 1 hour at room temperature. Slides were then incubated in 1% BSA in PBST with anti-phospho-H2AX (Ser 139) (EMD Millipore 05-636) overnight at 4°C. After washing three times in PBS, cells were incubated for 1 hour in 1% BSA in PBST containing goat anti-mouse A488-conjugated antibody at room temperature (Life Technolgies, A-11029).

For polarity assays, slides were incubated for 1 hour at 37°C (5% CO_2, 3% O_2) in a humidified chamber. After fixation with 4% PFA for 10 minutes, cells were washed with PBS, permeabilized with PBST for 20 minutes at room and then blocked with 10% donkey serum (Jackson ImmunoResearch, 017-000-121) in PBST for 30 minutes at room temperature. Slides were then incubated in 5% donkey serum in PBST with anti-alpha tubulin (Abcam, ab6160) and anti-Cdc42 (EMD Millipore, 07-1466) overnight at 4°C. After washing, cells were incubated for 1 hour in in PBST including donkey anti-rat A488-conjugated antibody (Jackson ImmunoResearch, 712-545-153) for tubulin and donkey anti-rabbit A594-conjugated antibody for Cdc42 (Jackson ImmunoResearch, 711-585-152) at room temperature.

At the end of incubation with secondary antibodies, slides were washed three times in PBS and mounted using VectaShield containing DAPI (Vector Laboratories, H-1200). Staining was visualized under a fluorescent microscope (Olympus IX71), and images were taken using a 100x oil objective lens. At least 100 cells were counted in each sample to assess the level of DNA damage and distribution of tubulin and Cdc42 in HSCs.

In all studies, investigators analyzing the samples were blinded to the identities of samples.

4.10: *In vitro* neutrophil function assays

Isolation of mouse bone marrow neutrophils: Bone marrow neutrophils were obtained using an immunomagnetic negative selection kit (Stem Cell Technologies, 19762) according to the manufecturer's instructions. After isolation, cytospin was performed with an aliquot from the cells followed by Diff-Quick staining as previously described. Purity of neutrophils was assessed in each sample and found to be >85% in all experiments. Prior to all experiments, isolated neutrophils were resuspended in HBSS (Life Technologies, 14170-112) supplemented with 0.2% endotoxin-free BSA (EMD Millipore, 126579) and incubated for 30 minutes at 37^{o}C and 5% CO_2.

ROS production: To determine extracellular superoxide production, 4 U/ml HRP (type XII; Sigma-Aldrich, P8415) and 5.5 μM isoluminol (VWR Scientific, TCA5300) were added to 0.4 x10^{6} neutrophils resuspended in HBSS supplemented with 0.2% endotoxin-free BSA. Then, cells were loaded into a 96-well MaxiSorp plate (Nunc, 436110). Chemiluminescence was measured using a microplate luminometer (Berthold Technologies, TriStar LB941). 1 μM fMLP (Genscript, RP12959) was injected into the mixture via the injection port of the luminometer. Luminescence was recorded for 20 minutes at 10 second intervals.

Neutrophil adhesion and detachment under shear flow: To examine neutrophil adhesion under shear flow, a Vena8 chamber (Cellix, V8CF-400-100-02P10) was coated with 10 μl of 10μg/ml fibronectin (Sigma-Aldrich, F1056) for 1 hour at 37^{o}C.

0.2 x 10^6 neutrophils resuspended in 100 µl of HBSS supplemented with 0.2% endotoxin-free BSA were stimulated 2 µM fMLP for 5 minutes at room temperature. Cells were loaded into the reservoir of the chamber and a shear flow of 10 dynes/cm^2 was applied to run the cells over the microchannel. Time lapse images were captured by Olympus IX71 microscope with a charge-coupled device (CCD) camera for 5 minutes with 60 ms exposure at 5 second intervals. Using a 60 ms exposure helped to differentiate the round adhered cells from elongated moving cells. At the end of 5 minutes, increasing shear flow rates of 0.5, 1, 2, 5, 7.5, 10 and 12 dynes/cm^2 was applied in the opposite direction for 1 minute each to determine the number of cells that detached from the surface. Time lapse images were taken for 7 minutes at 5 second intervals.

Chemotaxis: The EZ-TAXIScan (ECI Frontier, MIC-1000) was used to investigate chemotaxis of mouse neutrophils. After removal of bubbles and heating of the chamber to 37°C, 1.5 x 10^4 neutrophils in 1.5 µl of HBSS supplemented with 0.2% endotoxin-free BSA were loaded into the lower reservoir. 1 µl of 2 µM fMLP was loaded into the upper reservoir. Time lapse images were taken for 20 minutes at 30 second intervals. At least 20 cell tracks from each sample were analyzed using DIAS software (Soltech). Chemotaxis speed and directionality towards fMLP were determined by the cell tracks using Matlab (Mathworks).

***In vitro* bacterial killing:** Fresh culture of *E. coli* (strain 19138, ATCC) or *S. aureus* (strain 10390, ATCC) at an OD600 of 0.2 was opsonized with 10% autologous mouse serum in DPBS using an end-to-end rotator at 6 rpm and 37°C for 1 hour. 2.5 x 10^5 mouse bone marrow neutrophils were incubated with 1.25 x 10^6 *E. coli* or 2.5 x10^6

S. aureus in 100 µl DPBS supplemented with 10% autologous serum using an end-to-end rotator at 6 rpm and 37°C. Incubation times were 15 minutes, 30 minutes, 1 hour and 2 hours. After each time period, neutrophils were lysed by adding 900 µl ice-cold sterile ddH2O and incubated for 10 minutes for efficient lysis. Samples were vortexed vigorously for 5 seconds to disperse bacteria. Diluted aliquots were spread on LB agar plates for *E. coli* and blood agar plates for *S. aureus*. CFU were counted after incubating the plates overnight at 37^{o}C. Bacterial suspensions without any neutrophils were used as a control.

4.11: Detection of pro-IL1β cleavage by Proteinase 3

1.25 µg of recombinant human (rh) pro-IL1β (Sino Biological Inc., 10139-H070E) in 4 µl ddH_2O was mixed with with 0.5 µg rhPR3 (Novoprotein, C628) in 1 µl DPBS. Total reaction volume was adjusted to 15 µl with DPBS and samples were incubated at 37^{o}C for 30 minutes. Samples were run using SDS-PAGE gel electrophoresis and Coomassie Blue staining (Biorad, 161-0436) was performed according to the manufacturer's instructions.

To detect activity of generated IL1β fragments, aliquots from the previously described co-incubation experiment were added to HeLa cells grown in DMEM supplemented with 10% FBS. rh-IL1β (Peprotech, 200-01B) concentration was chosen as a positive control assuming total cleavage of rh-pro-IL1β by rhPR3. After 30 minutes, cells were lysed with Laemmli Sample Buffer (Biorad, 161-0737) supplemented with 2-Mercaptoethanol (Biorad, 161-0710).

4.12: Genotyping, qPCR, Western blotting and ELISA

Genotyping was performed by PCR of tail DNA with the following primers: 5'-TGCTTGGGAAGGAAAGAATG-3' (forward) and 5'-GAGCTGCAGTGAAGGTTGTG-3' (reverse).

For gene expression analysis, RNA was isolated from FACS sorted bone marrow subpopulations ($Gr1^+$ $CD11b^+$ neutrophils and $Lineage^-$ $Sca\text{-}1^+$ $c\text{-}Kit^+$ cells) using Picopure RNA isolation kit (Thermo Fisher Scientific, KIT0204). cDNA was synthesized using iScript cDNA synthesis kit (Bio-rad, 1708891) and quantitative RT-PCR was performed using a SYBR Green Quantitative RT-PCR kit (Bio-rad, 1708880). Primers used are listed below: Pr3_fwd, 5'-CCCTGATCCACCCGAGATTC-3'; Pr3_rev, 5'-GGTTCTCCTCGGGGTTGTAA-3'; Gapdh_fwd, 5'-AGAAGACTGTGGATGGCCCCTC-3'; Gapdh_rev, 5'-GATGACCTTGCCCACAGCCTT-3'.

Western blots were performed as previously described (Loison et al., 2014). To analyze PR3 expression in LSK cells, sorted LSK cells were loaded at a 10:1 ratio compared to LK cells and neutrophils. The antibodies against mouse PR3 (Santa Cruz Biotechnology, sc-19748) and gp91phox (Santa Cruz Biotechnology, sc-130543) were purchased from Santa Cruz. The antibody against mouse GAPDH (Encor, MCA-1D4) was purchased from Encor. To analyze $I\kappa B\alpha$ degradation in HeLa cells, antibodies against human $I\kappa B\alpha$ (Cell Signaling Technology, 9242) and pan-actin (Cytoskeleton, AAN01-A) were used.

Secreted $IL1\beta$ levels from mouse bone marrow neutrophils were detected by ELISA using a commercially available kit (R&D Systems, SMLB00C).

4.13: Statistical analysis

All values are mean ± SEM. Statistical significance for indicated data sets was performed by Student's t test capability on Prism (Graphpad). All data were analyzed using unpaired Student's t test except for caspase 3 activity by chemilluminescence and myeloid-lymphoid ratios in transplantation experiments, which were analyzed using paired Student's t test.

Chapter 5: Discussion

To our knowledge, PR3 expression in HSCs has not previously been reported. Our novel findings suggest that high PR3 expression levels are detected in HSPCs and PR3 is an intrinsic regulator of the stem cell compartment in the BM.

Functional changes occur in the HSC pool with ageing. HSC numbers rise with age, but aged HSCs exhibit a diminished repopulation capacity and are myeloid-biased (Morrison et al., 1996; Pang et al., 2011; Sudo et al., 2000). In aged HSCs, markers associated with DNA damage (Rossi et al., 2007a) and senescence increase (Flach et al., 2014; Janzen et al., 2006), while α-tubulin and Cdc42 become less polarized (Florian et al., 2012).

Here we reveal that *Pr3*$^{-/-}$ HSCs show many of the characteristics associated with aged HSCs. In the absence of PR3, we observed an increase in the frequency of HSCs and progenitor cells in the bone marrow. Competitive reconstitution experiments suggest that enhanced hematopoietic HSPC compartment is functional and LSK cells from *Pr3*$^{-/-}$ mice display enhanced regeneration potential at early time points. Yet, their long-term reconstitution capacity is defective at later stages in line with the development and maturation of lymphoid, particularly T, cells. We observed a consistent increase in the ratio of myeloid to lymphoid cells generated by *Pr3*$^{-/-}$ HSCs. We also saw higher levels of DNA damage and reduced cell polarity in *Pr3*$^{-/-}$ HSCs from young mice. Meanwhile, *Pr3*$^{-/-}$ HSCs from aged mice exhibited a more senescent phenotype.

In the absence of PR3, these aged phenotypes become evident at a younger age. Thus, PR3 contributes to the maintenance of healthy stem and progenitor cell

pools in the BM. Since PR3 regulates spontaneous HSC apoptosis by cleaving and activating pro-apoptotic caspase 3, our results also suggest that spontaneous cell death is a critical cellular process that controls aging of the quiescent HSC population (Figure 28).

We also found that *Pr3*$^{-/-}$ mice have a shorter lifespan. This is a surprising finding considering the limited number of cell types that express *Pr3*. While vulnerability to an infection due to a defect in neutrophil function cannot be completely excluded, we did not see a hallmark of infection or inflammation such as a change in blood count or spleen size in our cohort. Similarly, we did not see a major defect in neutrophil functions (Chapter 4). We could not use mice in which *Pr3* is deleted specifically in more mature myeloid cells (such as LysMCre-Pr3$^{floxp/floxp}$ mice) as a control in our cohort because *Pr3* and *LysM* are on the same chromosome. The histological analysis of various tissues from the ageing cohort is still ongoing.

PR3 is a serine protease mainly expressed in granulocytes and has been proposed as a key player in innate immunity. PR3 has been shown to play a role in neutrophil spontaneous death (Loison et al., 2014), and we now extend this finding to LSK cells, a population enriched with stem cells. While neutrophil spontaneous apoptosis is dependent on PR3-induced caspase 3 cleavage, caspase 8 and caspase 9 are not essential to this process but instead required for ligand-induced neutrophil apoptosis (Loison et al., 2014). Similarly, it is likely that HSC apoptosis induced by cytokine withdrawal is dependent on caspase 8 and 9, while spontaneous HSC apoptosis depends on PR3.

Figure 28

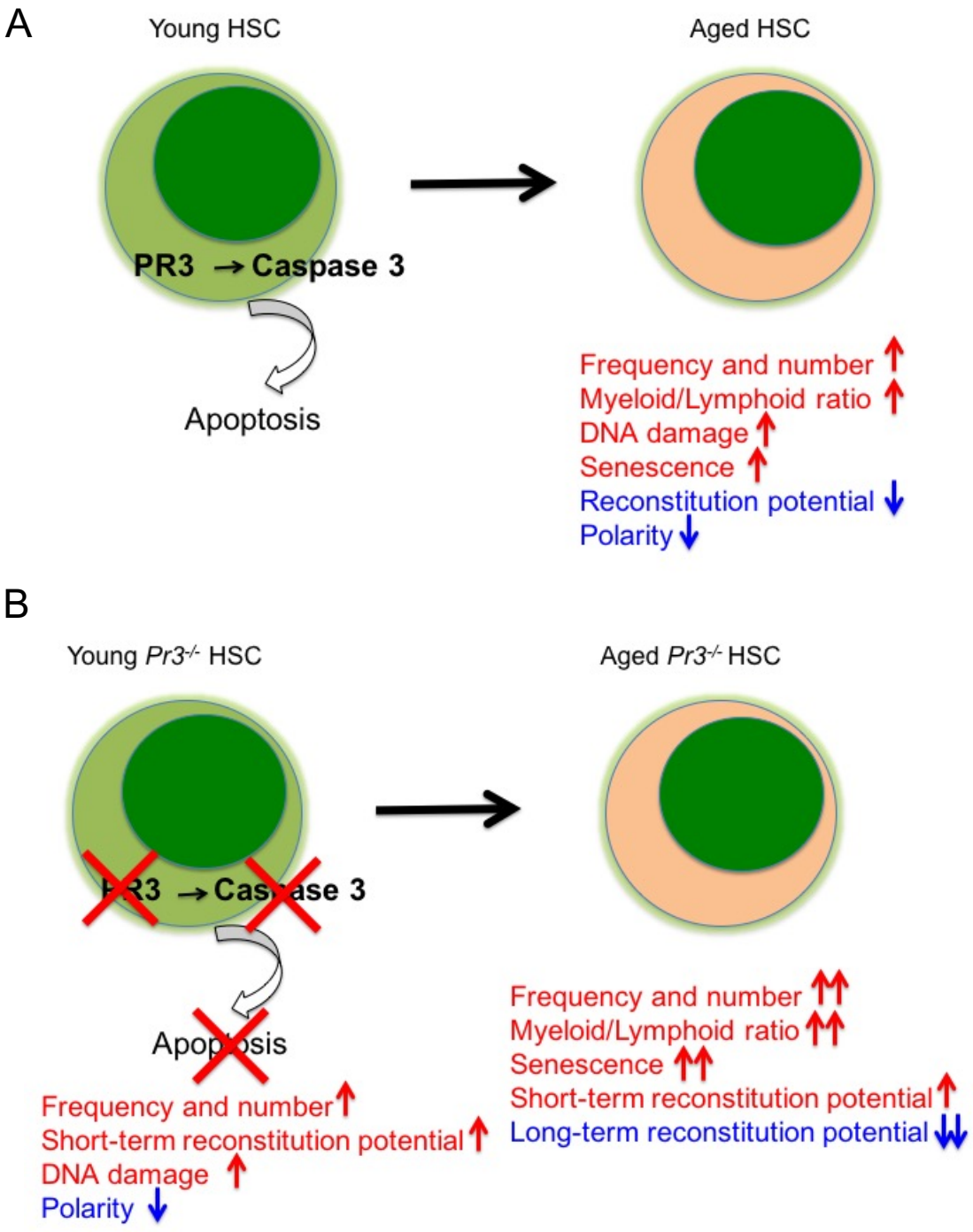

Figure 28. *Pr3* deficiency exacerbates HSC ageing. (A) Functional and phenotypic changes seen during HSC ageing. (B) Functional and phenotypic changes seen during HSC ageing in the absence of PR3.

We previously demonstrated that pro-caspase 3 is a direct PR3 target (Loison et al., 2014). Similar to *Pr3*$^{-/-}$ mice, caspase 3-deficient (Caspase 3$^{-/-}$) mice also have an expanded HSC pool (Janzen et al., 2008). Apoptosis was also decreased in Caspase 3-deficient HSCs *in vitro* but, intriguingly, there was increased proliferation in Caspase 3$^{-/-}$ HSCs as a consequence of hyperactive cytokine signaling. Janzen et al. attributed the expanded HSC pool in Caspase 3$^{-/-}$ mice to increased proliferation rather than decreased cell death (Janzen et al., 2008). However, we did not observe any differences in proliferation between WT and *Pr3*$^{-/-}$ mice or reduced survival in *Pr3*$^{-/-}$ HSCs *in vitro*. As noted above, the culture conditions used here contain hematopoietic cytokines that promote the expansion and differentiation of stem and progenitor cells. The cell death elicited by cytokines is likely to be mediated by caspase 9-dependent cleavage and caspase 3 activation and thus be independent of PR3. Additionally, cytokine-induced expansion and differentiation *in vitro* can mask the apoptosis rate of HSCs *in vivo*. Importantly, we detected reduced apoptosis in *Pr3*$^{-/-}$ LSK cells compared to WT LSK cells *in vivo* after depletion of BM macrophages. Of note, non-apoptotic roles for caspase 3 in hematopoiesis such as regulation of lymphocyte proliferation (Woo et al., 1998), differentiation (Yi and Yuan, 2009) and the silencing of type I IFN production in dying cells to render mitochondrial apoptosis immunologically silent (White et al., 2014) have also been described. It remains to be determined whether PR3 contributes to these non-apoptotic caspase 3 functions in hematopoiesis.

PR3 expression in cultured CD34^{+} cells is regulated by G-CSF and can confer cytokine-independent growth to a bone marrow-derived cell line (Lutz et al., 2000). While this finding was obtained *in vitro* with a pro-B cell line, our *in vivo* data suggest

that PR3 limits the HSPC compartments by driving the spontaneous turnover of HSCs. In another study, PR3 inhibition arrested growth in a promyelocytic leukemia cell line, HL-60, and promoted granulocytic differentiation (Bories et al., 1989). Similarly, we observed preferential myeloid development in PR3-deficient BM, although a higher proportion of myeloid cells were immature. These discrepancies can be explained by the differential functions of PR3 in the most primitive HSCs and progenitor cells. Additionally, the *in vitro* culture conditions may not closely resemble the *in vivo* BM environment for HSPC maintenance, self-renewal, and programmed death. Alternatively, in addition to the HSC-intrinsic defects seen in *Pr3*$^{-/-}$ HSCs, it is also possible that PR3 deficiency might lead to a block in maturation of neutrophils. This block could contribute to the preferential myeloid development. Due to the lack of well-established markers for immature myeloid cells (such as promyelocytes and myelocytes), this hypothesis could not be tested.

Intrinsic and extrinsic factors contribute to the stem cell fate. The HSPC pools undergo self-renewal and differentiation to ensure there are sufficient numbers of blood cells to fight infections and maintain homeostasis and host physiology. However, stem cells that have exhausted their proliferative potential or accumulated dangerous mutations need to undergo apoptosis to ensure that the HSC pool is healthy and to reduce the possibility of leukemia. The number of stem cells undergoing programmed cell death at a given point in time remains elusive. Inhibition of caspase activity can lead to enhanced engraftment of human CD34^{+} cells in NOD/SCID mice and increased *in vitro* clonogenicity of progenitors, confirming that cell death represents a significant fate for HSCs (V et al., 2010). Pharmacologic interventions such as antioxidative therapy,

rapamycin treatment, Cdc42 inhibition, and Bcl-2/Bcl-xL inhibition have all been shown to rejuvenate age-associated, HSC-intrinsic phenotypes (Chang et al., 2016; Chen et al., 2009; Florian et al., 2012; Ito et al., 2006). It is tempting to speculate that PR3 activation may be a physiological mechanism to rejuvenate the HSC compartment during ageing by inducing apoptosis of myeloid-skewed and/or damaged HSCs. Meanwhile, PR3 inhibition might be useful to accelerate and increase the efficiency of myeloid reconstitution during BM transplantation when the number of donor cells is limited.

In our studies looking at the role of PR3 in neutrophil function, we did not see a major defect in our assays in *Pr3*$^{-/-}$ neutrophils except for IL1β processing.

A previous study reported that PR3 can inhibit NADPH oxidase (Tal et al., 1998). Yet, this study looked at the ability of extracellular PR3 on unstimulated neutrophils whereas we directly investigated the intrinsic ability of PR3 to regulate ROS production. The previously proposed mechanism may indeed be valid to control excessive ROS production by suppressing distant cells after the generation of ROS and degranulation in stimulated cells, which leads to PR3 secretion to the extracellular space.

Although PR3 is not expressed on the cell surface of mouse neutrophils (Korkmaz et al., 2008), PR3 expression on the cell surface of human neutrophils has been reported to regulate the transmigration of a specific subset of neutrophils (Kuckleburg et al., 2012). Since Serpina1, an endogenous serine protease inhibitor, also inhibits neutrophil chemotaxis in a transwell assay (Stockley et al., 1990), we tested the effects of PR3 deficiency in *in vitro* adhesion and chemotaxis. There was no difference in the ability of *Pr3*$^{-/-}$ neutrophils to adhere to fibronectin and migrate towards

fMLP. These data along with the inhibitory effect of Serpina1 (Stockley et al., 1990) suggest that other serine proteases might compensate for PR3 deficiency.

In spite of the previously proposed role of PR3 in bacterial killing (Campanelli et al., 1990), *Pr3*$^{-/-}$ neutrophils could kill *E. coli* and *S. aureus* in both *in vitro* and *in vivo* studies as efficiently as wild-type neutrophils. In these studies, ROS and other serine proteases were sufficient to clear bacteria. It is important to note that we used self-limited infection models in bacteria-induced peritonitis studies. It remains to be determined if PR3 has a non-redundant role in more severe infection models (i.e. higher doses of bacteria), against other pathogens (i.e. *Streptococcus pneumoniae*) or in other infection models (i.e. pneumonia).

The role of PR3 in IL1β processing was first shown in THP-1 cells, a promonocytic leukemia cell line (Coeshott et al., 1999). Later studies identified that neutrophils deficient in Caspase 1, the central regulator of IL1β processing in macrophages, could secrete normal levels of IL1β (Greten et al., 2007). We found that PR3 was indeed essential for IL1β production in mouse neutrophils. In response to LPS, there was a 40% reduction in secreted IL1β levels in *Pr3*$^{-/-}$ neutrophils. This finding shows that other serine proteases could still process the proform of IL1β but with reduced efficiency. We also wanted to test the direct cleavage of pro-IL1β by PR3. Since an active recombinant mouse PR3 protein was not available, we used recombinant human proteins. We observed that PR3 cleaves pro-IL1β to generate mature fragments with full biological activity. These studies suggest that in acute infection models, where neutrophils are the primary source of IL1β secretion, neutrophil serine proteases can be utilized as potential targets with therapeutic potential. PR3

activation could lead to a more efficient immune response while resolution of inflammation might be accelerated with PR3 inhibition.

References

Adkison, A.M., Raptis, S.Z., Kelley, D.G., and Pham, C.T. (2002). Dipeptidyl peptidase I activates neutrophil-derived serine proteases and regulates the development of acute experimental arthritis. J Clin Invest *109*, 363-371.

Adolfsson, J., Borge, O.J., Bryder, D., Theilgaard-Monch, K., Astrand-Grundstrom, I., Sitnicka, E., Sasaki, Y., and Jacobsen, S.E. (2001). Upregulation of Flt3 expression within the bone marrow Lin(-)Sca1(+)c-kit(+) stem cell compartment is accompanied by loss of self-renewal capacity. Immunity *15*, 659-669.

Akashi, K., Traver, D., Miyamoto, T., and Weissman, I.L. (2000). A clonogenic common myeloid progenitor that gives rise to all myeloid lineages. Nature *404*, 193-197.

Alkalay, I., Yaron, A., Hatzubai, A., Orian, A., Ciechanover, A., and Ben-Neriah, Y. (1995). Stimulation-dependent I kappa B alpha phosphorylation marks the NF-kappa B inhibitor for degradation via the ubiquitin-proteasome pathway. Proc Natl Acad Sci U S A *92*, 10599-10603.

Allport, J.R., Lim, Y.C., Shipley, J.M., Senior, R.M., Shapiro, S.D., Matsuyoshi, N., Vestweber, D., and Luscinskas, F.W. (2002). Neutrophils from MMP-9- or neutrophil elastase-deficient mice show no defect in transendothelial migration under flow in vitro. J Leukoc Biol *71*, 821-828.

Antonchuk, J., Sauvageau, G., and Humphries, R.K. (2002). HOXB4-induced expansion of adult hematopoietic stem cells ex vivo. Cell *109*, 39-45.

Arai, F., Hirao, A., Ohmura, M., Sato, H., Matsuoka, S., Takubo, K., Ito, K., Koh, G.Y., and Suda, T. (2004). Tie2/angiopoietin-1 signaling regulates hematopoietic stem cell quiescence in the bone marrow niche. Cell *118*, 149-161.

Baici, A., Szedlacsek, S.E., Fruh, H., and Michel, B.A. (1996). pH-dependent hysteretic behaviour of human myeloblastin (leucocyte proteinase 3). Biochem J *317 (Pt 3)*, 901-905.

Baker, D.J., Childs, B.G., Durik, M., Wijers, M.E., Sieben, C.J., Zhong, J., Saltness, R.A., Jeganathan, K.B., Verzosa, G.C., Pezeshki, A.*, et al.* (2016). Naturally occurring p16(Ink4a)-positive cells shorten healthy lifespan. Nature *530*, 184-189.

Bank, U., Kupper, B., Reinhold, D., Hoffmann, T., and Ansorge, S. (1999). Evidence for a crucial role of neutrophil-derived serine proteases in the inactivation of interleukin-6 at sites of inflammation. FEBS Lett *461*, 235-240.

Beerman, I., Bhattacharya, D., Zandi, S., Sigvardsson, M., Weissman, I.L., Bryder, D., and Rossi, D.J. (2010). Functionally distinct hematopoietic stem cells modulate

hematopoietic lineage potential during aging by a mechanism of clonal expansion. Proc Natl Acad Sci U S A *107*, 5465-5470.

Beerman, I., Bock, C., Garrison, B.S., Smith, Z.D., Gu, H., Meissner, A., and Rossi, D.J. (2013). Proliferation-dependent alterations of the DNA methylation landscape underlie hematopoietic stem cell aging. Cell Stem Cell *12*, 413-425.

Beerman, I., Seita, J., Inlay, M.A., Weissman, I.L., and Rossi, D.J. (2014). Quiescent hematopoietic stem cells accumulate DNA damage during aging that is repaired upon entry into cell cycle. Cell Stem Cell *15*, 37-50.

Belaaouaj, A., Kim, K.S., and Shapiro, S.D. (2000). Degradation of outer membrane protein A in Escherichia coli killing by neutrophil elastase. Science *289*, 1185-1188.

Belaaouaj, A., McCarthy, R., Baumann, M., Gao, Z., Ley, T.J., Abraham, S.N., and Shapiro, S.D. (1998). Mice lacking neutrophil elastase reveal impaired host defense against gram negative bacterial sepsis. Nat Med *4*, 615-618.

Bernad, A., Kopf, M., Kulbacki, R., Weich, N., Koehler, G., and Gutierrez-Ramos, J.C. (1994). Interleukin-6 is required in vivo for the regulation of stem cells and committed progenitors of the hematopoietic system. Immunity *1*, 725-731.

Bories, D., Raynal, M.C., Solomon, D.H., Darzynkiewicz, Z., and Cayre, Y.E. (1989). Down-regulation of a serine protease, myeloblastin, causes growth arrest and differentiation of promyelocytic leukemia cells. Cell *59*, 959-968.

Brandt, J., Briddell, R.A., Srour, E.F., Leemhuis, T.B., and Hoffman, R. (1992). Role of c-kit ligand in the expansion of human hematopoietic progenitor cells. Blood *79*, 634-641.

Brun, A.C., Bjornsson, J.M., Magnusson, M., Larsson, N., Leveen, P., Ehinger, M., Nilsson, E., and Karlsson, S. (2004). Hoxb4-deficient mice undergo normal hematopoietic development but exhibit a mild proliferation defect in hematopoietic stem cells. Blood *103*, 4126-4133.

Bryder, D., and Jacobsen, S.E. (2000). Interleukin-3 supports expansion of long-term multilineage repopulating activity after multiple stem cell divisions in vitro. Blood *96*, 1748-1755.

Campanelli, D., Detmers, P.A., Nathan, C.F., and Gabay, J.E. (1990). Azurocidin and a homologous serine protease from neutrophils. Differential antimicrobial and proteolytic properties. J Clin Invest *85*, 904-915.

Campbell, E.J., Campbell, M.A., and Owen, C.A. (2000). Bioactive proteinase 3 on the cell surface of human neutrophils: quantification, catalytic activity, and susceptibility to inhibition. J Immunol *165*, 3366-3374.

Challen, G.A., Boles, N.C., Chambers, S.M., and Goodell, M.A. (2010). Distinct hematopoietic stem cell subtypes are differentially regulated by TGF-beta1. Cell Stem Cell *6*, 265-278.

Chambers, S.M., Boles, N.C., Lin, K.Y., Tierney, M.P., Bowman, T.V., Bradfute, S.B., Chen, A.J., Merchant, A.A., Sirin, O., Weksberg, D.C.*, et al.* (2007a). Hematopoietic fingerprints: an expression database of stem cells and their progeny. Cell Stem Cell *1*, 578-591.

Chambers, S.M., Shaw, C.A., Gatza, C., Fisk, C.J., Donehower, L.A., and Goodell, M.A. (2007b). Aging hematopoietic stem cells decline in function and exhibit epigenetic dysregulation. PLoS Biol *5*, e201.

Chang, J., Wang, Y., Shao, L., Laberge, R.M., Demaria, M., Campisi, J., Janakiraman, K., Sharpless, N.E., Ding, S., Feng, W.*, et al.* (2016). Clearance of senescent cells by ABT263 rejuvenates aged hematopoietic stem cells in mice. Nat Med *22*, 78-83.

Chen, C., Liu, Y., Liu, R., Ikenoue, T., Guan, K.L., Liu, Y., and Zheng, P. (2008). TSC-mTOR maintains quiescence and function of hematopoietic stem cells by repressing mitochondrial biogenesis and reactive oxygen species. J Exp Med *205*, 2397-2408.

Chen, C., Liu, Y., Liu, Y., and Zheng, P. (2009). mTOR regulation and therapeutic rejuvenation of aging hematopoietic stem cells. Sci Signal *2*, ra75.

Cheng, E.H., Wei, M.C., Weiler, S., Flavell, R.A., Mak, T.W., Lindsten, T., and Korsmeyer, S.J. (2001). BCL-2, BCL-X(L) sequester BH3 domain-only molecules preventing BAX- and BAK-mediated mitochondrial apoptosis. Mol Cell *8*, 705-711.

Cheng, T., Rodrigues, N., Shen, H., Yang, Y., Dombkowski, D., Sykes, M., and Scadden, D.T. (2000). Hematopoietic stem cell quiescence maintained by p21cip1/waf1. Science *287*, 1804-1808.

Cheshier, S.H., Morrison, S.J., Liao, X., and Weissman, I.L. (1999). In vivo proliferation and cell cycle kinetics of long-term self-renewing hematopoietic stem cells. Proc Natl Acad Sci U S A *96*, 3120-3125.

Chow, A., Lucas, D., Hidalgo, A., Mendez-Ferrer, S., Hashimoto, D., Scheiermann, C., Battista, M., Leboeuf, M., Prophete, C., van Rooijen, N.*, et al.* (2011). Bone marrow CD169+ macrophages promote the retention of hematopoietic stem and progenitor cells in the mesenchymal stem cell niche. J Exp Med *208*, 261-271.

Christensen, J.L., and Weissman, I.L. (2001). Flk-2 is a marker in hematopoietic stem cell differentiation: a simple method to isolate long-term stem cells. Proc Natl Acad Sci U S A *98*, 14541-14546.

Coeshott, C., Ohnemus, C., Pilyavskaya, A., Ross, S., Wieczorek, M., Kroona, H., Leimer, A.H., and Cheronis, J. (1999). Converting enzyme-independent release of tumor necrosis factor alpha and IL-1beta from a stimulated human monocytic cell line in the presence of activated neutrophils or purified proteinase 3. Proc Natl Acad Sci U S A *96*, 6261-6266.

Dimri, G.P., Lee, X., Basile, G., Acosta, M., Scott, G., Roskelley, C., Medrano, E.E., Linskens, M., Rubelj, I., Pereira-Smith, O.*, et al.* (1995). A biomarker that identifies senescent human cells in culture and in aging skin in vivo. Proc Natl Acad Sci U S A *92*, 9363-9367.

Domen, J., Cheshier, S.H., and Weissman, I.L. (2000). The role of apoptosis in the regulation of hematopoietic stem cells: Overexpression of Bcl-2 increases both their number and repopulation potential. J Exp Med *191*, 253-264.

Dublet, B., Ruello, A., Pederzoli, M., Hajjar, E., Courbebaisse, M., Canteloup, S., Reuter, N., and Witko-Sarsat, V. (2005). Cleavage of p21/WAF1/CIP1 by proteinase 3 modulates differentiation of a monocytic cell line. Molecular analysis of the cleavage site. J Biol Chem *280*, 30242-30253.

Dykstra, B., Olthof, S., Schreuder, J., Ritsema, M., and de Haan, G. (2011). Clonal analysis reveals multiple functional defects of aged murine hematopoietic stem cells. J Exp Med *208*, 2691-2703.

Enari, M., Sakahira, H., Yokoyama, H., Okawa, K., Iwamatsu, A., and Nagata, S. (1998). A caspase-activated DNase that degrades DNA during apoptosis, and its inhibitor ICAD. Nature *391*, 43-50.

Ergen, A.V., Boles, N.C., and Goodell, M.A. (2012). Rantes/Ccl5 influences hematopoietic stem cell subtypes and causes myeloid skewing. Blood *119*, 2500-2509.

Ernst, P., Fisher, J.K., Avery, W., Wade, S., Foy, D., and Korsmeyer, S.J. (2004). Definitive hematopoiesis requires the mixed-lineage leukemia gene. Dev Cell *6*, 437-443.

Flach, J., Bakker, S.T., Mohrin, M., Conroy, P.C., Pietras, E.M., Reynaud, D., Alvarez, S., Diolaiti, M.E., Ugarte, F., Forsberg, E.C.*, et al.* (2014). Replication stress is a potent driver of functional decline in ageing haematopoietic stem cells. Nature *512*, 198-202.

Florian, M.C., Dorr, K., Niebel, A., Daria, D., Schrezenmeier, H., Rojewski, M., Filippi, M.D., Hasenberg, A., Gunzer, M., Scharffetter-Kochanek, K.*, et al.* (2012). Cdc42 activity regulates hematopoietic stem cell aging and rejuvenation. Cell Stem Cell *10*, 520-530.

Garwicz, D., Lindmark, A., Hellmark, T., Gladh, M., Jogi, J., and Gullberg, U. (1997). Characterization of the processing and granular targeting of human proteinase 3 after

transfection to the rat RBL or the murine 32D leukemic cell lines. J Leukoc Biol *61*, 113-123.

Giuliani, A.L., Wiener, E., Lee, M.J., Brown, I.N., Berti, G., and Wickramasinghe, S.N. (2001). Changes in murine bone marrow macrophages and erythroid burst-forming cells following the intravenous injection of liposome-encapsulated dichloromethylene diphosphonate (Cl2MDP). Eur J Haematol *66*, 221-229.

Greten, F.R., Arkan, M.C., Bollrath, J., Hsu, L.C., Goode, J., Miething, C., Goktuna, S.I., Neuenhahn, M., Fierer, J., Paxian, S.*, et al.* (2007). NF-kappaB is a negative regulator of IL-1beta secretion as revealed by genetic and pharmacological inhibition of IKKbeta. Cell *130*, 918-931.

Grover, A., Mancini, E., Moore, S., Mead, A.J., Atkinson, D., Rasmussen, K.D., O'Carroll, D., Jacobsen, S.E., and Nerlov, C. (2014). Erythropoietin guides multipotent hematopoietic progenitor cells toward an erythroid fate. J Exp Med *211*, 181-188.

Henschler, R., Brugger, W., Luft, T., Frey, T., Mertelsmann, R., and Kanz, L. (1994). Maintenance of transplantation potential in ex vivo expanded CD34(+)-selected human peripheral blood progenitor cells. Blood *84*, 2898-2903.

Hock, H., Hamblen, M.J., Rooke, H.M., Schindler, J.W., Saleque, S., Fujiwara, Y., and Orkin, S.H. (2004a). Gfi-1 restricts proliferation and preserves functional integrity of haematopoietic stem cells. Nature *431*, 1002-1007.

Hock, H., Meade, E., Medeiros, S., Schindler, J.W., Valk, P.J., Fujiwara, Y., and Orkin, S.H. (2004b). Tel/Etv6 is an essential and selective regulator of adult hematopoietic stem cell survival. Genes Dev *18*, 2336-2341.

Holyoake, T.L., Freshney, M.G., McNair, L., Parker, A.N., McKay, P.J., Steward, W.P., Fitzsimons, E., Graham, G.J., and Pragnell, I.B. (1996). Ex vivo expansion with stem cell factor and interleukin-11 augments both short-term recovery posttransplant and the ability to serially transplant marrow. Blood *87*, 4589-4595.

Hsu, C.L., King-Fleischman, A.G., Lai, A.Y., Matsumoto, Y., Weissman, I.L., and Kondo, M. (2006). Antagonistic effect of CCAAT enhancer-binding protein-alpha and Pax5 in myeloid or lymphoid lineage choice in common lymphoid progenitors. Proc Natl Acad Sci U S A *103*, 672-677.

Hyatt, G., Melamed, R., Park, R., Seguritan, R., Laplace, C., Poirot, L., Zucchelli, S., Obst, R., Matos, M., Venanzi, E.*, et al.* (2006). Gene expression microarrays: glimpses of the immunological genome. Nat Immunol *7*, 686-691.

Imai, Y., Adachi, Y., Shi, M., Shima, C., Yanai, S., Okigaki, M., Yamashima, T., Kaneko, K., and Ikehara, S. (2010). Caspase inhibitor ZVAD-fmk facilitates engraftment of donor

hematopoietic stem cells in intra-bone marrow-bone marrow transplantation. Stem Cells Dev *19*, 461-468.

Ito, K., Hirao, A., Arai, F., Takubo, K., Matsuoka, S., Miyamoto, K., Ohmura, M., Naka, K., Hosokawa, K., Ikeda, Y.*, et al.* (2006). Reactive oxygen species act through p38 MAPK to limit the lifespan of hematopoietic stem cells. Nat Med *12*, 446-451.

Iwasaki, H., Mizuno, S., Arinobu, Y., Ozawa, H., Mori, Y., Shigematsu, H., Takatsu, K., Tenen, D.G., and Akashi, K. (2006). The order of expression of transcription factors directs hierarchical specification of hematopoietic lineages. Genes Dev *20*, 3010-3021.

Iwasaki, H., Mizuno, S., Wells, R.A., Cantor, A.B., Watanabe, S., and Akashi, K. (2003). GATA-1 converts lymphoid and myelomonocytic progenitors into the megakaryocyte/erythrocyte lineages. Immunity *19*, 451-462.

Janzen, V., Fleming, H.E., Riedt, T., Karlsson, G., Riese, M.J., Lo Celso, C., Reynolds, G., Milne, C.D., Paige, C.J., Karlsson, S.*, et al.* (2008). Hematopoietic stem cell responsiveness to exogenous signals is limited by caspase-3. Cell Stem Cell *2*, 584-594.

Janzen, V., Forkert, R., Fleming, H.E., Saito, Y., Waring, M.T., Dombkowski, D.M., Cheng, T., DePinho, R.A., Sharpless, N.E., and Scadden, D.T. (2006). Stem-cell ageing modified by the cyclin-dependent kinase inhibitor p16INK4a. Nature *443*, 421-426.

Jenne, D.E., Tschopp, J., Ludemann, J., Utecht, B., and Gross, W.L. (1990). Wegener's autoantigen decoded. Nature *346*, 520.

Karanu, F.N., Murdoch, B., Gallacher, L., Wu, D.M., Koremoto, M., Sakano, S., and Bhatia, M. (2000). The notch ligand jagged-1 represents a novel growth factor of human hematopoietic stem cells. J Exp Med *192*, 1365-1372.

Kessenbrock, K., Frohlich, L., Sixt, M., Lammermann, T., Pfister, H., Bateman, A., Belaaouaj, A., Ring, J., Ollert, M., Fassler, R.*, et al.* (2008). Proteinase 3 and neutrophil elastase enhance inflammation in mice by inactivating antiinflammatory progranulin. J Clin Invest *118*, 2438-2447.

Kiel, M.J., Yilmaz, O.H., Iwashita, T., Yilmaz, O.H., Terhorst, C., and Morrison, S.J. (2005). SLAM family receptors distinguish hematopoietic stem and progenitor cells and reveal endothelial niches for stem cells. Cell *121*, 1109-1121.

Kikushige, Y., Yoshimoto, G., Miyamoto, T., Iino, T., Mori, Y., Iwasaki, H., Niiro, H., Takenaka, K., Nagafuji, K., Harada, M.*, et al.* (2008). Human Flt3 is expressed at the hematopoietic stem cell and the granulocyte/macrophage progenitor stages to maintain cell survival. J Immunol *180*, 7358-7367.

Kim, J., Kundu, M., Viollet, B., and Guan, K.L. (2011). AMPK and mTOR regulate autophagy through direct phosphorylation of Ulk1. Nat Cell Biol *13*, 132-141.

Kohler, A., Schmithorst, V., Filippi, M.D., Ryan, M.A., Daria, D., Gunzer, M., and Geiger, H. (2009). Altered cellular dynamics and endosteal location of aged early hematopoietic progenitor cells revealed by time-lapse intravital imaging in long bones. Blood *114*, 290-298.

Kondo, M., Weissman, I.L., and Akashi, K. (1997). Identification of clonogenic common lymphoid progenitors in mouse bone marrow. Cell *91*, 661-672.

Korkmaz, B., Jaillet, J., Jourdan, M.L., Gauthier, A., Gauthier, F., and Attucci, S. (2009). Catalytic activity and inhibition of wegener antigen proteinase 3 on the cell surface of human polymorphonuclear neutrophils. J Biol Chem *284*, 19896-19902.

Korkmaz, B., Kuhl, A., Bayat, B., Santoso, S., and Jenne, D.E. (2008). A hydrophobic patch on proteinase 3, the target of autoantibodies in Wegener granulomatosis, mediates membrane binding via NB1 receptors. J Biol Chem *283*, 35976-35982.

Krishnamurthy, J., Torrice, C., Ramsey, M.R., Kovalev, G.I., Al-Regaiey, K., Su, L., and Sharpless, N.E. (2004). Ink4a/Arf expression is a biomarker of aging. J Clin Invest *114*, 1299-1307.

Kuckleburg, C.J., Tilkens, S.B., Santoso, S., and Newman, P.J. (2012). Proteinase 3 contributes to transendothelial migration of NB1-positive neutrophils. J Immunol *188*, 2419-2426.

Labbaye, C., Zhang, J., Casanova, J.L., Lanotte, M., Teng, J., Miller, W.H., Jr., and Cayre, Y.E. (1993). Regulation of myeloblastin messenger RNA expression in myeloid leukemia cells treated with all-trans retinoic acid. Blood *81*, 475-481.

Lacorazza, H.D., Yamada, T., Liu, Y., Miyata, Y., Sivina, M., Nunes, J., and Nimer, S.D. (2006). The transcription factor MEF/ELF4 regulates the quiescence of primitive hematopoietic cells. Cancer Cell *9*, 175-187.

Liang, Y., Van Zant, G., and Szilvassy, S.J. (2005). Effects of aging on the homing and engraftment of murine hematopoietic stem and progenitor cells. Blood *106*, 1479-1487.

Loison, F., Zhu, H., Karatepe, K., Kasorn, A., Liu, P., Ye, K., Zhou, J., Cao, S., Gong, H., Jenne, D.E.*, et al.* (2014). Proteinase 3-dependent caspase-3 cleavage modulates neutrophil death and inflammation. J Clin Invest *124*, 4445-4458.

Lopez-Boado, Y.S., Espinola, M., Bahr, S., and Belaaouaj, A. (2004). Neutrophil serine proteinases cleave bacterial flagellin, abrogating its host response-inducing activity. J Immunol *172*, 509-515.

Ludemann, J., Utecht, B., and Gross, W.L. (1990). Anti-neutrophil cytoplasm antibodies in Wegener's granulomatosis recognize an elastinolytic enzyme. J Exp Med *171*, 357-362.

Lundqvist, H., and Dahlgren, C. (1996). Isoluminol-enhanced chemiluminescence: a sensitive method to study the release of superoxide anion from human neutrophils. Free Radic Biol Med *20*, 785-792.

Lutz, P.G., Moog-Lutz, C., Coumau-Gatbois, E., Kobari, L., Di Gioia, Y., and Cayre, Y.E. (2000). Myeloblastin is a granulocyte colony-stimulating factor-responsive gene conferring factor-independent growth to hematopoietic cells. Proc Natl Acad Sci U S A *97*, 1601-1606.

MacIvor, D.M., Shapiro, S.D., Pham, C.T., Belaaouaj, A., Abraham, S.N., and Ley, T.J. (1999). Normal neutrophil function in cathepsin G-deficient mice. Blood *94*, 4282-4293.

Matsumoto, A., Takeishi, S., Kanie, T., Susaki, E., Onoyama, I., Tateishi, Y., Nakayama, K., and Nakayama, K.I. (2011). p57 is required for quiescence and maintenance of adult hematopoietic stem cells. Cell Stem Cell *9*, 262-271.

McKenzie, J.L., Gan, O.I., Doedens, M., Wang, J.C., and Dick, J.E. (2006). Individual stem cells with highly variable proliferation and self-renewal properties comprise the human hematopoietic stem cell compartment. Nat Immunol *7*, 1225-1233.

Medema, R.H., Kops, G.J., Bos, J.L., and Burgering, B.M. (2000). AFX-like Forkhead transcription factors mediate cell-cycle regulation by Ras and PKB through p27kip1. Nature *404*, 782-787.

Miller, C.L., and Eaves, C.J. (1997). Expansion in vitro of adult murine hematopoietic stem cells with transplantable lympho-myeloid reconstituting ability. Proc Natl Acad Sci U S A *94*, 13648-13653.

Morrison, S.J., Wandycz, A.M., Akashi, K., Globerson, A., and Weissman, I.L. (1996). The aging of hematopoietic stem cells. Nat Med *2*, 1011-1016.

Morrison, S.J., and Weissman, I.L. (1994). The long-term repopulating subset of hematopoietic stem cells is deterministic and isolatable by phenotype. Immunity *1*, 661-673.

Mortensen, M., Soilleux, E.J., Djordjevic, G., Tripp, R., Lutteropp, M., Sadighi-Akha, E., Stranks, A.J., Glanville, J., Knight, S., Jacobsen, S.E.*, et al.* (2011). The autophagy protein Atg7 is essential for hematopoietic stem cell maintenance. J Exp Med *208*, 455-467.

Muller, A.M., Medvinsky, A., Strouboulis, J., Grosveld, F., and Dzierzak, E. (1994). Development of hematopoietic stem cell activity in the mouse embryo. Immunity *1*, 291-301.

Nakamura, N., Ramaswamy, S., Vazquez, F., Signoretti, S., Loda, M., and Sellers, W.R. (2000). Forkhead transcription factors are critical effectors of cell death and cell cycle arrest downstream of PTEN. Mol Cell Biol *20*, 8969-8982.

Nerlov, C., Querfurth, E., Kulessa, H., and Graf, T. (2000). GATA-1 interacts with the myeloid PU.1 transcription factor and represses PU.1-dependent transcription. Blood *95*, 2543-2551.

Nijnik, A., Woodbine, L., Marchetti, C., Dawson, S., Lambe, T., Liu, C., Rodrigues, N.P., Crockford, T.L., Cabuy, E., Vindigni, A.*, et al.* (2007). DNA repair is limiting for haematopoietic stem cells during ageing. Nature *447*, 686-690.

Notta, F., Zandi, S., Takayama, N., Dobson, S., Gan, O.I., Wilson, G., Kaufmann, K.B., McLeod, J., Laurenti, E., Dunant, C.F.*, et al.* (2016). Distinct routes of lineage development reshape the human blood hierarchy across ontogeny. Science *351*, aab2116.

Ogawa, M. (1993). Differentiation and proliferation of hematopoietic stem cells. Blood *81*, 2844-2853.

Ogawa, M., Matsuzaki, Y., Nishikawa, S., Hayashi, S., Kunisada, T., Sudo, T., Kina, T., Nakauchi, H., and Nishikawa, S. (1991). Expression and function of c-kit in hemopoietic progenitor cells. J Exp Med *174*, 63-71.

Okuda, T., van Deursen, J., Hiebert, S.W., Grosveld, G., and Downing, J.R. (1996). AML1, the target of multiple chromosomal translocations in human leukemia, is essential for normal fetal liver hematopoiesis. Cell *84*, 321-330.

Olofsson, T., Nilsson, E., and Olsson, I. (1984). Characterization of the cells in myeloid leukemia that produce leukemia associated inhibitor (LAI) and demonstration of LAI-producing cells in normal bone marrow. Leuk Res *8*, 387-396.

Olofsson, T., and Olsson, I. (1980a). Biochemical characterization of a leukemia-associated inhibitor (LAI) suppressing normal granulopoiesis in vitro. Blood *55*, 983-991.

Olofsson, T., and Olsson, I. (1980b). Suppression of normal granulopoiesis in vitro by a leukemia-associated inhibitor (LAI) of acute and chronic leukemia. Blood *55*, 975-982.

Opferman, J.T., Iwasaki, H., Ong, C.C., Suh, H., Mizuno, S., Akashi, K., and Korsmeyer, S.J. (2005). Obligate role of anti-apoptotic MCL-1 in the survival of hematopoietic stem cells. Science *307*, 1101-1104.

Orkin, S.H., and Zon, L.I. (2008). Hematopoiesis: an evolving paradigm for stem cell biology. Cell *132*, 631-644.

Osawa, M., Hanada, K., Hamada, H., and Nakauchi, H. (1996). Long-term lymphohematopoietic reconstitution by a single CD34-low/negative hematopoietic stem cell. Science *273*, 242-245.

Padrines, M., Wolf, M., Walz, A., and Baggiolini, M. (1994). Interleukin-8 processing by neutrophil elastase, cathepsin G and proteinase-3. FEBS Lett *352*, 231-235.

Pang, W.W., Price, E.A., Sahoo, D., Beerman, I., Maloney, W.J., Rossi, D.J., Schrier, S.L., and Weissman, I.L. (2011). Human bone marrow hematopoietic stem cells are increased in frequency and myeloid-biased with age. Proc Natl Acad Sci U S A *108*, 20012-20017.

Park, I.K., Qian, D., Kiel, M., Becker, M.W., Pihalja, M., Weissman, I.L., Morrison, S.J., and Clarke, M.F. (2003). Bmi-1 is required for maintenance of adult self-renewing haematopoietic stem cells. Nature *423*, 302-305.

Paul, F., Arkin, Y., Giladi, A., Jaitin, D.A., Kenigsberg, E., Keren-Shaul, H., Winter, D., Lara-Astiaso, D., Gury, M., Weiner, A.*, et al.* (2015). Transcriptional Heterogeneity and Lineage Commitment in Myeloid Progenitors. Cell *163*, 1663-1677.

Pederzoli, M., Kantari, C., Gausson, V., Moriceau, S., and Witko-Sarsat, V. (2005). Proteinase-3 induces procaspase-3 activation in the absence of apoptosis: potential role of this compartmentalized activation of membrane-associated procaspase-3 in neutrophils. J Immunol *174*, 6381-6390.

Pendergraft, W.F., 3rd, Rudolph, E.H., Falk, R.J., Jahn, J.E., Grimmler, M., Hengst, L., Jennette, J.C., and Preston, G.A. (2004). Proteinase 3 sidesteps caspases and cleaves p21(Waf1/Cip1/Sdi1) to induce endothelial cell apoptosis. Kidney Int *65*, 75-84.

Perera, N.C., Schilling, O., Kittel, H., Back, W., Kremmer, E., and Jenne, D.E. (2012). NSP4, an elastase-related protease in human neutrophils with arginine specificity. Proc Natl Acad Sci U S A *109*, 6229-6234.

Pham, C.T. (2006). Neutrophil serine proteases: specific regulators of inflammation. Nat Rev Immunol *6*, 541-550.

Porcher, C., Swat, W., Rockwell, K., Fujiwara, Y., Alt, F.W., and Orkin, S.H. (1996). The T cell leukemia oncoprotein SCL/tal-1 is essential for development of all hematopoietic lineages. Cell *86*, 47-57.

Preston, G.A., Zarella, C.S., Pendergraft, W.F., 3rd, Rudolph, E.H., Yang, J.J., Sekura, S.B., Jennette, J.C., and Falk, R.J. (2002). Novel effects of neutrophil-derived proteinase 3 and elastase on the vascular endothelium involve in vivo cleavage of NF-

kappaB and proapoptotic changes in JNK, ERK, and p38 MAPK signaling pathways. J Am Soc Nephrol *13*, 2840-2849.

Rao, J., Zhang, F., Donnelly, R.J., Spector, N.L., and Studzinski, G.P. (1998). Truncation of Sp1 transcription factor by myeloblastin in undifferentiated HL60 cells. J Cell Physiol *175*, 121-128.

Rao, N.V., Rao, G.V., Marshall, B.C., and Hoidal, J.R. (1996). Biosynthesis and processing of proteinase 3 in U937 cells. Processing pathways are distinct from those of cathepsin G. J Biol Chem *271*, 2972-2978.

Rao, N.V., Wehner, N.G., Marshall, B.C., Gray, W.R., Gray, B.H., and Hoidal, J.R. (1991). Characterization of proteinase-3 (PR-3), a neutrophil serine proteinase. Structural and functional properties. J Biol Chem *266*, 9540-9548.

Rarok, A.A., Stegeman, C.A., Limburg, P.C., and Kallenberg, C.G. (2002). Neutrophil membrane expression of proteinase 3 (PR3) is related to relapse in PR3-ANCA-associated vasculitis. J Am Soc Nephrol *13*, 2232-2238.

Reya, T., Duncan, A.W., Ailles, L., Domen, J., Scherer, D.C., Willert, K., Hintz, L., Nusse, R., and Weissman, I.L. (2003). A role for Wnt signalling in self-renewal of haematopoietic stem cells. Nature *423*, 409-414.

Robertson, S.E., Young, J.D., Kitson, S., Pitt, A., Evans, J., Roes, J., Karaoglu, D., Santora, L., Ghayur, T., Liew, F.Y.*, et al.* (2006). Expression and alternative processing of IL-18 in human neutrophils. Eur J Immunol *36*, 722-731.

Ross, E.A., Anderson, N., and Micklem, H.S. (1982). Serial depletion and regeneration of the murine hematopoietic system. Implications for hematopoietic organization and the study of cellular aging. J Exp Med *155*, 432-444.

Rossi, D.J., Bryder, D., Seita, J., Nussenzweig, A., Hoeijmakers, J., and Weissman, I.L. (2007a). Deficiencies in DNA damage repair limit the function of haematopoietic stem cells with age. Nature *447*, 725-729.

Rossi, D.J., Bryder, D., Zahn, J.M., Ahlenius, H., Sonu, R., Wagers, A.J., and Weissman, I.L. (2005). Cell intrinsic alterations underlie hematopoietic stem cell aging. Proc Natl Acad Sci U S A *102*, 9194-9199.

Rossi, D.J., Seita, J., Czechowicz, A., Bhattacharya, D., Bryder, D., and Weissman, I.L. (2007b). Hematopoietic stem cell quiescence attenuates DNA damage response and permits DNA damage accumulation during aging. Cell Cycle *6*, 2371-2376.

Rube, C.E., Fricke, A., Widmann, T.A., Furst, T., Madry, H., Pfreundschuh, M., and Rube, C. (2011). Accumulation of DNA damage in hematopoietic stem and progenitor cells during human aging. PLoS One *6*, e17487.

Satoh, Y., Matsumura, I., Tanaka, H., Ezoe, S., Sugahara, H., Mizuki, M., Shibayama, H., Ishiko, E., Ishiko, J., Nakajima, K.*, et al.* (2004). Roles for c-Myc in self-renewal of hematopoietic stem cells. J Biol Chem *279*, 24986-24993.

Schmidt, M., Fernandez de Mattos, S., van der Horst, A., Klompmaker, R., Kops, G.J., Lam, E.W., Burgering, B.M., and Medema, R.H. (2002). Cell cycle inhibition by FoxO forkhead transcription factors involves downregulation of cyclin D. Mol Cell Biol *22*, 7842-7852.

Shimizu, S., Eguchi, Y., Kamiike, W., Matsuda, H., and Tsujimoto, Y. (1996). Bcl-2 expression prevents activation of the ICE protease cascade. Oncogene *12*, 2251-2257.

Sieburg, H.B., Rezner, B.D., and Muller-Sieburg, C.E. (2011). Predicting clonal self-renewal and extinction of hematopoietic stem cells. Proc Natl Acad Sci U S A *108*, 4370-4375.

Siminovitch, L., Till, J.E., and McCulloch, E.A. (1964). Decline in Colony-Forming Ability of Marrow Cells Subjected to Serial Transplantation into Irradiated Mice. J Cell Physiol *64*, 23-31.

Simsek, T., Kocabas, F., Zheng, J., Deberardinis, R.J., Mahmoud, A.I., Olson, E.N., Schneider, J.W., Zhang, C.C., and Sadek, H.A. (2010). The distinct metabolic profile of hematopoietic stem cells reflects their location in a hypoxic niche. Cell Stem Cell *7*, 380-390.

Skold, S., Rosberg, B., Gullberg, U., and Olofsson, T. (1999). A secreted proform of neutrophil proteinase 3 regulates the proliferation of granulopoietic progenitor cells. Blood *93*, 849-856.

Sorensen, O.E., Follin, P., Johnsen, A.H., Calafat, J., Tjabringa, G.S., Hiemstra, P.S., and Borregaard, N. (2001). Human cathelicidin, hCAP-18, is processed to the antimicrobial peptide LL-37 by extracellular cleavage with proteinase 3. Blood *97*, 3951-3959.

Spangrude, G.J., Heimfeld, S., and Weissman, I.L. (1988). Purification and characterization of mouse hematopoietic stem cells. Science *241*, 58-62.

Spector, N.L., Hardy, L., Ryan, C., Miller, W.H., Jr., Humes, J.L., Nadler, L.M., and Luedke, E. (1995). 28-kDa mammalian heat shock protein, a novel substrate of a growth regulatory protease involved in differentiation of human leukemia cells. J Biol Chem *270*, 1003-1006.

Stockley, R.A., Shaw, J., Afford, S.C., Morrison, H.M., and Burnett, D. (1990). Effect of alpha-1-proteinase inhibitor on neutrophil chemotaxis. Am J Respir Cell Mol Biol *2*, 163-170.

Sturrock, A., Franklin, K.F., and Hoidal, J.R. (1996). Human proteinase-3 expression is regulated by PU.1 in conjunction with a cytidine-rich element. J Biol Chem *271*, 32392-32402.

Sturrock, A., Franklin, K.F., Wu, S., and Hoidal, J.R. (1998). Characterization and localization of the genes for mouse proteinase-3 (Prtn3) and neutrophil elastase (Ela2). Cytogenet Cell Genet *83*, 104-108.

Sturrock, A.B., Espinosa, R., 3rd, Hoidal, J.R., and Le Beau, M.M. (1993). Localization of the gene encoding proteinase-3 (the Wegener's granulomatosis autoantigen) to human chromosome band 19p13.3. Cytogenet Cell Genet *64*, 33-34.

Sudo, K., Ema, H., Morita, Y., and Nakauchi, H. (2000). Age-associated characteristics of murine hematopoietic stem cells. J Exp Med *192*, 1273-1280.

Sugawara, S., Uehara, A., Nochi, T., Yamaguchi, T., Ueda, H., Sugiyama, A., Hanzawa, K., Kumagai, K., Okamura, H., and Takada, H. (2001). Neutrophil proteinase 3-mediated induction of bioactive IL-18 secretion by human oral epithelial cells. J Immunol *167*, 6568-6575.

Sugimori, T., Cooley, J., Hoidal, J.R., and Remold-O'Donnell, E. (1995). Inhibitory properties of recombinant human monocyte/neutrophil elastase inhibitor. Am J Respir Cell Mol Biol *13*, 314-322.

Sun, J., Ramos, A., Chapman, B., Johnnidis, J.B., Le, L., Ho, Y.J., Klein, A., Hofmann, O., and Camargo, F.D. (2014). Clonal dynamics of native haematopoiesis. Nature *514*, 322-327.

Swanton, E., Savory, P., Cosulich, S., Clarke, P., and Woodman, P. (1999). Bcl-2 regulates a caspase-3/caspase-2 apoptotic cascade in cytosolic extracts. Oncogene *18*, 1781-1787.

Takizawa, H., Regoes, R.R., Boddupalli, C.S., Bonhoeffer, S., and Manz, M.G. (2011). Dynamic variation in cycling of hematopoietic stem cells in steady state and inflammation. J Exp Med *208*, 273-284.

Tal, T., Sharabani, M., and Aviram, I. (1998). Cationic proteins of neutrophil azurophilic granules: protein-protein interaction and blockade of NADPH oxidase activation. J Leukoc Biol *63*, 305-311.

Till, J.E., and Mc, C.E. (1961). A direct measurement of the radiation sensitivity of normal mouse bone marrow cells. Radiat Res *14*, 213-222.

Tothova, Z., Kollipara, R., Huntly, B.J., Lee, B.H., Castrillon, D.H., Cullen, D.E., McDowell, E.P., Lazo-Kallanian, S., Williams, I.R., Sears, C*., et al.* (2007). FoxOs are

critical mediators of hematopoietic stem cell resistance to physiologic oxidative stress. Cell *128*, 325-339.

Tsai, F.Y., Keller, G., Kuo, F.C., Weiss, M., Chen, J., Rosenblatt, M., Alt, F.W., and Orkin, S.H. (1994). An early haematopoietic defect in mice lacking the transcription factor GATA-2. Nature *371*, 221-226.

Ueda, T., Tsuji, K., Yoshino, H., Ebihara, Y., Yagasaki, H., Hisakawa, H., Mitsui, T., Manabe, A., Tanaka, R., Kobayashi, K.*, et al.* (2000). Expansion of human NOD/SCID-repopulating cells by stem cell factor, Flk2/Flt3 ligand, thrombopoietin, IL-6, and soluble IL-6 receptor. J Clin Invest *105*, 1013-1021.

V, M.S., Kale, V.P., and Limaye, L.S. (2010). Expansion of cord blood CD34 cells in presence of zVADfmk and zLLYfmk improved their in vitro functionality and in vivo engraftment in NOD/SCID mouse. PLoS One *5*, e12221.

Vas, V., Senger, K., Dorr, K., Niebel, A., and Geiger, H. (2012). Aging of the microenvironment influences clonality in hematopoiesis. PLoS One *7*, e42080.

von Vietinghoff, S., Tunnemann, G., Eulenberg, C., Wellner, M., Cristina Cardoso, M., Luft, F.C., and Kettritz, R. (2007). NB1 mediates surface expression of the ANCA antigen proteinase 3 on human neutrophils. Blood *109*, 4487-4493.

Wang, L.C., Swat, W., Fujiwara, Y., Davidson, L., Visvader, J., Kuo, F., Alt, F.W., Gilliland, D.G., Golub, T.R., and Orkin, S.H. (1998). The TEL/ETV6 gene is required specifically for hematopoiesis in the bone marrow. Genes Dev *12*, 2392-2402.

White, M.J., McArthur, K., Metcalf, D., Lane, R.M., Cambier, J.C., Herold, M.J., van Delft, M.F., Bedoui, S., Lessene, G., Ritchie, M.E.*, et al.* (2014). Apoptotic caspases suppress mtDNA-induced STING-mediated type I IFN production. Cell *159*, 1549-1562.

Wiesner, O., Litwiller, R.D., Hummel, A.M., Viss, M.A., McDonald, C.J., Jenne, D.E., Fass, D.N., and Specks, U. (2005). Differences between human proteinase 3 and neutrophil elastase and their murine homologues are relevant for murine model experiments. FEBS Lett *579*, 5305-5312.

Willis, S.N., Chen, L., Dewson, G., Wei, A., Naik, E., Fletcher, J.I., Adams, J.M., and Huang, D.C. (2005). Proapoptotic Bak is sequestered by Mcl-1 and Bcl-xL, but not Bcl-2, until displaced by BH3-only proteins. Genes Dev *19*, 1294-1305.

Wilson, A., Murphy, M.J., Oskarsson, T., Kaloulis, K., Bettess, M.D., Oser, G.M., Pasche, A.C., Knabenhans, C., Macdonald, H.R., and Trumpp, A. (2004). c-Myc controls the balance between hematopoietic stem cell self-renewal and differentiation. Genes Dev *18*, 2747-2763.

Witko-Sarsat, V., Canteloup, S., Durant, S., Desdouets, C., Chabernaud, R., Lemarchand, P., and Descamps-Latscha, B. (2002). Cleavage of p21waf1 by proteinase-3, a myeloid-specific serine protease, potentiates cell proliferation. J Biol Chem *277*, 47338-47347.

Witko-Sarsat, V., Cramer, E.M., Hieblot, C., Guichard, J., Nusbaum, P., Lopez, S., Lesavre, P., and Halbwachs-Mecarelli, L. (1999). Presence of proteinase 3 in secretory vesicles: evidence of a novel, highly mobilizable intracellular pool distinct from azurophil granules. Blood *94*, 2487-2496.

Wolf, B.B., Schuler, M., Echeverri, F., and Green, D.R. (1999). Caspase-3 is the primary activator of apoptotic DNA fragmentation via DNA fragmentation factor-45/inhibitor of caspase-activated DNase inactivation. J Biol Chem *274*, 30651-30656.

Woo, M., Hakem, R., Soengas, M.S., Duncan, G.S., Shahinian, A., Kagi, D., Hakem, A., McCurrach, M., Khoo, W., Kaufman, S.A.*, et al.* (1998). Essential contribution of caspase 3/CPP32 to apoptosis and its associated nuclear changes. Genes Dev *12*, 806-819.

Xing, Z., Ryan, M.A., Daria, D., Nattamai, K.J., Van Zant, G., Wang, L., Zheng, Y., and Geiger, H. (2006). Increased hematopoietic stem cell mobilization in aged mice. Blood *108*, 2190-2197.

Yagi, M., Ritchie, K.A., Sitnicka, E., Storey, C., Roth, G.J., and Bartelmez, S. (1999). Sustained ex vivo expansion of hematopoietic stem cells mediated by thrombopoietin. Proc Natl Acad Sci U S A *96*, 8126-8131.

Yamada, Y., Warren, A.J., Dobson, C., Forster, A., Pannell, R., and Rabbitts, T.H. (1998). The T cell leukemia LIM protein Lmo2 is necessary for adult mouse hematopoiesis. Proc Natl Acad Sci U S A *95*, 3890-3895.

Yamazaki, S., Iwama, A., Takayanagi, S., Eto, K., Ema, H., and Nakauchi, H. (2009). TGF-beta as a candidate bone marrow niche signal to induce hematopoietic stem cell hibernation. Blood *113*, 1250-1256.

Yang, J., Liu, X., Bhalla, K., Kim, C.N., Ibrado, A.M., Cai, J., Peng, T.I., Jones, D.P., and Wang, X. (1997). Prevention of apoptosis by Bcl-2: release of cytochrome c from mitochondria blocked. Science *275*, 1129-1132.

Yang, J.J., Preston, G.A., Pendergraft, W.F., Segelmark, M., Heeringa, P., Hogan, S.L., Jennette, J.C., and Falk, R.J. (2001). Internalization of proteinase 3 is concomitant with endothelial cell apoptosis and internalization of myeloperoxidase with generation of intracellular oxidants. Am J Pathol *158*, 581-592.

Yang, L., Bryder, D., Adolfsson, J., Nygren, J., Mansson, R., Sigvardsson, M., and Jacobsen, S.E. (2005). Identification of Lin(-)Sca1(+)kit(+)CD34(+)Flt3- short-term

hematopoietic stem cells capable of rapidly reconstituting and rescuing myeloablated transplant recipients. Blood *105*, 2717-2723.

Yi, C.H., and Yuan, J. (2009). The Jekyll and Hyde functions of caspases. Dev Cell *16*, 21-34.

Yuan, Y., Shen, H., Franklin, D.S., Scadden, D.T., and Cheng, T. (2004). In vivo self-renewing divisions of haematopoietic stem cells are increased in the absence of the early G1-phase inhibitor, p18INK4C. Nat Cell Biol *6*, 436-442.

Zasloff, M. (2002). Antimicrobial peptides of multicellular organisms. Nature *415*, 389-395.

Zen, K., Guo, Y.L., Li, L.M., Bian, Z., Zhang, C.Y., and Liu, Y. (2011). Cleavage of the CD11b extracellular domain by the leukocyte serprocidins is critical for neutrophil detachment during chemotaxis. Blood *117*, 4885-4894.

Zhang, J., Grindley, J.C., Yin, T., Jayasinghe, S., He, X.C., Ross, J.T., Haug, J.S., Rupp, D., Porter-Westpfahl, K.S., Wiedemann, L.M.*, et al.* (2006). PTEN maintains haematopoietic stem cells and acts in lineage choice and leukaemia prevention. Nature *441*, 518-522.

Zhang, P., Behre, G., Pan, J., Iwama, A., Wara-Aswapati, N., Radomska, H.S., Auron, P.E., Tenen, D.G., and Sun, Z. (1999). Negative cross-talk between hematopoietic regulators: GATA proteins repress PU.1. Proc Natl Acad Sci U S A *96*, 8705-8710.

Zhang, P., Zhang, X., Iwama, A., Yu, C., Smith, K.A., Mueller, B.U., Narravula, S., Torbett, B.E., Orkin, S.H., and Tenen, D.G. (2000). PU.1 inhibits GATA-1 function and erythroid differentiation by blocking GATA-1 DNA binding. Blood *96*, 2641-2648.

Zhu, J., Nathan, C., Jin, W., Sim, D., Ashcroft, G.S., Wahl, S.M., Lacomis, L., Erdjument-Bromage, H., Tempst, P., Wright, C.D.*, et al.* (2002). Conversion of proepithelin to epithelins: roles of SLPI and elastase in host defense and wound repair. Cell *111*, 867-878.

Zimmer, M., Medcalf, R.L., Fink, T.M., Mattmann, C., Lichter, P., and Jenne, D.E. (1992). Three human elastase-like genes coordinately expressed in the myelomonocyte lineage are organized as a single genetic locus on 19pter. Proc Natl Acad Sci U S A *89*, 8215-8219.

Appendix

Abbreviations

AGM: Aorta-gonad mesonephros

ANCA: Anti-neutrophil cytoplasmic antibodies

ANG-1: Angiopoietin 1

BAD: Bcl-2 associated death promoter

BCL-2: B cell lymphoma 2

BCL-xL: B cell lymphoma-extra large

BID: BH3 interacting-domain death agonist

BIM: Bcl-2-like protein 11

BM: Bone marrow

BMI1: Polycomb group ring finger protein 4

BRDU: Bromodeoxyuridine

C12FDG: 5-dodecanoylaminofluorescein di-β-D-galactopyranoside

C/EBPα: CCAAT-enhancer-binding protein alpha

CDC42: Cell division cycle 42

CFC: Colony-forming cell

CLP: Common lymphoid progenitor

CMP: Common myeloid progenitor

DMSO: Dimethylsulfoxide

DPPI: Dipeptidyl peptidase I

EPO: Erythropoietin

fMLP: N-Formylmethionyl-leucyl-phenylalanine

FOXO: Forkhead box protein O

FLT3L: Ligand for Flt3 receptor

FRET: Fluorescence resonance energy transfer

G-CSF: Granulocyte colony-stimulating factor

G-CSFR: Granulocyte colony-stimulating factor receptor

GATA1: GATA binding protein 1

GATA2: GATA binding protein 2

GFI1: Growth factor independent 1

GM-CSF: Granulocyte-macrophage colony-stimulating factor

GMP: Granulocyte/macrophage progenitor

γH2AX: Histone 2A family member X after phosphorylation of Serine 139

H4K16ac: Acetylation of lysine 16 on the tail of histone H4

hCAP18: Human cathelicidin

HOXB4: Homeobox B4

HSC: Hematopoietic stem cell

HSP28: 28 kD heat shock protein

HSPC: Hematopoietic stem and progenitor cell

IκBα: NF-κB inhibitor alpha

IL-1β: Interleukin 1 beta

IL-3: Interleukin 3

IL-6: Interleukin 6

IL-8: Interleukin 8

IL-11: Interleukin 11

IL-18: Interleukin 18

LK: Lineage$^-$ Sca-1$^-$ c-Kit$^+$ cells

LMO2: Lim-domain only 2

LPS: Lipopolysaccharide

LSK: Lineage$^-$ Sca-1$^+$ c-Kit$^+$ cells

LT-HSC: Long-term hematopoietic stem cell

MCL1: Myeloid cell leukemia 1

MEP: Megakaryocyte/erythrocyte progenitor

MLL: Mixed lineage leukemia protein

MPP: Multipotent progenitor cell

mTOR: Mammalian target of rapamycin

NE: Neutrophil elastase

NOD/SCID: Non-obese diabetic/severe combined immunodeficiency

PBS: Phosphate-buffered saline

PI3K: Phosphatidylinositol 3-kinase

PMA: Phorbol myristate acetate

PR3: Proteinase 3

PTEN: Phosphatase and tensin homolog

ROS: Reactive oxygen species

RUNX1: Runt related transcription factor 1

SA-β-GAL: Senescence-associated beta-galactosidase

SCF: Stem cell factor

SERPIN: Serine protease inhibitor

TGFβ: Transforming growth factor beta

TPO: Thrombopoietin

SCL/TAL1: T cell acute lymphocytic leukemia protein 1

SLAM: Signaling lymphocytic activation molecule

ST-HSC: Short-term hematopoietic stem cell

TEL/ETV6: Ets variant 6

TNFα: Tumor necrosis factor alpha

TUNEL: terminal deoxynucleotidyl transferase dUTP nick end labeling

WG: Wegener's granulomatosis

WT: Wild-type